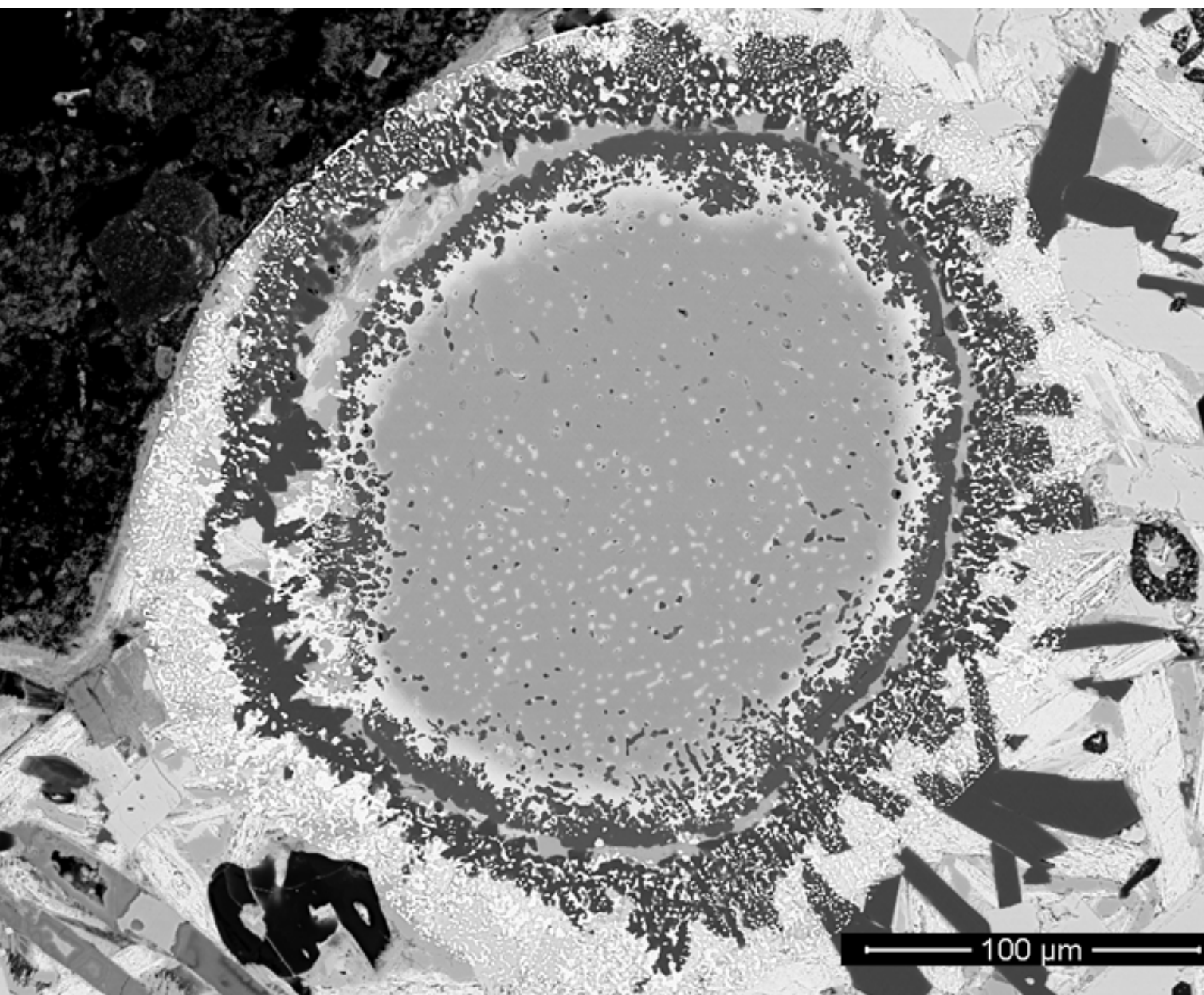


ROMAN AND MEDIEVAL LITHARGE CAKES A SCIENTIFIC EXAMINATION

TECHNOLOGY REPORT

Brice Girbal



This report has been prepared for use on the internet and the images within it have been down-sampled to optimise downloading and printing speeds.

Please note that as a result of this down-sampling the images are not of the highest quality and some of the fine detail may be lost. Any person wishing to obtain a high resolution copy of this report should refer to the ordering information on the following page.

ROMAN AND MEDIEVAL LITHARGE CAKES

A SCIENTIFIC EXAMINATION

Brice Girbal

© English Heritage

ISSN 1749-8775

The Research Department Report Series incorporates reports from all the specialist teams within the English Heritage Research Department: Archaeological Science; Archaeological Archives; Historic Interiors Research and Conservation; Archaeological Projects; Aerial Survey and Investigation; Archaeological Survey and Investigation; Architectural Investigation; Imaging, Graphics and Survey, and the Survey of London. It replaces the former Centre for Archaeology Reports Series, the Archaeological Investigation Report Series and the Architectural Investigation Report Series.

Many of these are interim reports which make available the results of specialist investigations in advance of full publication. They are not usually subject to external refereeing, and their conclusions may sometimes have to be modified in the light of information not available at the time of the investigation. Where no final project report is available, readers are advised to consult the author before citing these reports in any publication. Opinions expressed in Research Department reports are those of the author(s) and are not necessarily those of English Heritage.

Requests for further hard copies, after the initial print run, can be made by emailing:

Res.reports@english-heritage.org.uk

or by writing to:

English Heritage, Fort Cumberland, Fort Cumberland Road, Eastney, Portsmouth PO4 9LD

Please note that a charge will be made to cover printing and postage.

SUMMARY

The refining of silver alloys to obtain the silver they contain (cupellation) has been undertaken for thousands of years. The primary material evidence for this process comprises a lead-rich waste known as litharge cakes. Studies conducted by Bayley and Eckstein (2006) and Bayley (2009) suggested that cupellation in the medieval period was more successful/advanced than in Roman times based on the higher PbO/Cu₂O ratio in the medieval litharge cakes. The analyses of a further forty five litharge fragments from twelve archaeological sites has found no correlation between the PbO/Cu₂O ratio and time period. The microstructural and chemical analyses showed that there were two major compositions; a clay/vegetable ash mixture and bone ash. No correlation was identified between hearth lining composition and the PbO/Cu₂O ratio. However, it is argued that the clay/vegetable ash was more absorbent than the bone ash litharge cakes. It was also noticed that 90% of the medieval litharge was clay/vegetable ash while they accounted for only 50% of the Roman litharge. This may be indicative of a compositional preference in certain time periods. Unfortunately the dating is poor in most cases limiting more comprehensive interpretations. Nevertheless there is no evidence to suggest a more effective practice at either period.

ACKNOWLEDGEMENTS

I would like to thank Sarah Paynter and Harriet White for moral and technical support and David Dungworth for his guidance. I feel it important to thank Justine Bayley for providing the assemblage and initiating this project. Thank you to all past English Heritage staff who helped collate and sample the litharge fragments. I am also grateful to Roger Wilkes for taking photographs of the original litharge fragments.

ARCHIVE LOCATION

Litharge fragments have been sent back to respective commercial units but the mounted samples are kept in the Archaeological Conservation and Technology Laboratory, English Heritage, Fort Cumberland, Fort Cumberland Road, Eastney, Portsmouth, PO4 9LD

DATE OF RESEARCH

Nov-Dec 2010

CONTACT DETAILS

Technology Team, English Heritage, Fort Cumberland, Fort Cumberland Road, Eastney, Portsmouth, PO4 9LD

Brice Girbal, Tel: 023 9285 6785: brice.girbal@english-heritage.org.uk

INTRODUCTION

The production (smelting) and refining (cupellation) of silver are amongst the oldest metallurgical processes known; and for thousands of years (until the 20th century AD) these basic processes remained mostly unaltered. Remains from silver refining are linked with three processes: silver production, silver recycling and silver assaying (Bayley and Eckstein 1997).

The production of silver usually involved the smelting of silver-rich lead ores such as cerussite and galena (although other mineral sources are known – Kassianidou 2003, 198–199). Lead has an affinity for silver which tends to concentrate in the metal. This results in the formation of a lead bullion rich in silver (argentiferous lead) which must then be refined by cupellation. The argentiferous lead is melted in a shallow cupellation hearth under oxidising conditions. Because a much lower partial pressure of oxygen is required to oxidise lead (or copper) than silver, lead oxidises (litharge, PbO) forming a layer on top of the molten metal while the silver remains in a metallic state. However, oxygen diffuses very slowly through a layer of litharge meaning that it must be continually removed so that the rest of the lead can continue to oxidise. Much of the litharge was raked off the surface of the melt but some of it was absorbed by the hearth lining. The cupellation hearth is thus lined with porous, calcium-rich material which absorbs the litharge and any other metal oxides (impurities) by capillary action, while the silver (still in its metallic state) remains on the surface due to its high surface tension (Bayley and Eckstein 2006).

An essentially identical process was also employed to refine/recycle impure silver (debased or alloyed with other metals such as copper or tin). In this case, lead was added and melted with the impure silver. The lead reacts with the base metal impurities, oxidising them to form fusible compounds which are then absorbed by the lining as discussed above. This is the process that produced all the litharge cakes studied here.

The third process linked with silver refining is assaying which is a quantitative method in which the aim is to investigate the purity of a small sample of a given metal or ore. Two steps are required for this; first the silver must be concentrated in a lead button and then cupelled. The first step may be achieved by 'scorification' whereby the ore/metal is smelted in a shallow (earthenware) dish under oxidising conditions (Bayley and Eckstein 1997, 109–110). This results in a very pure argentiferous lead which can then be refined by cupellation in smaller bowls of the same calcium-rich material (cupels). The refined product (silver) is then weighed and the weight loss (from the start of the process) indicates the purity of the metal/ore.

Two primary sources of evidence (documentary and archaeological) have enabled these processes to be better understood. Although some of the earliest documents remain vague (Tereygeol and Thomas 2003, 172) several later ones provide more detailed accounts of the processes associated with the production and refining of silver. Some of the most complete available in English are Theophilus's *De diversis artibus* (Hawthorne

and Smith 1979), Agricola's *De re metallica* (Hoover and Hoover 1950) and Biringuccio's *Pirotechnica* (Smith and Gnudi 1990). The more general aspects of the process will be described below but for a more complete summary of documentary sources related to cupellation refer to Bayley (2008a) and Nriagu (1985).

Of interest to this study, documentary sources describe both the cupellation process and the making of the cupellation hearth linings. The processes involved share similarities in all sources with minor variations. The ashes (of various composition) making the hearth lining are mixed with water (or other binding agent) and compacted into a small bowl/hearth. This is left to dry and when ready is put into the fire/furnace directly under the blowing hole so that the process is an oxidising one. Lead is melted and then the metal to be refined is placed into the lined hearth (although different sources argue for the metal to be added first and then the lead). The whole is covered with charcoal and melted. As the lead oxidises it forms a layer on top of the melted bath (scum) which is removed with the aid of a wooden stick. Biringuccio states that the liquid lead and copper (oxides) float on top of the silver and is allowed to gradually flow out of the hearth until the silver is almost reached (the rest of the lead and impurities presumably being absorbed by the lining). Knowing when the process is completed seems to be ascertained visually and it is said that if the liquid is agitated/spitting then it is still impure and more lead must be added (Theophilus also mentions the addition of crushed glass). This process must be repeated until the metal achieves a particular visual shine indicative of pure silver.

The most common archaeological remains for silver refining are the lead oxide impregnated cupellation hearth linings (litharge cakes) and cupels discussed above. These are mainly composed of litharge (PbO – to which they owe their name) with varying proportions of other impurities like Cu₂O (sometimes in metallic form), SnO₂ and the lining material such as P₂O₅, CaO and SiO₂. It is, however, in some cases hard to identify which processes these litharge cakes have resulted from (Bayley and Eckstein 1997, 109–111). Silicate ceramics are unlikely to have been used for cupellation as the PbO would react aggressively with the silica forming a lead silicate glass in turn causing the breakdown of the lining but would have been suitable for the process of scorification. It has also been suggested that litharge from production sites would contain almost no base metal oxides (impurities such as copper and tin) which one would expect to find in significant quantities in litharge from recycling (Bayley and Eckstein 1997, 108). Unfortunately no concrete evidence for the refining of silver from newly smelted lead (production sites) has been found in Britain for the Medieval period (perhaps because the litharge was re-smelted to recover the lead). On the other hand there is ample evidence (in the form of litharge cakes) of cupellation as a means of refining (recycling) debased silver (Bayley 2008, 133–134).

Although the archaeological evidence combined with documentary sources have helped our understanding of the different processes associated with silver refining, very little has been done with the archaeological finds; especially regarding litharge cakes. This study will further the work started by Bayley and Eckstein (2006) undertaking microstructural and

compositional analyses of forty five fragments of litharge dating from the Roman to medieval period.

BACKGROUND

Recent studies of cupellation hearth linings have been concerned with two main issues: determining their composition and judging the efficiency of the technology. Few studies, however, have dealt specifically with litharge cakes. Indeed the majority of the work published can be summarised in three articles; Bayley (2008) and Bayley and Eckstein (1997; 2006). Due to the lack of published resources on litharge cakes it has been necessary to draw upon the more abundant research conducted on their smaller counterparts — cupels (Martín-Torres *et al*/2008; Martín-Torres *et al*/2009; Tereygeol and Thomas 2003; White, 2010a; White 2010b) even though there is no evidence for this small scale cupellation in Britain before the sixteenth century (Bayley and Eckstein 1997, 107).

Bayley and Eckstein's (2006) pilot study discussed the efficiency of Roman and medieval cupellation. It comprised the microstructural and chemical analyses (scanning electron microscope — SEM) of six litharge cakes with the addition of a further three in 2009 (Bayley 2009). They argued that the efficiency of the cupellation process can be determined by the quantity of copper present in the litharge. Analyses of the nine fragments showed that silver was only detected in considerable amounts when the Cu/Pb ratio was high. The oxidised copper forms as free copper oxide (Cu_2O) as opposed to a copper lead oxide ($\text{PbO}\cdot\text{Cu}_2\text{O}$) when insufficient lead is added to the process. As up to 44% of silver dissolves in Cu_2O (but not in $\text{PbO}\cdot\text{Cu}_2\text{O}$) significant amounts of silver are absorbed with the copper oxide into the calcium rich lining. The silver separates on cooling but cannot then be retrieved, resulting in silver loss (Bayley and Eckstein 2006). This is also supported by Tereygeol and Thomas' (2003) cupellation experiments which have shown that the losses of silver were proportionally greater when the metal refined had a higher Cu to Ag ratio. Ideally, according to the Cu_2O -PbO phase diagram, the Pb/Cu ratio should be around 16 to prevent formation of free copper oxide (Riche and Gelis 1888, 156; Tereygeol and Thomas 2003).

On the other hand, Martín-Torres *et al* (2009, 438) have argued that silver traces in cupels should not directly reflect the (in)efficiency of the process, as the silver content (if any) of the metal processed cannot be known. They propose instead that when silver is detected in several cupels from the same site, they can be compared and inferences can be made as to the reproducibility of the process. For example, their study compares cupels from two different sites; the Oberstockstall cupels all have (apart from one) similar silver contents (clustering around 200ppm) while the Kapfenberg cupels have a much broader scatter of silver losses. From this it can be inferred that there was a more effective standard practice in Oberstockstall while the more erratic silver losses in the

Kapfenberg cupels may be due to a more experimental process, or indicative of less skilled/experienced artisans (Martinón-Torres *et al*/2009). This approach, however, has some limitations. It requires an assemblage of several well preserved cupellation hearth linings which is rare, especially when dealing with litharge cakes. Good context information is required in order to evaluate their provenance (temporal and spatial), for instance whether they are from the same workshop. This can be problematic for urban sites (where the majority of the litharge cakes investigated in this report were found) as layers may contain residual material from several periods. Nevertheless, when the material and archaeological information permit this kind of evaluation it is very informative.

Silver losses can be caused by the lack of skill of the craftsman, the addition of insufficient lead, or even the quality of the cupellation linings. This latter brings us to the composition of the litharge cakes. Problematically, the original microstructures of hearth linings are often blurred by the large amounts of impregnated lead oxide. Indeed the chemical compositions are dominated mainly by the metal oxides (PbO, Cu₂O and occasionally SnO₂ and ZnO) which the lining was designed to absorb. Unused cupellation hearth linings would be ideal to investigate the original compositions. Unfortunately, such artefacts are rare as it is the litharge (PbO) which acts as a consolidant (bonding agent) enabling them to resist post depositional deterioration. However, Bayley and Eckstein (2006) as well as Martinón-Torres *et al* (2008, 10; 2009, 439) circumvent this dilemma by neglecting all elements heavier than nickel (assuming that these are contaminants absorbed by the linings during use) and re-normalising the remaining elements to 100%. This new composition, although not fully quantitative, can then be taken as representative of the original hearth lining before use.

Three main materials/recipes seem to have been used in the litharge cakes analysed by Bayley and Eckstein (2006). These were bone ash, a mixture of bone/plant ash, and clay marl (lime-rich clay). The main constituent (~85%) of bone ash is the mineral hydroxylapatite [Ca₅(PO₄)₃(OH)] while the rest is mainly calcium carbonate (~10%) along with other compounds (~5%) (Martinón-Torres *et al*/2008, 10; 2009, 439). If the main constituents of the hearth lining are CaO and P₂O₅ then it is most likely pure bone ash. A mixture of ashes may contain more MgO while clay marl would be rich in SiO₂ and Al₂O₃ but deficient in P₂O₅. Martinón-Torres *et al* (2008; 2009) have developed a strategy for calculating the percentage of bone ash and any other material that may have been mixed with it (excipient). This involves calculating the weight ratio of CaO to P₂O₅ but is based on two assumptions: that the excipient (like clay and plant ashes) did not contain significant quantities of phosphorus and that the CaO/P₂O₅ ratio in bone is relatively stable and predictable. If a CaO/P₂O₅ ratio of 1.2 is accepted (this may vary between animals and body parts, but is a good estimate — see Martinón-Torres *et al*/2008; 2009 for full limitations), the CaO contributed by the bone ash can be calculated by multiplying the P₂O₅ content by 1.2. This gives the approximate proportion of bone ash which can then be removed and the remainder re-normalised giving the chemical composition of the excipient. One can then go further by working out the ratio of bone ash to excipient by following these simple equations (Martinón-Torres *et al*/2009, 439):

$$\text{Bone ash \%} = \text{P}_2\text{O}_5 + (\text{P}_2\text{O}_5 \times 1.2) \%$$

$$\text{Excipient \%} = \sum \text{normalised lining raw composition (100\%)} - \text{bone ash \%}$$

The analyses of the nine Roman and Medieval litharge cakes (Bayley and Eckstein 2006; Bayley 2009) using similar methodologies discussed above has evoked several points of interest. Higher silver losses were noticed in Roman litharge, perhaps because the silver being refined was less pure than Medieval. On the other hand, the lower Cu/Pb ratios in the Medieval litharge suggests they had a greater understanding of the process than their Roman predecessors. However, subsequent semi-quantitative (preliminary) X-Ray Fluorescence (XRF) analyses on a greater number of litharge fragments have hinted that this pattern may not stand when a larger assemblage is examined (Bayley 2009). The analyses also indicated that there is no correlation between the composition of the hearth lining and the effectiveness of the cupellation process (Bayley and Eckstein 2006, 152).

AIMS AND OBJECTIVES

This study will build upon Bayley and Eckstein's research, using similar methodologies, with the aim to further understanding of cupellation processes through the scientific analysis of its main waste product, litharge cakes. This will involve the microstructural and compositional (SEM-EDS) examination of forty-five litharge cake fragments from twelve sites, which come from contexts dating to the first to fourteenth centuries AD.

Several questions will be addressed:

1. Are Roman and Medieval litharge cakes compositionally different?
2. Was Roman cupellation technology less effective than Medieval? Are there consistently greater losses of silver in Roman or Medieval litharge? What does this imply/infer about cupellation technology in Roman and Medieval England?
3. Is there a correlation between cupellation hearth lining composition and effectiveness of process?
4. Can specific technological processes be identified/recognised through the scientific analysis of litharge cakes?
5. Can socio-political-cultural behaviours be inferred through the choice of materials and technological processes?
6. Are the scientific and sampling methodologies used suitable to achieve the aim of this study?

METHODOLOGY

Visual Analysis

The original assemblage of forty (including CGI/2/3) litharge fragments was collected over several decades of research (by Justine Bayley) but most of these (after having been sampled) had been returned to the respective archaeological units or museums for archive and were unavailable to the author. All descriptions of these fragments were based on sketches (by Justine Bayley) and photographs (by Roger Wilkes — Appendix 1). Five fragments of litharge from Dunkirt Barn (Cunliffe and Poole 2008) were added to the assemblage by the author and examined visually. Distinctive characteristics such as colour, texture, shape, weight (g) and size (cm — to the nearest mm) were considered and recorded. This visual analysis is important to reveal which processes the fragments have resulted from, in turn suggesting possible technological traits (Bayley *et al*/2001). Please refer to Appendix 1 for photographs of individual litharge fragments.

Microstructural and Chemical Analysis

Samples were then selected for micro-structural and chemical analysis. The forty samples had already been cut, embedded in resin and polished. The other five (from Dunkirt Barn) were chosen to represent a good proportion of the fragments available; special care was taken to get a complete profile of the fragments. The most solid were cut with a Buehler Isomet low speed saw while the more brittle ones were broken by hand and one edge ground flat with rough wet and dry paper. The samples were then embedded in epoxy resin (Struers epo-thin) and polished to a 1-micron finish. Once embedded, sections of some of the larger fragments were cut to facilitate grinding and polishing as well as enabling them to fit on the SEM stage. For photographs showing the macrostructure at low magnification of the cut samples please refer to Appendix 2.

The polished samples were then carbon coated and examined using a scanning electron microscope (SEM – FEI Inspect F). This allowed the identification of individual micro-structural phases such as litharge (PbO) and copper-lead oxide (PbO.Cu₂O). Images were collected using the back-scattered electron detector — the brightness of each region being proportional to its average atomic number. The chemical composition of each sample was obtained using the energy dispersive X-ray spectrometer (Oxford Instruments SDD X-act EDS) attached to the SEM. The data was collected in several different ways: random bulks, stratigraphic bulks and spot analyses. Random bulk analyses were taken for each sample at magnifications between 100x to 350x depending on the size of the crystalline structures. An average composition was determined by taking the mean of 5 to 20 bulk readings per sample; the more homogenous the sample the fewer readings were required to reach a reliable average. Areas analysed were carefully selected to show a

good representation of the crystalline phases while areas of unusual heterogeneity (corrosion or contamination) or ones making up a minor percentage of the overall sample were avoided. For samples with known orientations, stratigraphic bulk analyses were taken. This involved taking bulk analyses at 250x (approximately 1.2mm²) starting at the top and taking a reading every 0.8mm to the bottom. A spot mode which allows an accurate reading of an area about 10 micron² was used to confirm the crystalline phases present.

Compositions for the bulk analyses were calculated assuming that all elements were present as oxides (stoichiometric) while the spot analyses of metals were calculated as elements. Analytical parameters were kept constant at an accelerating voltage of 25kV, spot size of 5 (approximately 1.2nA), processing time of 5 and acquisition time of 120 seconds per spectrum. The spectra were de-convoluted using the Oxford Instruments INCA software. Compositions were normalised to 100wt% to allow comparisons of samples with varying degrees of porosity.

To verify the reliability of the chemical data retrieved by SEM-EDS two high-lead glass standards (DLH1 and DLH2) were analysed. It is important here to stress the lack of, and need for, litharge standards which would provide better (more suitable) comparative data. Nevertheless, ten areas per standard were examined (Appendix 3) and the results compared to the reported values. These confirm that the data presented are accurate. The SEM-EDS has a detection limit for most elements of ~0.1wt% and ~0.2wt% for P₂O₅, SO₃ and BaO. However, due to the high-lead matrixes of the litharge fragments, detection limits for certain elements were dramatically affected. The results for these (Au₂O₃, SnO₂, As₂O₃ and SO₂) were plotted in cumulative frequency graphs enabling more realistic detection limits to be ascertained — 0.5wt% for Au₂O₃, 0.6wt% for SnO₂, 0.3wt% for As₂O₃ and 1.1wt% for SO₃. Due to the Au M-peak interference with the Pb L-peak the data for Au was collected from its L-peak. The S contents for all samples were unreliable (most were between 0.5 to 1.0wt%) and therefore are not given in the data tables. Samples Lith9, Lith10 and CG2 all had detectable S but these happen to be the smallest samples in the assemblage and the presence of Cl suggested that the S content was probably associated with corrosion or post-depositional contamination.

The data was rounded to one decimal place while compositions below the detection limit of the measured element were labelled <detection limit (eg <0.1). The elements analysed were Na, Mg, Al, Si, P, S, K, Ca, Mn, Fe, Ni, Cu, As, Ag, Sn, Au and Pb. Any element below the detection limit in all samples is not displayed in the data tables. Although some of the metals were present in metallic form they were measured as (stoichiometric) oxides.

Four samples were selected for X-ray diffraction (XRD). These were approximately 1cm³ in size and taken as close to the SEM samples as possible so that the same material was analysed. They were then crushed manually with a steel pestle and mortar and sieved (Endecotts - 125 micron aperture). The process was repeated until all the material was ground to a fine powder. After each sample the pestle and mortar was cleaned with a

fine brush and compressed air so as to avoid cross-sample contamination. The fine powders were then analysed in the Bruker D8 Advance XRD with a LynxEye detector and copper anode X-ray tube. Analytical parameters were kept constant with a 0.11 discriminator lower level and 0.14 discriminator window width. The tube was set at 40mA and 40kV while the probe was effectuated at a 2 theta angle of 10° to 75°. The increment step size remained at 0.02 and the scan speed at 0.2 sec/step. The spectra were scrutinised using the X'Pert Highscore software by PANalytical and the mineral phases were identified using the ICDD (International Centre for Diffraction Data) database.

THE ASSEMBLAGE

Forty-five litharge fragments from twelve sites were examined in this study. Twenty-five fragments were from Lincoln with 10 of these from Saltergate, 14 from Flaxengate and one from Swan Lane. These were found in medieval contexts which contained significant quantities of residual Roman material and Bayley (2008b, 29–42) has suggested a late Roman date for these cupellation residues. There were also five fragments from Abbots Ann (Dunkirt Barn) as well as one from Grange Farm, Gillingham, Kent, one from York (Driffield Terrace) and another from Merida, Spain all Roman in date. Five fragments found in medieval contexts were from Winchester; four from Brook Street and one from Wolvesey Palace. In addition, two from Dublin, three from York (Coppergate) and one from London (No 1 Poultry) were also medieval in date. All the samples analysed in this study are listed in Table 1.

The litharge fragments ranged in size from approximately 1 to 10cm in length, 1 to 5.6cm in width and 0.8 to 4.2cm in depth; the majority being very fragmentary – below 4cm in length. Apart from size, their morphological appearance was quite similar (Figs 1 to 6). In colour they all varied in shades of light to dark grey with most displaying greenish or brownish patches. The greenish colour is undoubtedly due to the copper content of the litharge fragments while the brown patches may be residues of soil, a clay lining or even the original ash. In texture they were quite rough to the touch, in most cases one side appeared to be rougher sometimes with small protrusions of material. Some of the larger fragments displayed a curved profile but the majority of fragments were amorphous in shape. An orientation (top-bottom) was easy to determine for those with curved profiles. However, it was harder to discern for the smaller, amorphous shaped fragments. As a gross generalisation the bottom surfaces appeared to be rougher (Figs 1 and 4). The orientations of the fragments were reassessed once samples had been cut and again once they had been analysed in the SEM. This allowed an orientation to be determined for some of the smaller fragments and confirmed previous suggestions for the larger fragments. Those too fragmentary for an orientation to be determined were noted in Table 1. For photographs of individual litharge fragments please refer to Appendix 1.

Table 1. The litharge fragments sampled.

Lith No	Town	Site	Site No	Context	Context Date	Likely Date	Weight (g)	Sample
1	Winchester	Wolvesey Palace	RF 5682	Tr. 205	L14th?	medieval	25	fragment
2	Winchester	Brook St	8167	1039	13th	medieval	25	T-B
3	Winchester	Brook St	RF 9072	1053	L11-12th	L11-12th	23	T-B
4	Winchester	Brook St	RF 9071	1053	L11-12th	L11-12th	115	Misplaced
5	Winchester	Brook St	RF 9073	1056	L11-12th	L11-12th	120	T-
6	Lincoln	Saltergate D	28 [RN2059]	1	-	Roman	520 [435]	T-B
7	Lincoln	Saltergate F I	26 [RN2444]	35	EM-ML11	Roman	20	T-
8	Lincoln	Saltergate F I	48 [RN2659]	68	EM-ML11	Roman	30	T-B
9	Lincoln	Saltergate D I	84 [RN2852]	75	E-EM13	Roman		fragment
10	Lincoln	Saltergate F I	69 [RN2904]	44	E-ML11	Roman	60	T-
11	Lincoln	Saltergate F	87 [RN3030]	96	E-EM11	Roman		fragment
12	Lincoln	Saltergate F	75 [RN3072]	44	E-ML11	Roman	25	T-
13	Lincoln	Saltergate D	165 [RN3196]	105	L10	Roman	14	T-
14	Lincoln	Saltergate D	183 [RN3322]	121	-	Roman	70	fragment
15	Lincoln	Saltergate F	507 [RN3695]		ML9-M10	Roman	20	fragment
16	Lincoln	Flaxengate	M4	BCU	E10	Roman	450	T-B
17	London	No 1 Poultry	2860	6036		10-11th		T-B
18	York	Driffeld Terrace	462	4059		Roman		B-
19	Gillingham	Grange Farm	-	201				T-B
20	Merida, Spain					Roman		fragment
21&28	Lincoln	Flaxengate	M40	BVD	9	Roman	325	(2F) frag
22	Lincoln	Flaxengate	M47	BXN	9	Roman	260	B-
23	Lincoln	Flaxengate	M33	BNF	9/10	Roman	110	T-
24	Lincoln	Flaxengate	M14	BDS	9/10	Roman	50	T-
25	Lincoln	Flaxengate	Ae456	B106	M10	Roman	40	B-
26	Lincoln	Flaxengate	Ae269	BXN	9	Roman	80	B-
27	Lincoln	Flaxengate	M22 & Fe280	BDQ	9/10	Roman	360	(2F) T-B
29	Lincoln	Flaxengate	Ae163	BPM	9	Roman	25	fragment
30	Lincoln	Flaxengate	M31	BPM	9	Roman	30	fragment
31	Lincoln	Flaxengate	M30	BPM	9	Roman	100	fragment
32	Lincoln	Flaxengate	M38	BDS	9/10	Roman	10	NS
33	Lincoln	Flaxengate	M41	BPH	L12	Roman	50	(2F) frag
34	Lincoln	Flaxengate	M6	BDG	E10	Roman	20	fragment
35	Lincoln	Swan Lane	674	386	L4	Roman		B-
36	Abbotts Ann	Dunkirt Barn	DB06	F1548	Roman	Roman	20	T-B
37	Abbotts Ann	Dunkirt Barn	DB06	F1578	Roman	Roman	142	T-B
38	Abbotts Ann	Dunkirt Barn	DB06	F1580	Roman	Roman	93	T-B
39	Abbotts Ann	Dunkirt Barn	DB06	1058	Roman	Roman	20	fragment
40	Abbotts Ann	Dunkirt Barn	DB06	1060	Roman	Roman	20	fragment
41	Dublin		E71	2812		10-11th		fragment
42	Dublin		E71	8319		10-11th		fragment
CG1	York	Coppergate	16179	32194	EM10-ML10	10th	50	fragment
CG2	York	Coppergate	7409	20999	EM10-ML10	10th	170	fragment
CG3	York	Coppergate	58	2143	L11-16	medieval	90	fragment

In sample column:

T-B = full section from top to bottom of litharge cake

T- = section includes upper surface but not bottom edge

B- = section includes bottom edge but not top surface

fragment = orientation of sample unknown/unsure

2F = two fragments sampled

NS = not sampled



Fig 1. Bottom of lith05.



Fig 2. Top of lith05.



Fig 3. Side view of lith05.



Fig 4. Bottom of lith27.



Fig 5. Top of lith27.



Fig 6. Side view of lith27.

MICROSTRUCTURAL ANALYSES

Out of the 45 fragments, 42 samples were analysed in this study. Two fragments were not analysed – lith04 which was misplaced and lith32 which was not sampled. All of the litharge in the assemblage except 2 (lith24 and lith26 discussed later) have microstructures typical of precious metal cupellation hearth linings (Martinón-Torres *et al* 2008; 2009; Bayley and Eckstein 2006). Table 2 shows the crystalline phases, metal and metal oxides present in each sample.

Two major microstructural groupings were apparent: those with complex lead-rich microstructures and many different crystalline structures (group 1) and those predominantly composed of bone ash (group 2).

Group 1

Group 1 comprised 24 of the litharge cakes in the assemblage; all three samples from Brook Street, nine from Saltergate, one from Flaxengate, one from No 1 Poultry, one from Grange Farm, one from Merida, three from Dunkirt Barn, both samples from Dublin and all three samples from Coppergate. Their microstructures tended to be quite complex, heavily broken down by a dominant lead oxide (with a mixture of other elements) structure. The samples were reasonably similar microstructurally and contained many crystalline phases. These were mainly present as concentrations of tiny/small dark grains scattered all over the samples. Spot analyses were taken for each crystalline phase and while some matched well known mineral phases, others were given an approximate chemical formula based on their composition.

Table 2. The crystalline phases, metal oxides and metals present in each sample.

Lith No	Composition	Age	Crystalline phases	Metal oxides	Metals
1	Group 2	M	Apatite, 2a	Cu ₂ O, Cu ₂ (CO ₃)(OH) ₂ , PbCu ₂ O ₂ , PbO	Cu, Ag
2	Group 1	M	Apatite, 1a, 1c, 2a, 4a	Cu ₂ O, PbCu ₂ O ₂ , PbO	Cu
3	Group 1	M	1a, 2a, 4a	Cu ₂ O, PbCu ₂ O ₂ , PbO	Cu
5	Group 1	M	1a, 1d, 2a, 4a	PbCu ₂ O ₂ , PbO, PbO ₂	Cu
6	Group 1	R	1a, 2a, 2b, 3a	PbO, PbO ₂	
7	Group 1	R	Apatite, 1b, 2a, 2b, 2d, 4a	Cu ₂ O, PbCu ₂ O ₂ , PbO ₂ , PbO	Cu, Ag
8	Group 1	R	1a, 2a, 2b, 2d, 4a	Cu ₂ O, PbCu ₂ O ₂ , PbO	Cu
9	Group 1	R	Apatite, 4a	Cu ₂ (CO ₃)(OH) ₂ , PbO, PbO ₂	
10	Group 1	R	1a, 2a, 4a	PbCu ₂ O ₂ , PbO, PbO ₂ , Ca(SnZr)O ₃	Cu
11	Group 1	R	Corroded	Cu ₂ O, Cu ₂ (CO ₃)(OH) ₂ , PbO	Cu
12	Group 1	R	1b, 2a, 3a, 4a	PbO, PbO ₂	Cu
13	Group 1	R	2a, 2c, 4a	Cu ₂ O, Cu ₂ (CO ₃)(OH) ₂ , PbCu ₂ O ₂ , PbO, Pb ₃ O ₄	Cu, Ag
14	Group 2	R	Apatite	Cu ₂ O, PbO, PbO ₂	Cu
15	Group 1	R	Apatite, 4a	Cu ₂ O, Cu ₂ (CO ₃)(OH) ₂ , PbO, PbO ₂	Cu
16	Group 2	R	Apatite	Cu ₂ O, Cu ₂ (CO ₃)(OH) ₂ , PbCu ₂ O ₂ , PbO, PbO ₂ , Pb ₃ O ₄ , Ca(SnZr)O ₃	Cu, Ag
17	Group 1	M	1b	PbO, PbO ₂	Cu
18	Group 2	R	Apatite, 4b	Cu ₂ O, Cu ₂ (CO ₃)(OH) ₂ , PbCu ₂ O ₂ , PbO	Cu, Ag
19	Group 1		1b, 1c, 2a, 2b	Cu ₂ O, PbCu ₂ O ₂ , PbO	Cu
20	Group 1	R	2b, 3a, 3c	Cu ₂ (CO ₃)(OH) ₂ , PbCu ₂ O ₂ , PbO	Cu
21	Group 2	R	Apatite	Cu ₂ O, Cu ₂ (CO ₃)(OH) ₂ , PbO	Cu
22	Group 2	R	Apatite	Cu ₂ O, Cu ₂ (CO ₃)(OH) ₂ , PbCu ₂ O ₂ , PbO	Cu
23	Group 2	R	Apatite	Cu ₂ O, Cu ₂ (CO ₃)(OH) ₂ , PbCu ₂ O ₂ , PbO	Cu, Ag
24	Other	R	1b, 2c, 3b	Cu ₂ O, PbO, PbO ₂ , SnO ₂	Cu
25	Group 1	R	1b	Cu ₂ O, PbO, PbO ₂	Cu
26	Other	R	1d	Cu ₂ O, Cu ₂ (CO ₃)(OH) ₂ , PbCu ₂ O ₂ , PbO, PbO ₂ , tin copper oxide	Cu
27	Group 2	R	Apatite	Cu ₂ O, Cu ₂ (CO ₃)(OH) ₂ , PbCu ₂ O ₂ , PbO	Cu, Ag
29	Group 2	R	Apatite	Cu ₂ O, Cu ₂ (CO ₃)(OH) ₂ , PbO, PbO ₂	Cu
30	Group 2	R	Apatite	Cu ₂ O, PbCu ₂ O ₂ , PbO, PbO ₂	Cu
31	Group 2	R	Apatite	PbO, PbO ₂	
33	Group 2	R	Apatite, 1c	Cu ₂ O, Cu ₂ (CO ₃)(OH) ₂ , PbCu ₂ O ₂ , PbO, Pb ₂ SnO ₄ , Ca(SnZr)O ₃	Cu, Au
34	Group 2	R	Apatite	Cu ₂ O, Cu ₂ (CO ₃)(OH) ₂ , PbCu ₂ O ₂ , PbO, Pb ₃ O ₄	Ag
35	Group 2	R	Apatite, 1c	Cu ₂ O, Cu ₂ (CO ₃)(OH) ₂ , PbCu ₂ O ₂ , PbO, PbO ₂	Cu, Ag
36	Group 1	R	1a, 1d, 2a	Cu ₂ O, PbCu ₂ O ₂ , PbO, PbO ₂	Cu, Ag
37	Group 2	R	Apatite, 1a, 1c	Cu ₂ O, PbCu ₂ O ₂ , PbO, PbO ₂	Cu
38	Group 2	R	Apatite, 1c, 2a	Cu ₂ O, Cu ₂ (CO ₃)(OH) ₂ , PbO, PbO ₂	Cu
39	Group 1	R	2a, 2b, 4a	Cu ₂ O, Cu ₂ (CO ₃)(OH) ₂ , PbCu ₂ O ₂ , PbO	Cu, Ag
40	Group 1	R	1a, 1c, 2a, 2b, 4a	PbCu ₂ O ₂ , PbO, PbO ₂ , Ca(SnZr)O ₃	Cu, Ag
41	Group 1	M	Apatite 1c, 2b, 4a, 4b	PbO, PbO ₂	
42	Group 1	M	1c, 2a, 4a	Cu ₂ O, PbO, PbO ₂	Cu, Ag
CG1	Group 1	M	4a	Cu ₂ O, PbO, PbO ₂	Cu
CG2	Group 1	M	1c, 2a, 4a	PbO, PbO ₂	Cu
CG3	Group 1	M	1c, 2a, 3a, 4a	PbO, PbO ₂	Cu

One of the most abundant crystalline phase was a calcium phosphate silicate often heavily impregnated with PbO. Four major compositions were observed close to the following:

Ia – $\text{Ca}_{12}\text{PKSi}_6\text{O}_{27}$ – tiny (<15 most around 5 micron) globular mid to dark grey grains often in large concentrations, sometimes forming circular concentrations up to 80 microns in diameter (Fig 7 and 8).

Ib – $\text{Ca}_8\text{P}_2\text{Si}_2\text{O}_{17}$ – tiny (<15 micron) globular dark grey grains (Fig 9).

Ic – Silicocarnotite $\text{Ca}_5\text{P}_2\text{SiO}_{12}$ – small (up to 300 micron) angular elongated, euhedral (sometimes more anhedral) shaped black grains usually in small spread out concentrations and sometimes in larger concentrations (Fig 10 to 12)

Id – $\text{Ca}_4\text{PSi}_6\text{Pb}_{10}\text{CuO}_{29}$ – Similar to Ia but with varying proportions of Pb and Cu.

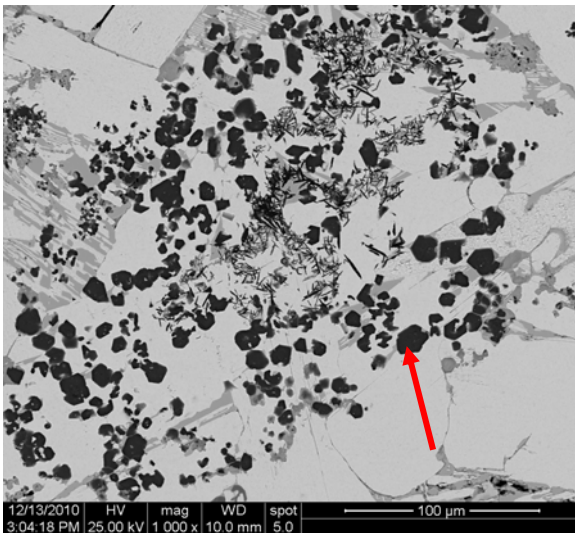


Fig 7. Crystalline phase Ia in lith06.

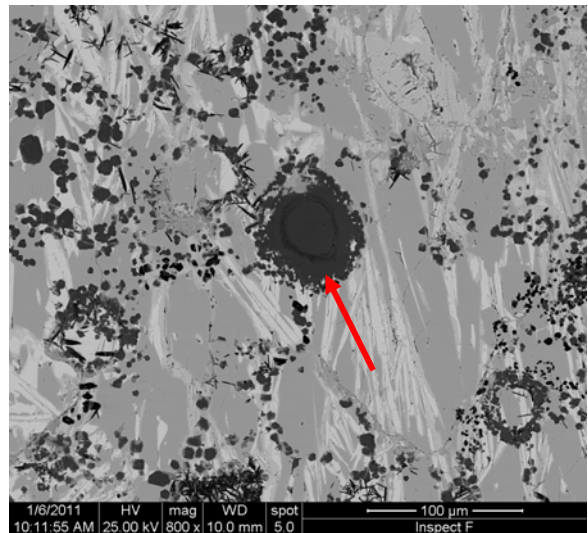


Fig 8. Crystalline phase Ia in lith40.

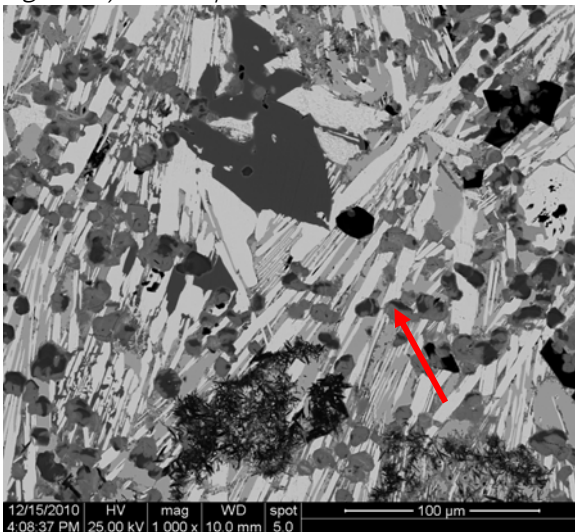


Fig 9. Crystalline phase Ib in lith19.

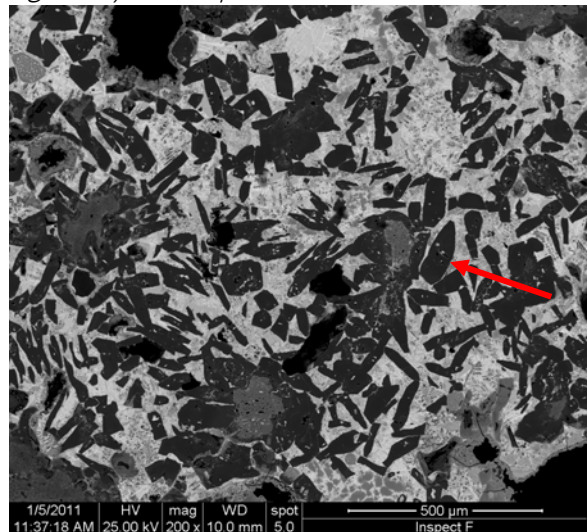


Fig 10. Crystalline phase Ic in lith38.



Fig 11. Crystalline phase 1c in lith41.

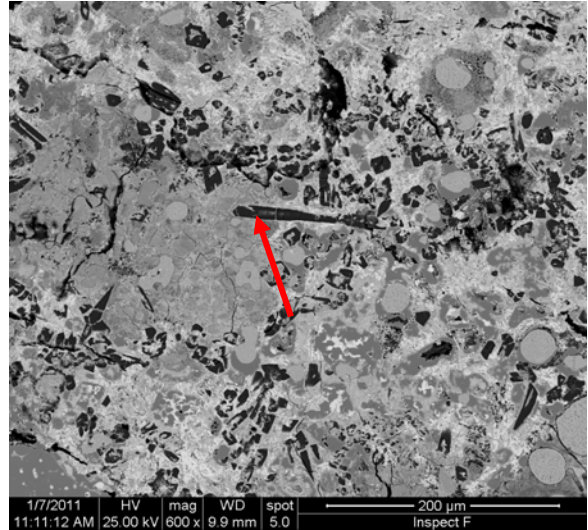


Fig 12. Crystalline phase 1c in lith42.

There were also some calcium magnesium silicates. Four major compositions were apparent:

2a – Monticellite $\text{Ca}(\text{Mg,Fe})[\text{SiO}_4]$ – small (10 to 50 micron most around 10 to 30 micron) angular sometimes hexagonal dark grey grains, often in sparse and open concentrations (Figs 13 to 15).

2b – Merwinite $\text{Ca}_3\text{Mg}[\text{SiO}_4]_2$ – tiny (<7 micron) globular dark grey grains, often in concentrations and usually as tight concentrations of tiny needle like grains, sometimes these needles can reach up to 20 microns in length (Figs 16 and 17).

2c – Akermanite $\text{Ca}_2[\text{MgSi}_2\text{O}_7]$ – small very elongated (up to 60 micron in length) rectangular dark grey grains, often in some concentrations, some very rectangular (10 to 20 micron) black grains (Figs 18 and 19).

2d – $\text{CaMg}_2\text{SiO}_5$ – small (up to 25 micron) globular elongated dark grey grains in large concentrations (Fig 20).

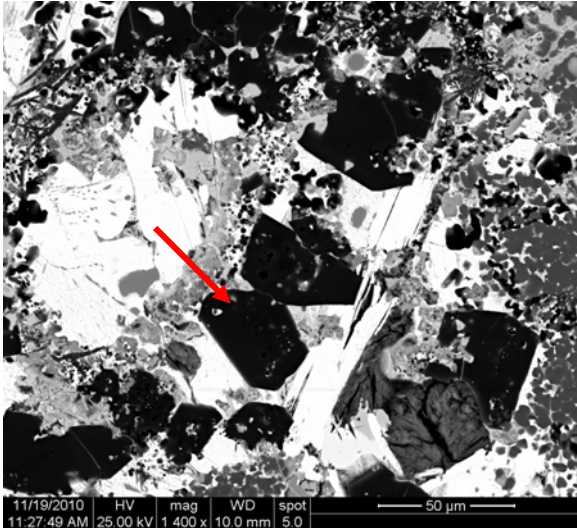


Fig 13. Crystalline phase 2a in lith10.

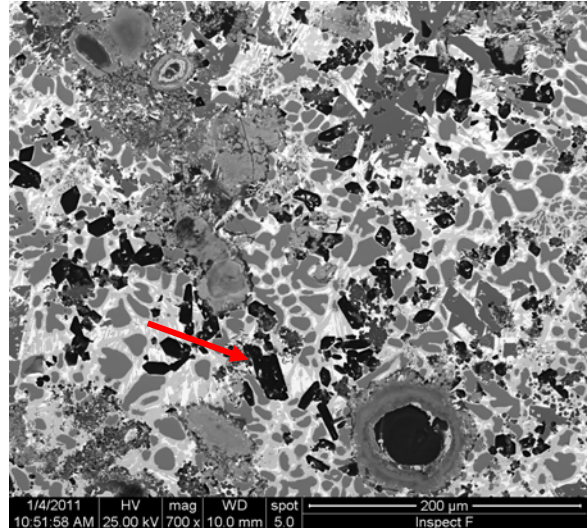


Fig 14. Crystalline phase 2a in lith36.

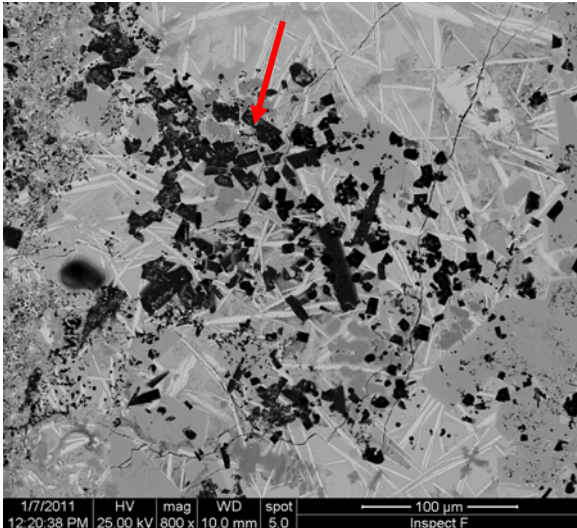


Fig 15. Crystalline phase 2a in lith42.

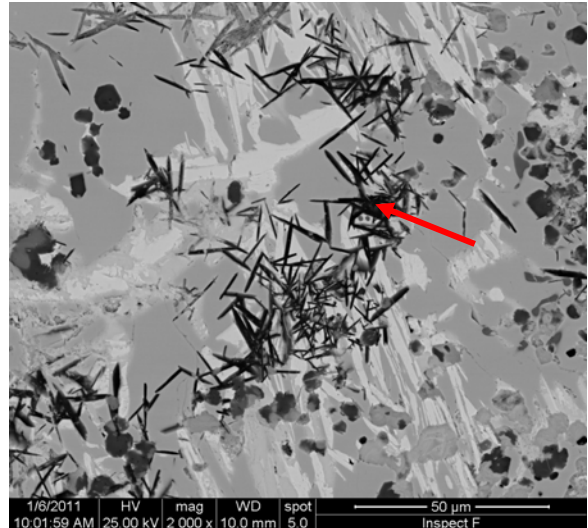


Fig 16. Crystalline phase 2b in lith40.

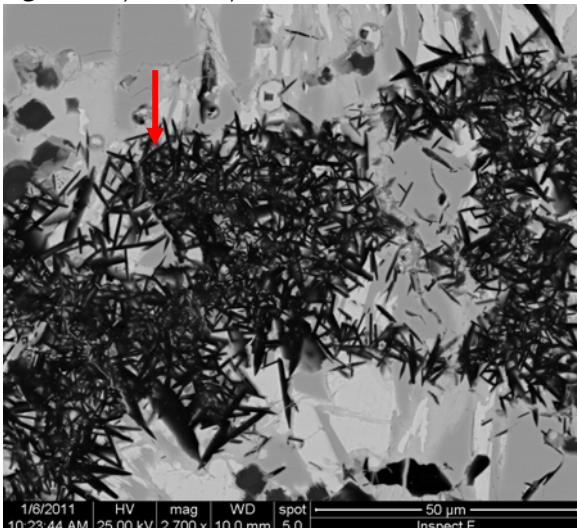


Fig 17. Crystalline phase 2b in lith40.

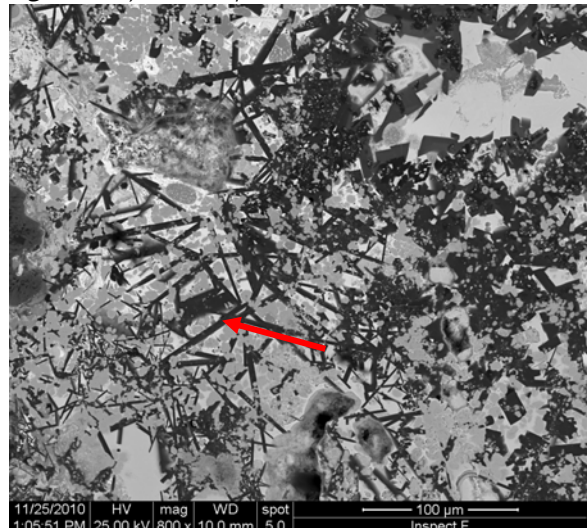


Fig 18. Crystalline phase 2c in lith13.

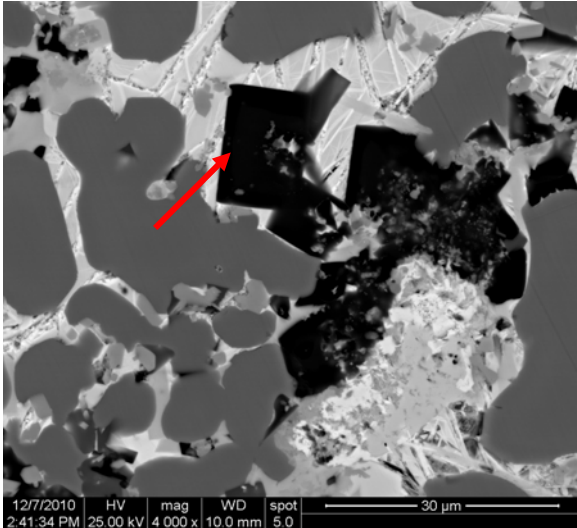


Fig 19. Crystalline phase 2c in lith24.

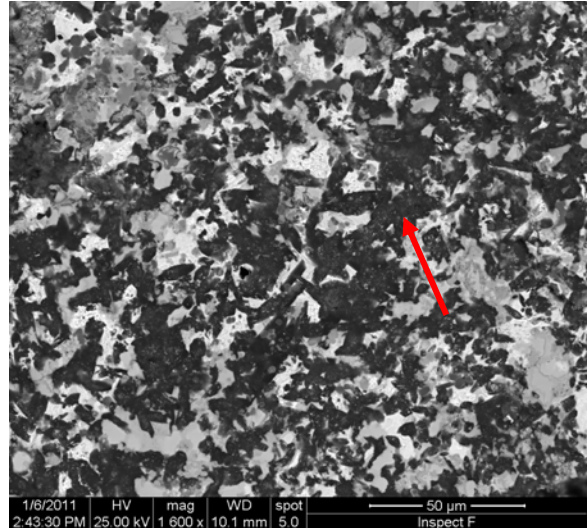


Fig 20. Crystalline phase 2d in lith41.

Another common group of crystalline phases were calcium aluminium silicates. These had three major compositions:

3a – Gehlenite $\text{Ca}_2\text{Al}_2\text{SiO}_7$ – small (up to 25 micron but mainly <10 micron) elongated angular black grains, most often in concentrations of tiny needles (<10 microns), sometimes forming larger ring like structures (Figs 21 to 23).

3b – $\text{Ca}_4\text{Al}_2\text{Si}_2\text{Sn}_2\text{O}_{15}$ – small (10 to 20 micron) square mid grey grains in circular concentrations. Only present in lith24 (Figs 24 and 25).

3c – $\text{Ca}_{10}\text{Al}_{10}\text{SiO}_{27}$ – small (about 15 micron) almost circular dark grains (Fig 26).

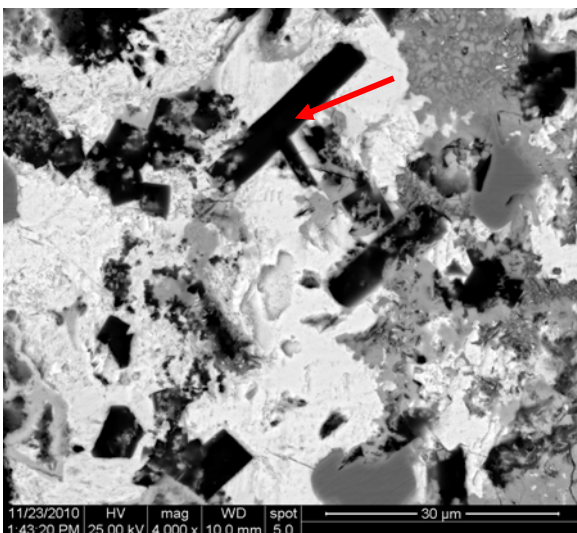


Fig 21. Crystalline phase 3a in lith12.

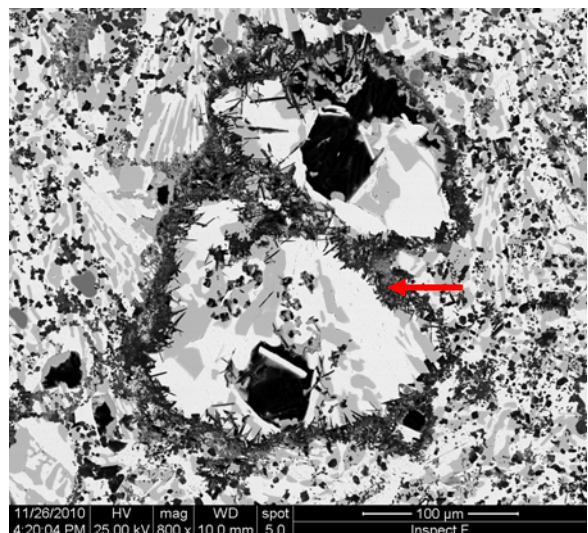


Fig 22. Crystalline phase 3a in lith20.

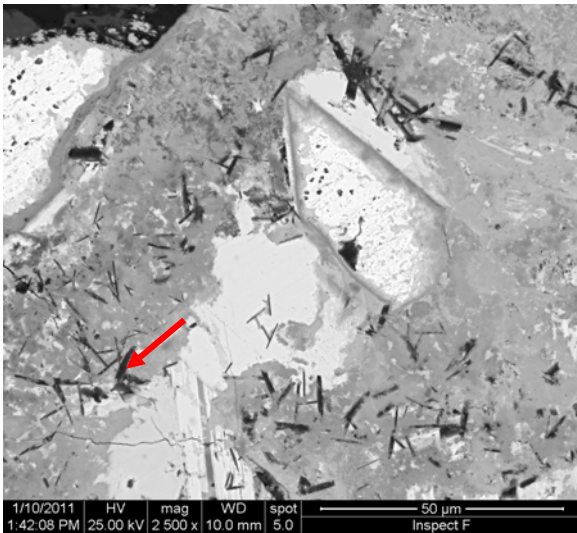


Fig 23. Crystalline phase 3a in CG3.

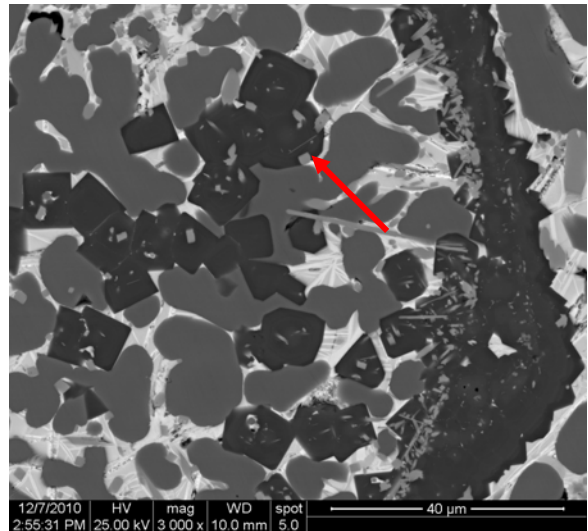


Fig 24. Crystalline phase 3b in lith24.

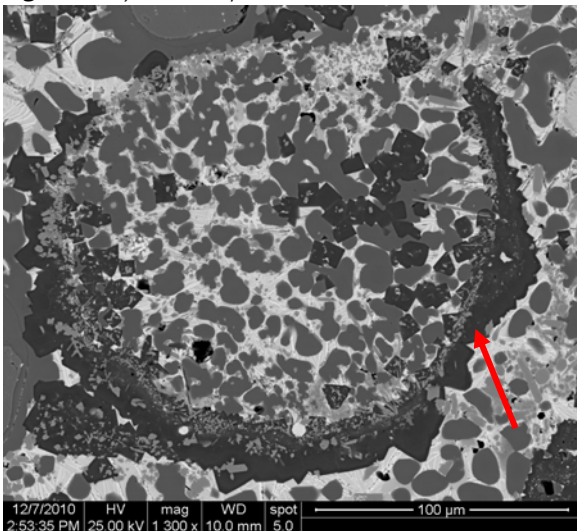


Fig 25. Crystalline phase 3b in lith24.

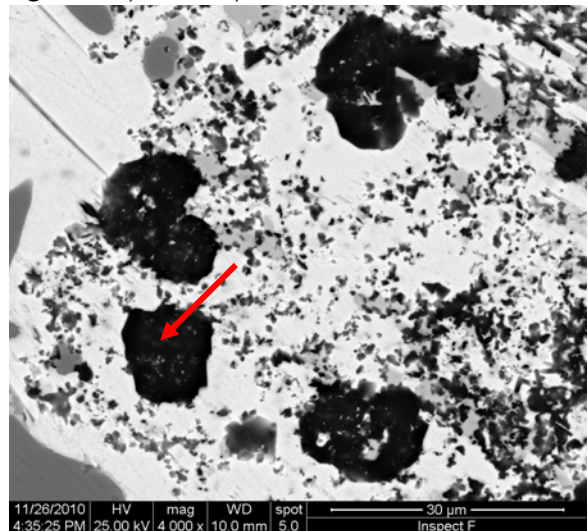


Fig 26. Crystalline phase 3c in lith20.

The crystalline phases also included (sodium) potassium aluminium silicates. Two major compositions were apparent:

4a – Kalsilite $K[AlSiO_4]$ – tiny (<10 micron) angular to sub-angular black grains, often very concentrated making up larger grains (Figs 27 to 32).

4b – Nepheline $Na_3(Na,K)[Al_4Si_4O_{16}]$ – small (10 to 40 micron but mainly 15 to 25 micron) very angular sometime rectangular black grains (Figs 33 and 34).

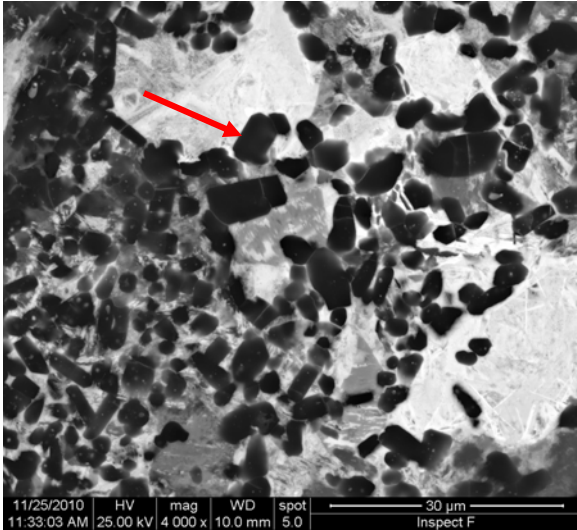


Fig 27. Crystalline phase 4a in lith13.

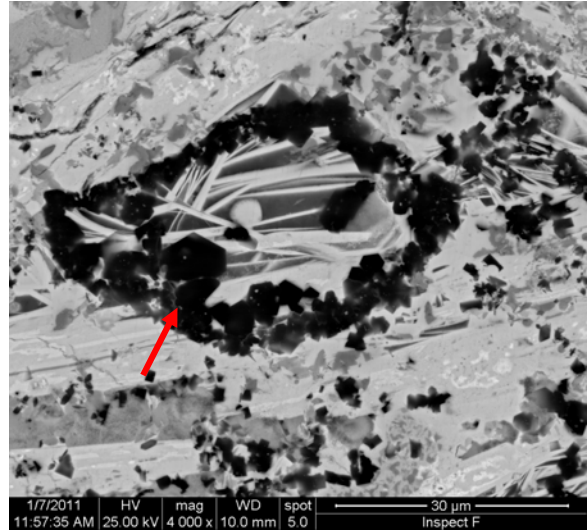


Fig 28. Crystalline phase 4a in lith42.

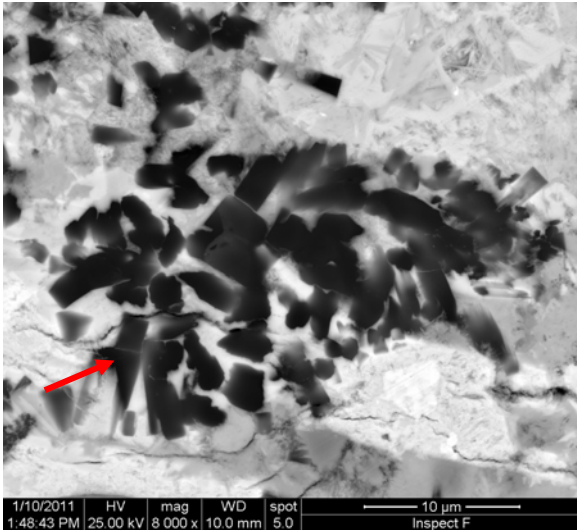


Fig 29. Crystalline phase 4a in CG3.

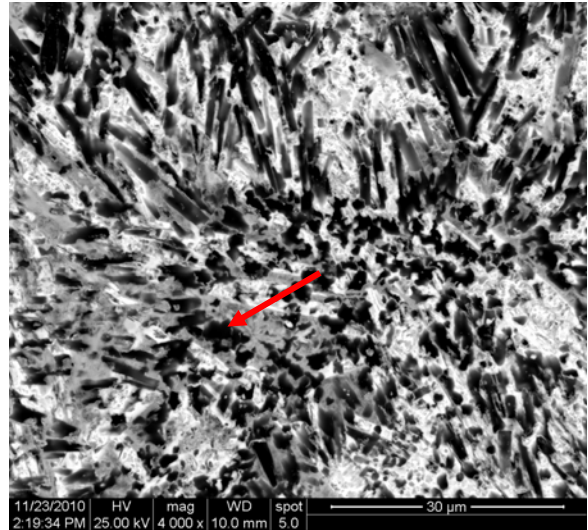


Fig 30. Crystalline phase 4a in lith12.

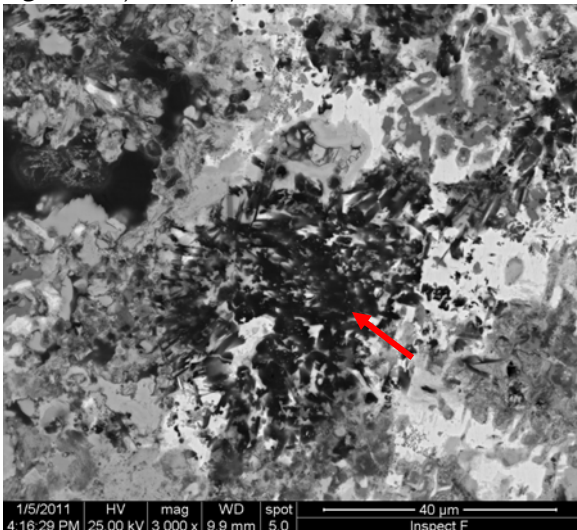


Fig 31. Crystalline phase 4a in lith39.

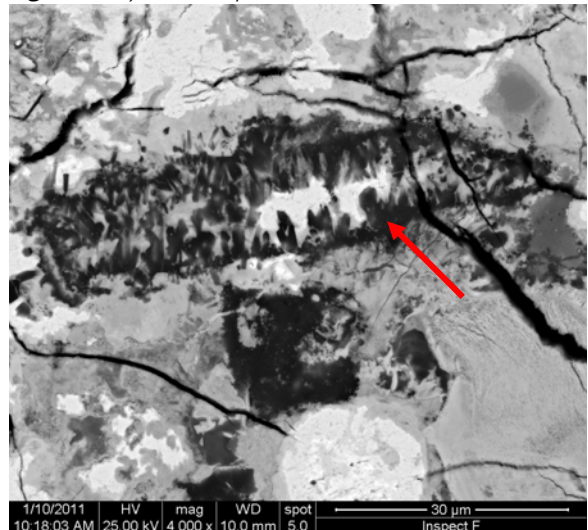


Fig 32. Crystalline phase 4a in CG2.

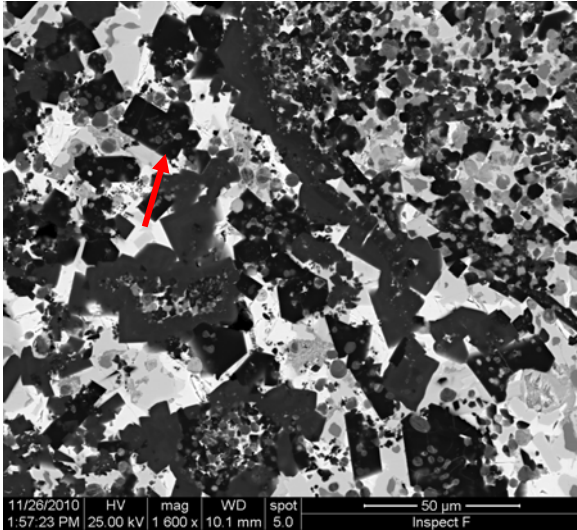


Fig 33. Crystalline phase 4b in lith18.

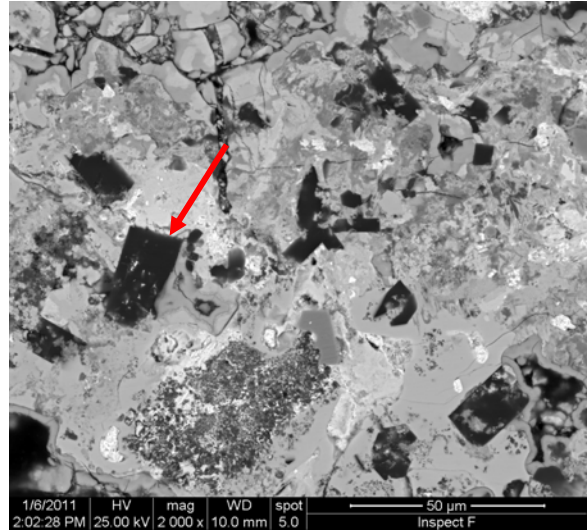


Fig 34. Crystalline phase 4b in lith41.

The majority of the samples were composed of lead oxide (occasionally metallic lead but sparse). The lead oxide took two different forms. Litharge (PbO – although XRD analyses proved that both litharge and massicot were present) mostly occurred as well formed white laths but could also be amorphous (Figs 35 and 36). The other was lead dioxide (PbO_2 – also sometimes as cerussite PbCO_3), slightly darker in colour and not as clearly defined, often surrounding areas of litharge or concentrated around larger holes and natural edges. The matrix in-between these laths and areas of pure lead oxides were made of two major phases. When clear litharge laths were present the matrix was mainly copper lead oxide (PbCu_2O_2 lead oxocuprate – Figs 35 and 36). Some of the surviving top edges of the litharge cakes were comprised of these well formed litharge laths bounded by PbCu_2O_2 . This was usually present in a well defined layer or crust not more than a few mm thick (Figs 37 and 38).

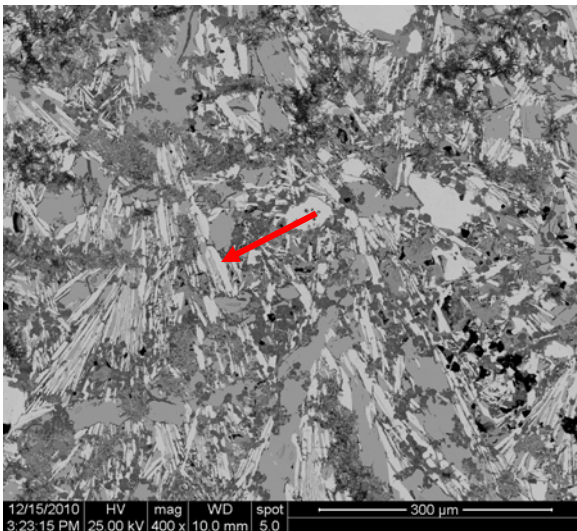


Fig 35. White PbO laths (red arrow) and PbCu_2O_2 matrix in lith19.

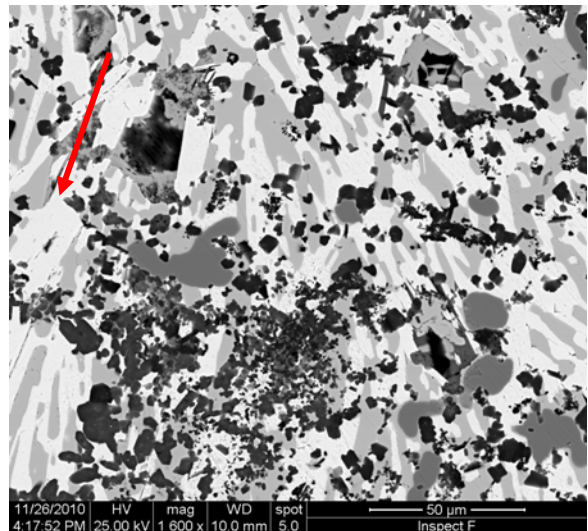


Fig 36. White PbO laths (red arrow) and PbCu_2O_2 matrix in lith20.

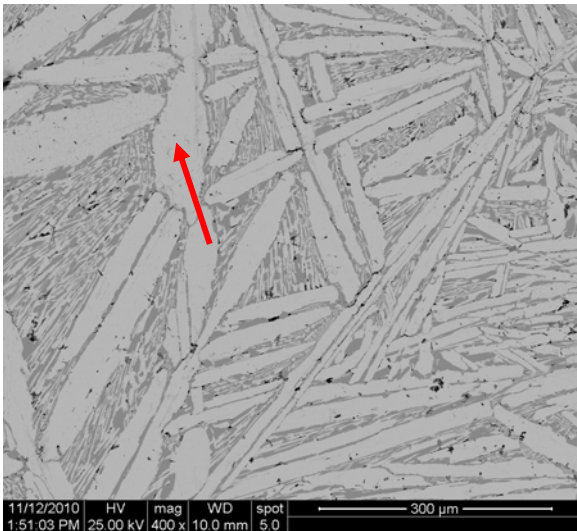


Fig 37. White PbO laths (red arrow) and PbCu₂O₂ matrix on top edge of lith03.

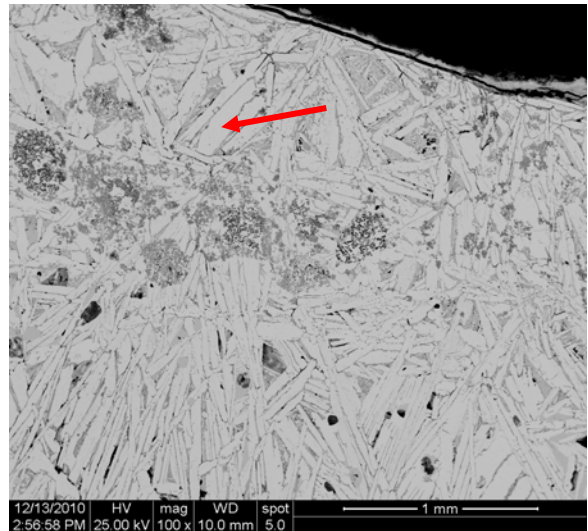


Fig 38. White PbO laths (red arrow) and PbCu₂O₂ matrix on top edge of lith06.

Not all samples displayed such clear microstructures and many were quite complex. In these cases the matrix was dominated by different shades of light to mid grey litharge containing varying proportions of Ca, Si and P (Figs 39 to 42). These lead solutions (which may also be corrosion) were present in most samples and when the sample orientations were known it was noticeable that the solutions were concentrated towards the bottom. In other cases some samples (eg lith I I) were entirely composed of this solution. It may also not be surprising that areas close to Si rich grains (quartz — SiO₄) contained stronger concentrations of Si. For example, there tended to be greater Si contents in the litharge nearer the bottom of certain samples. This is presumably due to the fact that it was in proximity to the clay hearth. Similarly, areas close to pure Ca areas (CaCO₃) were richer in Ca.

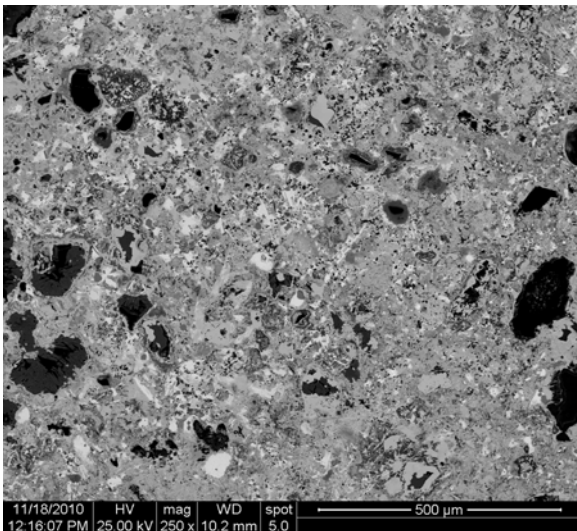


Fig 39. More complex PbO matrix in lith08.

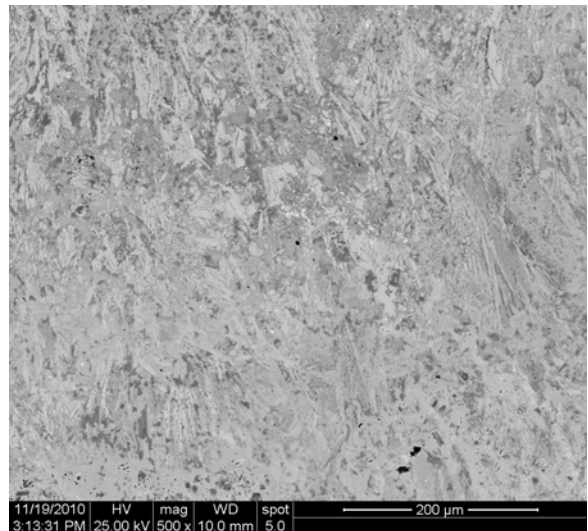


Fig 40. More complex PbO matrix in lith I I.

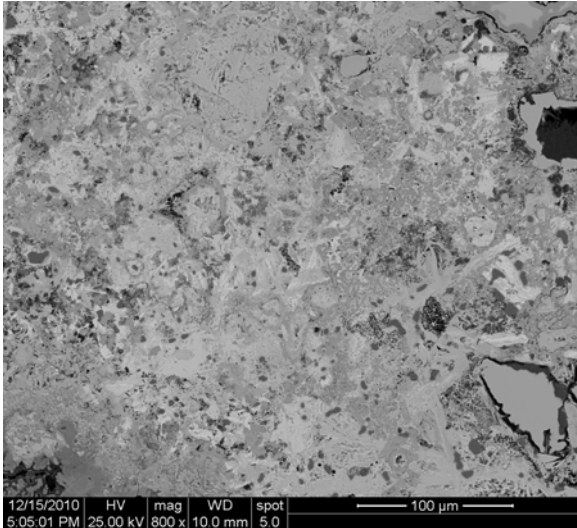


Fig 41. More complex PbO matrix (perhaps corrosion) on bottom of lith 19.

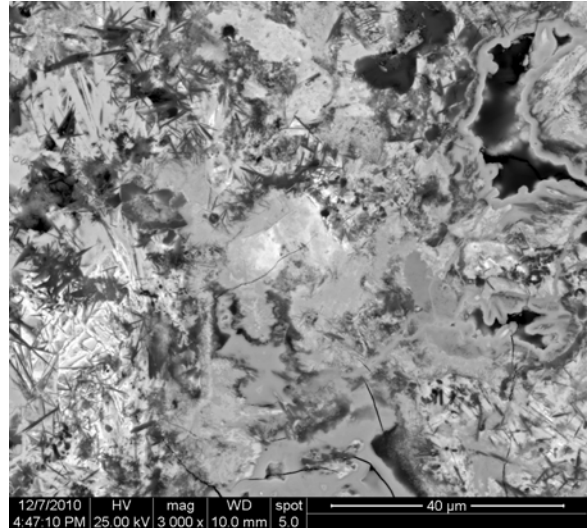


Fig 42. More complex PbO matrix (perhaps corrosion) in lith 25.

Another abundant phase was copper. This was mainly present in a metallic state forming well rounded globular prills of varying sizes (10 to 200 microns — Fig 43). Samples had varying proportions of copper with some almost fully covered in it while others had only a few tiny prills. When the metallic copper was present in larger quantities it tended to form in networks of globular, almost dendritic prills (up to several cm in size — Fig 44). Most samples also had copper oxides present in two oxidation states. The most common was cuprous oxide (Cu_2O) which tended to concentrate around metallic prills (Fig 45) and was more rarely present as free globules or amorphous patches spread around the samples. In some cases the Cu_2O also precipitated within PbO areas forming eutectics in-between PbO laths (Fig 46). It was noticed when the majority of sample depth was available that there were greater concentrations of copper (metallic and oxide) in the top and middle parts of the samples. Malachite ($\text{Cu}_2(\text{CO}_3)(\text{OH})_2$) was also present in some samples but in smaller quantities, tending to concentrate near the natural edges or around larger porosity (Figs 47 and 48). This would indicate that it is a corrosion product – most likely a post-depositional phenomenon.



Fig 43. Metallic copper prills in lith36.

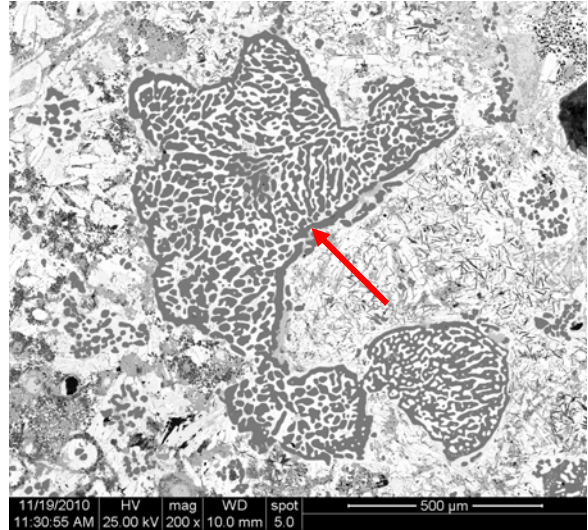


Fig 44. Metallic copper prill network in lith 10.

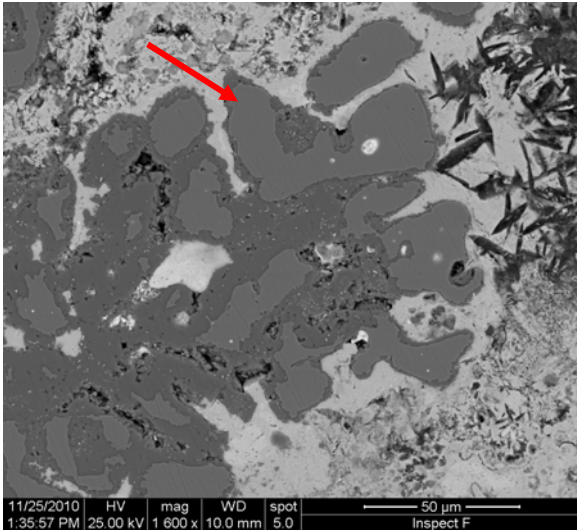


Fig 45. Metallic prills (red arrow) surrounded by Cu_2O (dark grey) in lith 13.

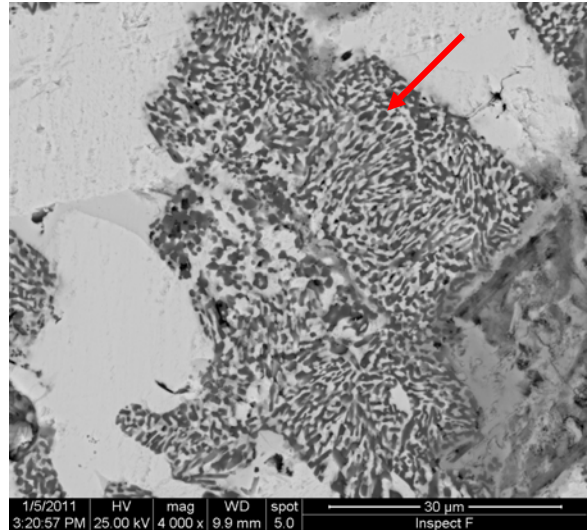


Fig 46. Cu_2O and PbO eutectic in lith39.

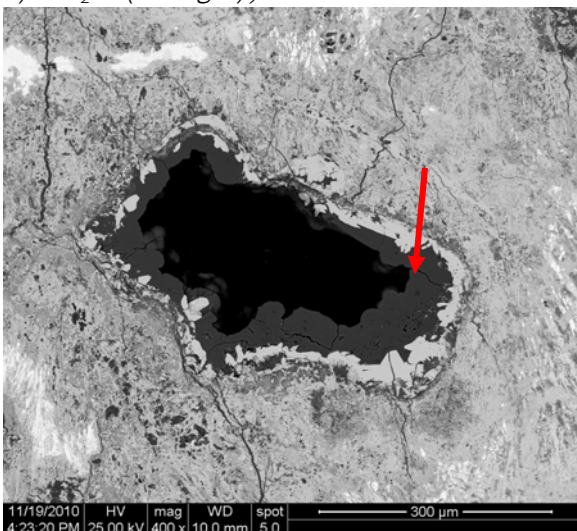


Fig 47. Malachite around pore in lith 11.

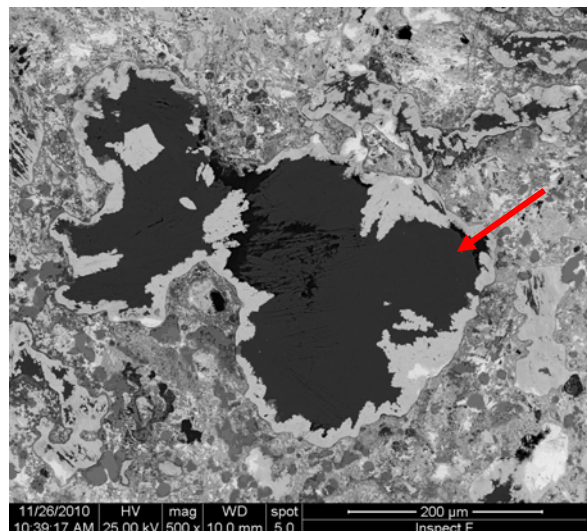


Fig 48. Malachite filling pore in lith 15.

Group 2

The bone ash litharge (group 2) was very distinctive and comprised 16 of the litharge fragments in the assemblage: one from Wolvesey Palace, one from Saltergate, one from Driffild Terrace, 10 from Flaxengate, one from Swan Lane and two from Dunkirt Barn. These were characterised by large apatite grain [hydroxylapatite — $\text{Ca}_5(\text{PO}_4)_3(\text{OH})$] inclusions dominating the majority of the structure (Figs 49 and 50). These ranged in size from 20 to 2200 microns, averaging around 100 to 500 microns. The apatite grains were at different stages of breaking down with some heavily impregnated with PbO (Fig 51) while others remained relatively pure and whole. Those more severely PbO impregnated appeared to break down and precipitate into tiny Ca-P -rich (sometimes with Si) grains (Fig 52).

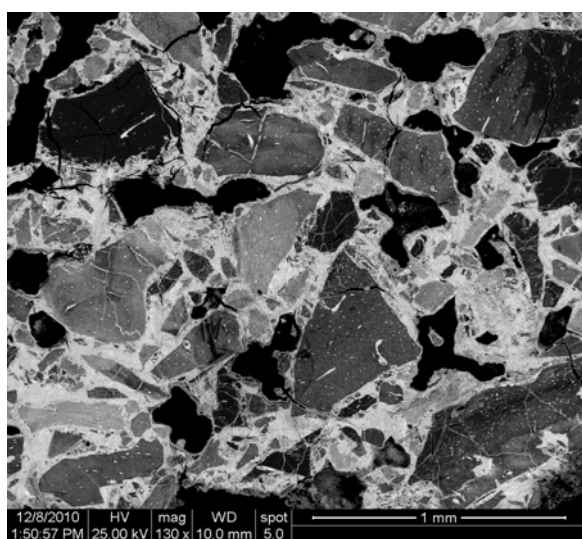


Fig 49. Large apatite grains in lith27.

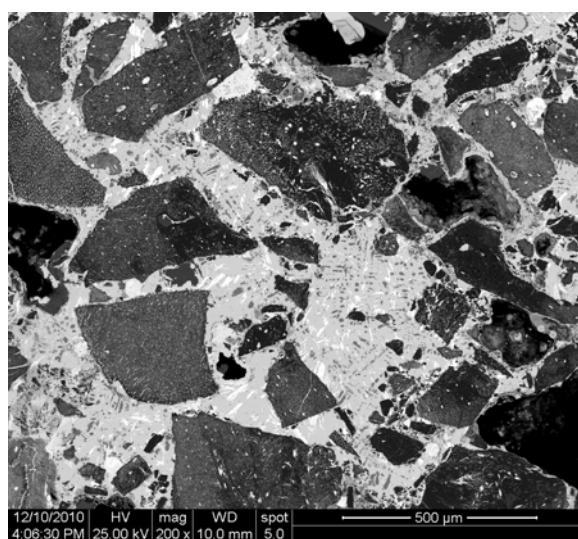


Fig 50. Large apatite grains in lith34.



Fig 51. Apatite grain breaking down in lith21.

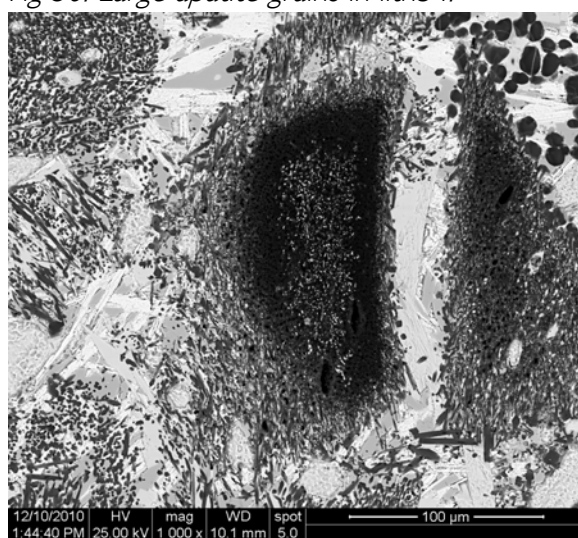


Fig 52. Apatite grain breaking down in lith33.

It was also noticeable that the samples were reasonably pure without any other distinct crystalline mineral phases. A few (in particular lith37 and lith38) did contain some calcium

phosphate silicates mainly in the form of crystalline structure 1c (discussed above). These have very low Si contents (about 10wt%) which suggests that they were formed due to either minor additions of Si-rich clay marl or even a reaction with the underlying clay lining as opposed to any large additions of Si-rich material. Two bone ash samples (lith01 and lith38) also contained tiny amounts of monticellite (2a — $\text{Ca}(\text{Mg,Fe})[\text{SiO}_4]$) and one sample some nepheline (4b — $\text{Na}_3(\text{Na,K})[\text{Al}_4\text{Si}_4\text{O}_{16}]$) which could have formed due to the addition of small amounts of vegetable ash. Another possibility is the contribution from the fuel (charcoal) ash during firing. Indeed charcoal was identified on the edges of certain litharge samples. It is therefore conceivable that there was some (if only small) contamination from the fuel used. The lack of any other major crystalline mineral phase in these samples would suggest that the hearth linings originally consisted of pure bone ash.

In the bone ash samples the matrix (in between the apatite grains) was mainly composed of PbO (litharge and massicot) and PbO_2 (lead dioxide). The litharge often appeared as white laths or amorphous areas while the lead dioxide appeared as a light grey often surrounding areas of litharge or around holes and edges. In some cases lead oxocuprate (PbCu_2O_2) was present filling the areas in between the litharge laths (Figs 53 and 54). Like group 1 some samples had lead oxide solutions and corrosion containing varying proportions of Ca, Si and P (Figs 55 and 56). However, these tended to be mainly (if not wholly) Ca- and P-rich especially around large apatite grains in the process of breaking down. Copper was present mainly in metallic form, often forming networks of well rounded globular prills (Fig 57). These varied greatly in size and quantity from sample to sample with greater concentrations in the top and middle parts of the samples. The copper also took an oxidised form (Cu_2O) mainly concentrating around the metallic copper but in some cases forming as globular grains similar in size and shape to the metallic prills (Figs 58 and 59). In some instances like lith23 the majority of the matrix was composed of Cu_2O . Malachite ($\text{Cu}_2(\text{CO}_3)(\text{OH})_2$) was also present concentrating near the natural edges or larger porosity (Fig 60).

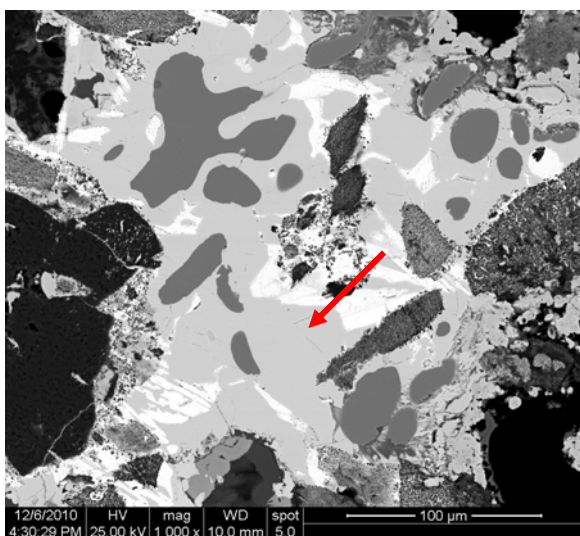


Fig 53. White PbO amorphous areas and PbCu_2O_2 matrix (red arrow) in lith22.

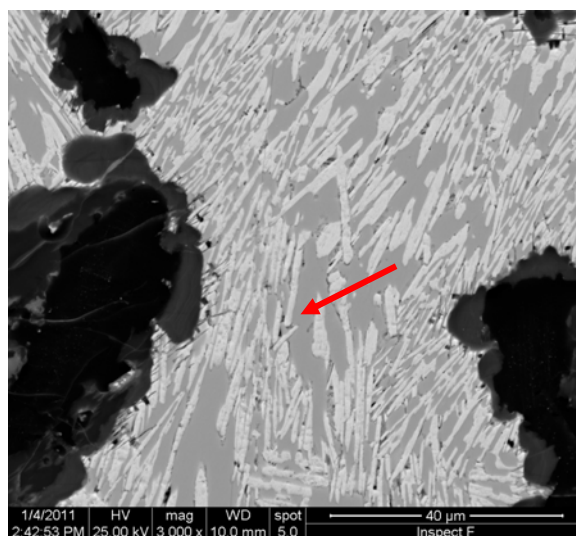


Fig 54. White PbO laths and PbCu_2O_2 matrix (red arrow) in lith37.

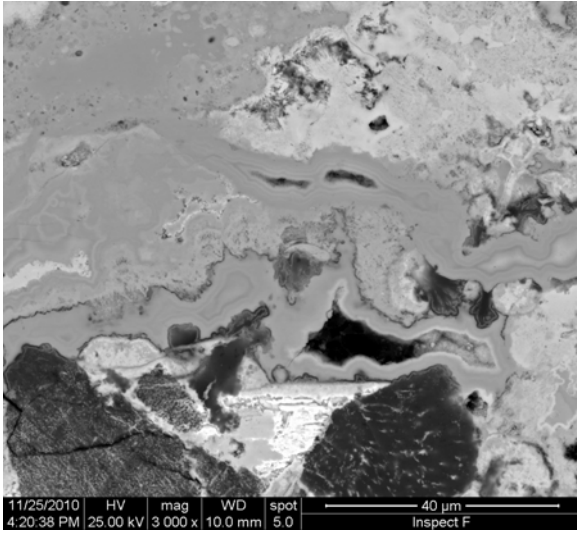


Fig 55. PbO , CaO and P_2O_5 matrix in lith14.

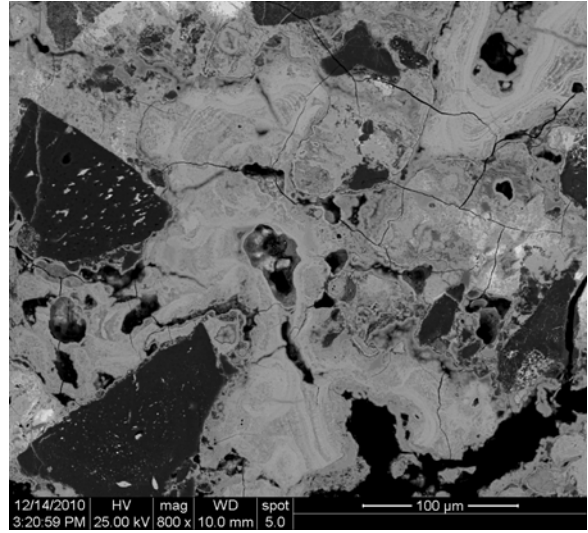


Fig 56. PbO , CaO and P_2O_5 matrix in lith16.

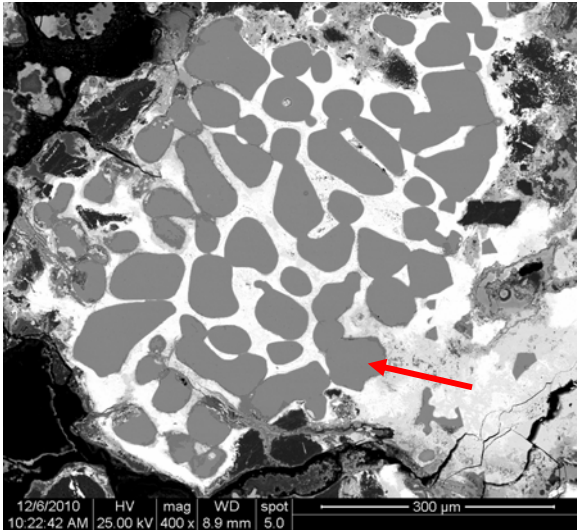


Fig 57. Metallic copper prills in lith21.

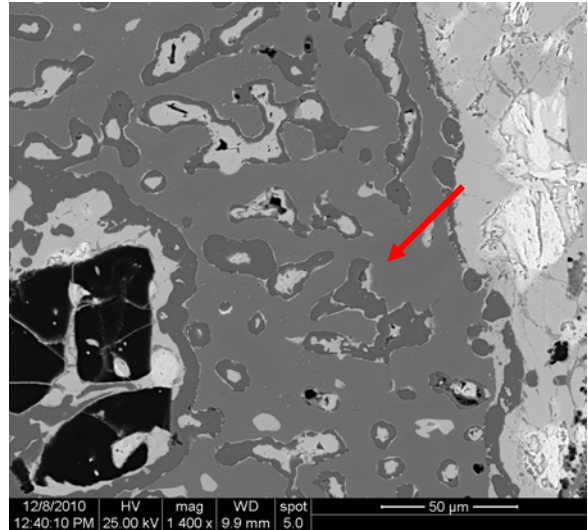


Fig 58. Copper network and Cu_2O in lith27.

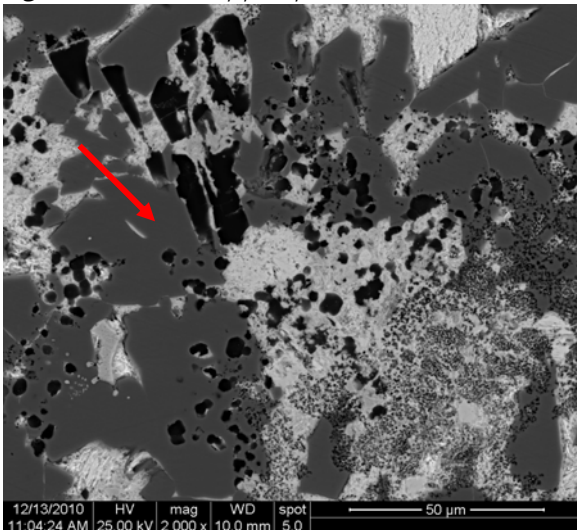


Fig 59. Cu_2O grains in lith35.

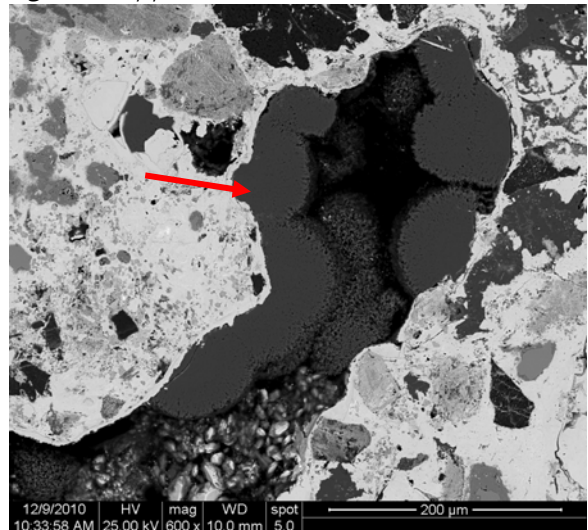


Fig 60. Malachite around hole in lith29.

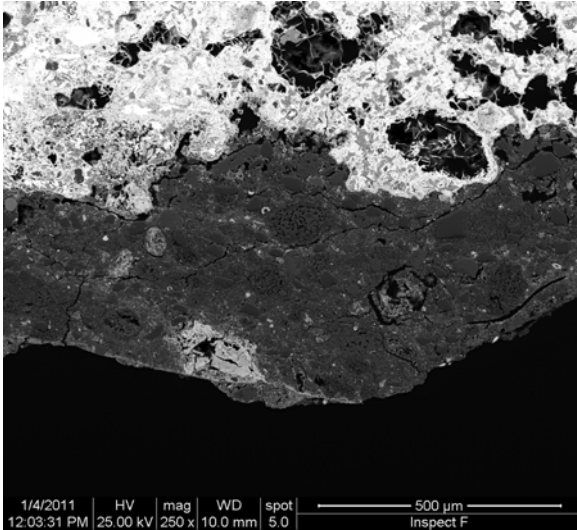


Fig 61. Quartz/feldspar grains in Ca rich matrix on bottom of lith36.

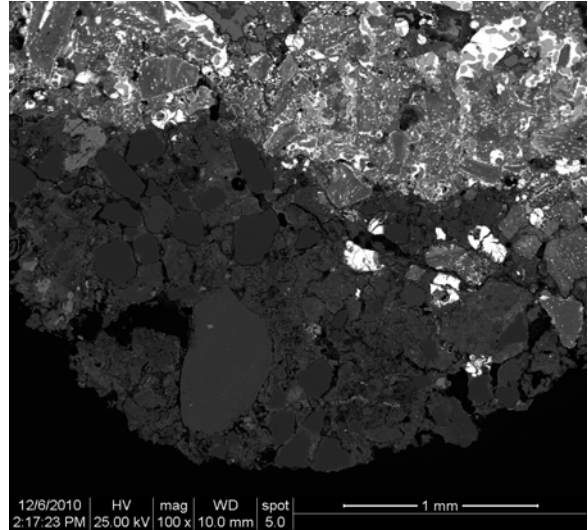


Fig 62. Quartz/feldspar grains in Ca rich matrix on bottom of lith21.

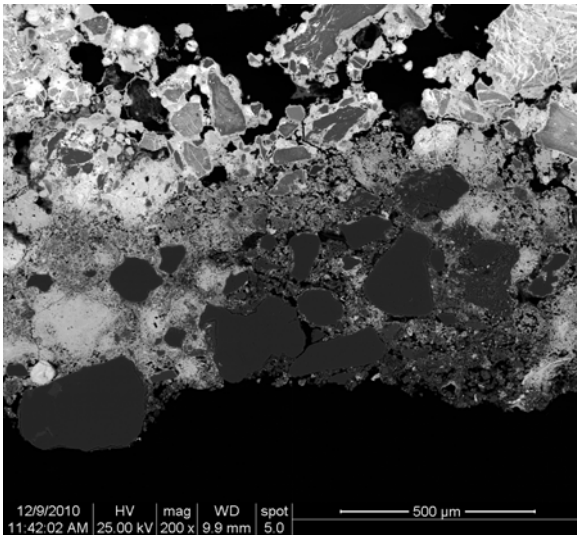


Fig 63. Quartz/feldspar grains in Ca rich matrix on bottom of lith29.

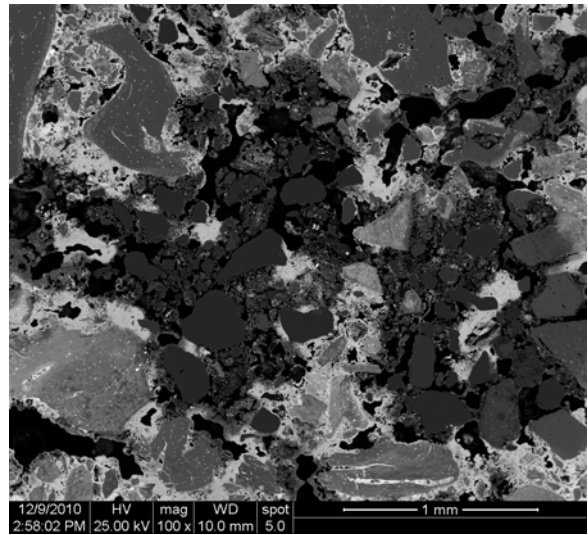


Fig 64. Quartz/feldspar grains in Ca rich matrix in lith31.

The majority of the samples in group 1 and some of group 2 had some quartz (SiO_2) and feldspar (KAlSi_3O_8). These were mainly present on the edges (Figs 61 and 62) and in some cases must have been adhering soil as the fragments were not cleaned prior to sampling. However, it was apparent that the quartz and feldspar crystals in some samples had reacted with the PbO (Figs 63 and 64). This suggests that they were perhaps part of the original hearth lining composition or that they were part of the clay hearth. The matrix found in-between the quartz was often Ca-rich so it is possible that some of these residues are non-impregnated clay marl. In some rare cases there were crystalline CaCO_3 fragments – most likely chalk (Figs 65 and 66). These are very few but did occur, for example in lith41. Calcium carbonate in solution was more common (CaCO_3 – Figs 67 and 68). These were dark areas mainly found close to edges or bordering/filling larger holes and cavities. Due to the Ca-rich nature of the hearth lining material this secondary calcite is probably *partly allochthonous* (Cau Ontiveros *et al* 2002). The Ca in the hearth

lining would almost certainly have calcinated when heated (above 825°C) producing CaO (quicklime) but due to the unstable nature of quicklime it would have reacted with CO₂ (re-carbonation) on cooling reverting back to CaCO₃.

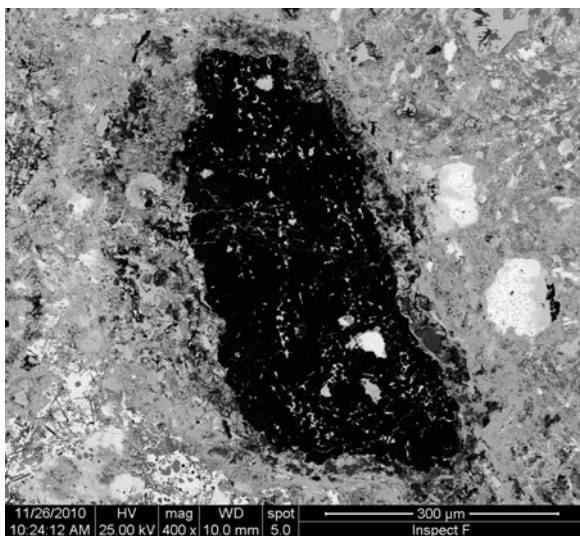


Fig 65. A CaCO₃ grain in lith15.

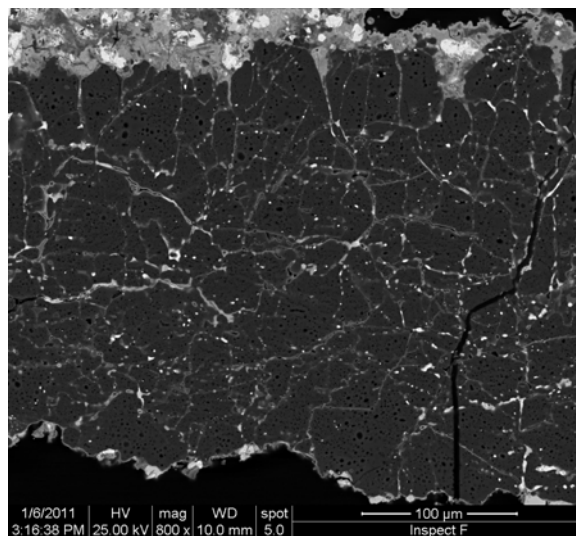


Fig 66. A CaCO₃ grain in lith41.

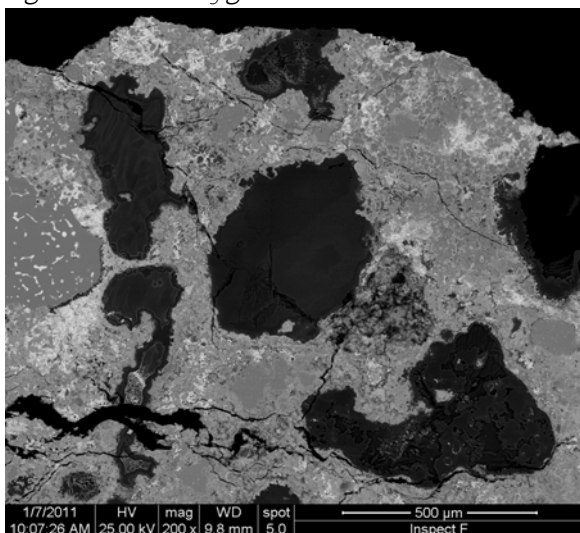


Fig 67. CaCO₃ areas in lith42.

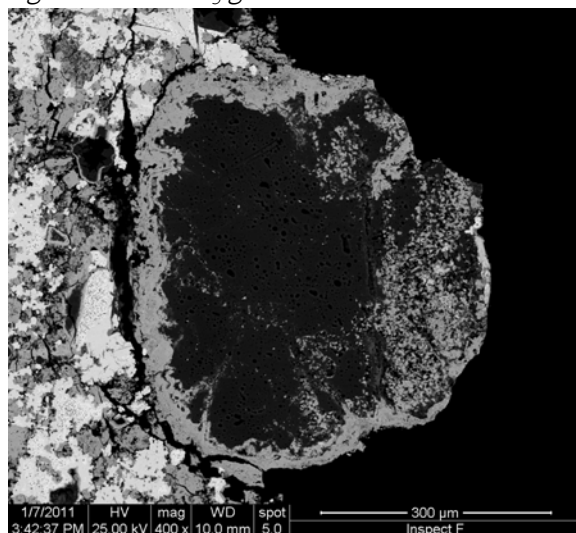


Fig 68. A CaCO₃ area in CGI.

Tin was found in six samples and present in three major oxides: lith24 contained tin dioxide (cassiterite – SnO₂); lith10, lith16, lith33 and lith40 all had a perovskite compound (Ca(SnZr)O₃); lith33 had lead ortho-stannate (Pb₂SnO₄) and lith26 had a Cu-Sn oxide mixture. The tin dioxide crystals are small (20 to 60 micron) elongated and needle like (Fig 69). The perovskite compound grains are 5 to 50 microns in size and square to rectangular in shape (Figs 70 and 71). The lead ortho-stannate crystals are mainly square/rectangular, up to 50 micron in size but differ from the perovskite compound by being lighter in colour (Fig 72). These oxides tend to concentrate nearer the top and sometimes centre of the samples. Lith26 differs from the others as the tin does not form any clear crystalline structure but seems to be mixed in a copper solution. While the tin

oxide in the other samples may be residues of small amounts of metallic tin in the metal refined, lith26 was probably a bronze.

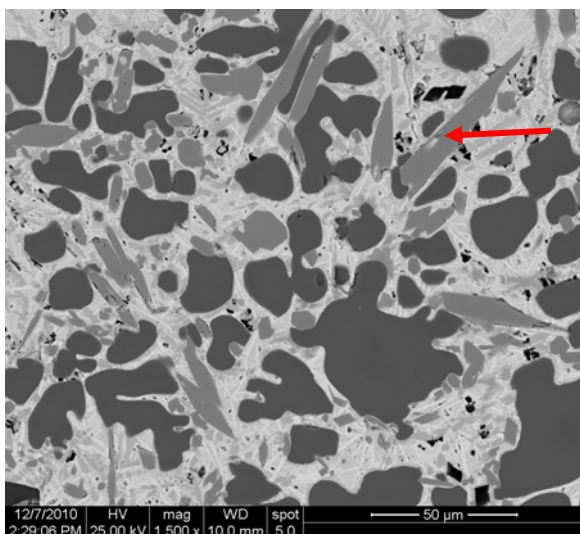


Fig 69. SnO_2 in lith24.

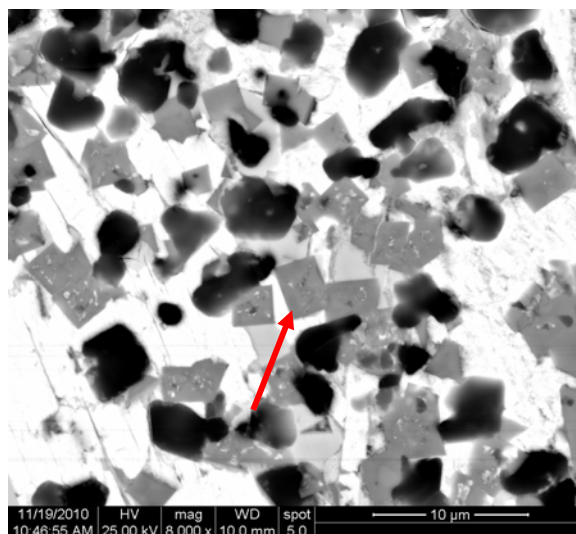


Fig 70. $\text{Ca}(\text{SnZr})\text{O}_3$ in lith10.

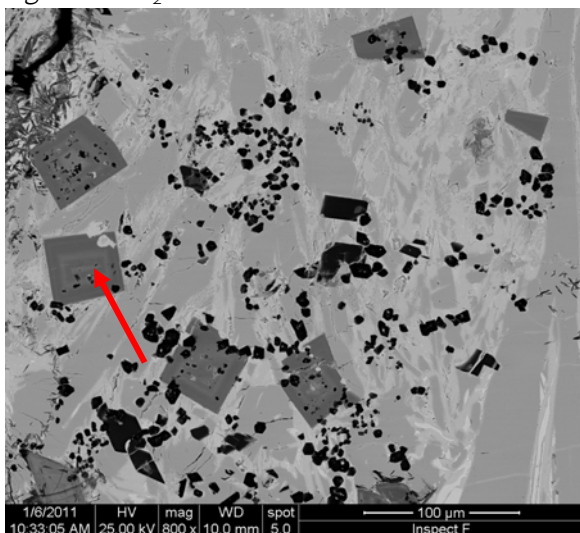


Fig 71. $\text{Ca}(\text{SnZr})\text{O}_3$ in lith40.

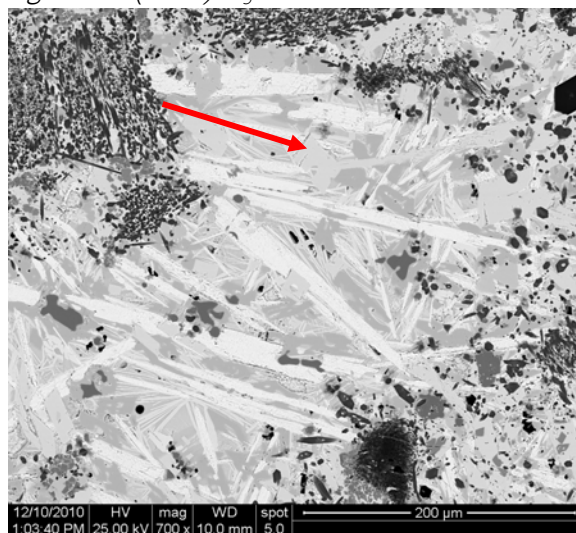


Fig 72. Pb_2SnO_4 in lith33.

Many of the samples in the assemblage contained Ag (Table 2). The majority of the silver was present in solid solutions within the metallic Cu prills which contained as much as ~6wt% (Ag is soluble in Cu up to 9wt% at 780°C) and in the cuprous oxide (Cu_2O) containing as much as ~4wt%. However, some of the samples contained visible Ag metallic prills. These prills, mostly circular in shape and ranging from 5 to 300 micron in size, were often in proximity or bound by Cu metal (Figs 73 and 74). Some metallic prills formed close to the Cu-Ag eutectic – 28wt% Cu and 72wt% Ag (Figs 75 and 76). The varying compositions of Ag and Cu alloys present in the litharge reflect the increase of either Cu or Ag on either side of the eutectic. For example, the increased Ag in Fig 74 resulted in the creation of mostly Ag-rich prills with some Cu. The Ag and Cu would have separated on cooling and solidified below 780°C. It was also noticed that the metallic Ag (especially well rounded prills) tended to concentrate close to the top edge of the

samples. It is possible that some of the prills infiltrated the lining in cracks or porosity explaining their presence close to the upper surface. One sample (lith33) contained two metallic Au prills around 40 micron in size. There was also one Au prill (250 micron wide) heavily mixed with copper. The Au seemed to concentrate towards the edges of the prill forming tiny droplets. This may be evidence of Au dissolved in copper but in the process of separating during cooling.

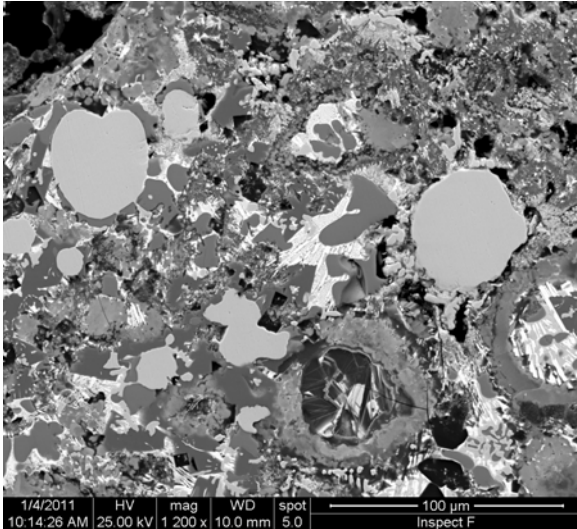


Fig 73. Circular Ag prills in lith36.

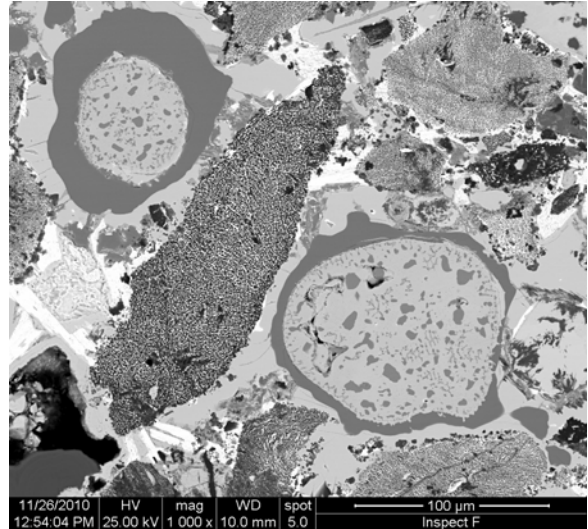


Fig 74. Circular Ag prills in lith18.

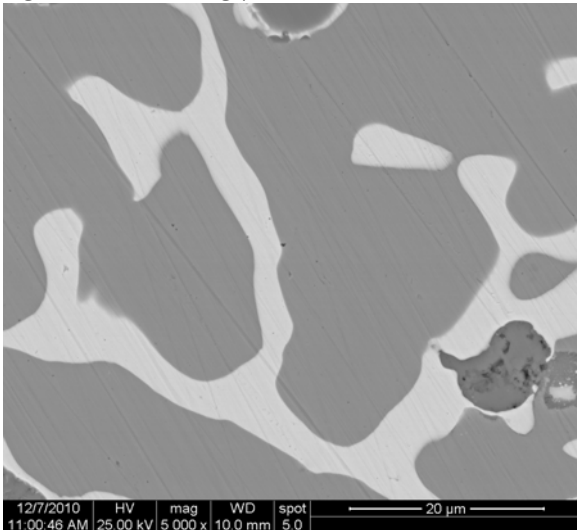


Fig 75. Ag-Cu eutectic in lith23.

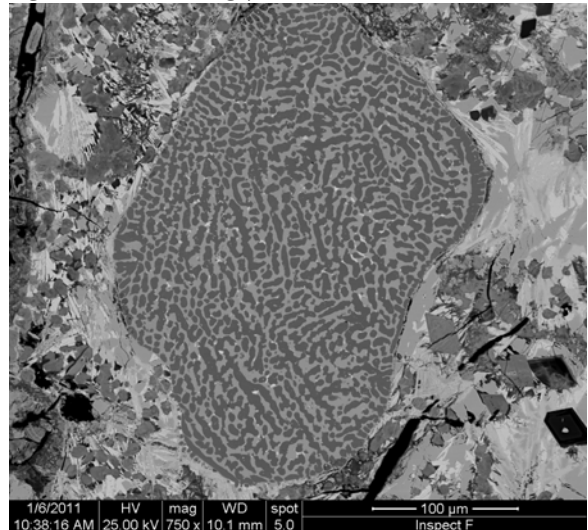


Fig 76. Ag-Cu eutectic in lith40.

CHEMICAL ANALYSES

Table 3. Average chemical composition of all litharge cake samples.

Samples	Na ₂ O	MgO	Al ₂ O ₃	SiO ₂	P ₂ O ₅	K ₂ O	CaO	MnO	Fe ₂ O ₃	Cu ₂ O	AgO	SnO ₂	PbO
Lith01	<0.1	0.3	0.2	3.1	12.3	<0.1	19.0	<0.1	0.4	13.1	0.2	<0.6	51.1
Lith02	<0.1	1.1	0.9	7.5	1.3	0.6	7.2	0.1	0.3	6.7	<0.1	<0.6	74.3
Lith03	<0.1	1.3	1.0	9.4	1.4	0.4	11.7	0.2	0.4	5.3	<0.1	<0.6	68.8
Lith05	<0.1	1.2	0.4	7.8	1.5	0.5	9.2	<0.1	<0.1	10.1	<0.1	<0.6	69.3
Lith06	<0.1	1.8	0.7	4.4	0.9	0.2	7.2	<0.1	<0.1	4.1	<0.1	<0.6	80.7
Lith07	<0.1	1.0	1.3	8.9	1.4	0.6	6.1	<0.1	0.3	14.6	<0.1	<0.6	65.8
Lith08	<0.1	1.7	1.2	9.2	1.1	1.2	8.8	<0.1	0.3	8.1	<0.1	<0.6	68.3
Lith09	<0.1	0.7	0.8	5.1	2.8	<0.1	3.5	0.1	0.7	5.5	<0.1	<0.6	80.8
Lith10	<0.1	1.3	0.9	6.1	1.0	0.8	6.0	<0.1	<0.1	18.1	0.2	<0.6	65.5
Lith11	<0.1	<0.1	<0.1	3.1	1.8	<0.1	1.3	<0.1	<0.1	22.3	0.2	<0.6	71.1
Lith12	<0.1	1.8	0.9	6.7	1.2	0.2	5.4	<0.1	<0.1	13.4	<0.1	<0.6	70.3
Lith13	<0.1	2.3	1.4	11.7	1.2	0.4	9.2	0.1	0.4	16.7	0.4	<0.6	56.3
Lith14	<0.1	0.2	0.3	1.8	20.3	<0.1	29.4	<0.1	0.5	3.1	<0.1	<0.6	44.3
Lith15	<0.1	1.6	1.3	5.6	1.5	0.2	5.9	<0.1	0.1	7.8	<0.1	<0.6	76.1
Lith16	<0.1	0.2	0.1	1.5	13.3	<0.1	22.2	<0.1	<0.1	14.3	1.1	0.8	46.3
Lith17	<0.1	0.7	1.5	7.6	1.3	<0.1	10.6	<0.1	0.2	20.7	<0.1	0.9	56.5
Lith18	<0.1	0.6	0.2	1.7	15.0	<0.1	20.4	<0.1	0.1	23.0	1.2	<0.6	37.6
Lith19	<0.1	1.2	1.0	6.3	1.3	0.8	5.4	0.2	0.4	19.9	0.5	<0.6	63.1
Lith20	<0.1	0.9	2.1	5.7	0.3	<0.1	12.3	<0.1	0.5	10.6	<0.1	<0.6	67.6
Lith21	<0.1	0.1	0.1	2.3	18.0	<0.1	23.6	<0.1	0.2	19.0	0.1	<0.6	36.2
Lith22	<0.1	0.4	0.1	1.7	15.8	<0.1	24.1	<0.1	<0.1	13.6	<0.1	<0.6	44.1
Lith23	<0.1	0.2	<0.1	0.5	17.6	<0.1	23.2	<0.1	<0.1	25.5	1.8	<0.6	31.0
Lith24	0.3	0.1	0.5	3.8	0.5	0.3	1.2	<0.1	0.2	57.0	0.1	10.8	25.2
Lith25	<0.1	0.7	1.5	6.8	4.8	0.3	12.2	0.1	1.1	4.6	<0.1	<0.6	68.0
Lith26	<0.1	0.2	2.2	17.4	0.6	0.4	0.7	<0.1	1.8	54.7	0.1	11.3	10.6
Lith27	<0.1	0.3	<0.1	1.2	15.2	<0.1	23.5	<0.1	<0.1	14.1	0.3	<0.6	45.3
Lith29	<0.1	0.2	0.3	2.8	10.3	0.1	14.6	<0.1	<0.1	18.0	<0.1	<0.6	53.3
Lith30	<0.1	0.3	0.3	1.2	12.6	<0.1	19.4	<0.1	<0.1	12.1	<0.1	<0.6	53.8
Lith31	0.2	0.3	0.7	6.1	22.7	0.1	29.8	<0.1	1.0	2.0	<0.1	<0.6	36.7
Lith33	<0.1	0.1	0.2	3.3	11.0	<0.1	16.6	<0.1	0.2	7.3	<0.1	1.9	59.4
Lith34	<0.1	0.3	0.1	1.7	18.9	<0.1	27.2	<0.1	<0.1	16.5	1.4	<0.6	33.6
Lith35	<0.1	0.3	0.2	2.2	13.9	<0.1	20.8	<0.1	<0.1	14.0	0.8	<0.6	47.7
Lith36	<0.1	1.2	1.0	8.2	1.1	1.0	7.5	0.2	0.3	23.7	1.6	<0.6	54.2
Lith37	<0.1	0.3	0.1	3.4	12.6	0.6	20.9	<0.1	<0.1	16.4	0.3	<0.6	45.0
Lith38	<0.1	0.3	0.2	2.7	14.4	0.2	22.3	<0.1	0.1	15.2	<0.1	<0.6	44.3
Lith39	<0.1	1.4	0.7	5.5	1.1	0.2	5.6	<0.1	<0.1	21.3	0.6	<0.6	63.5
Lith40	<0.1	1.2	0.7	5.6	1.1	0.3	4.4	<0.1	<0.1	17.2	0.2	0.7	68.5
Lith41	0.6	1.1	2.5	14.3	4.1	1.4	12.7	0.2	1.4	0.8	<0.1	<0.6	60.8
Lith42	<0.1	0.7	0.5	5.3	1.6	0.2	5.4	<0.1	<0.1	32.9	1.8	<0.6	51.5
CG1	<0.1	1.0	1.5	9.4	1.4	0.5	11.3	0.2	0.3	5.2	<0.1	<0.6	69.0
CG2	<0.1	0.8	1.2	5.6	2.0	0.6	10.6	0.2	0.3	4.5	<0.1	<0.6	74.2
CG3	<0.1	1.1	1.0	8.3	1.0	<0.1	6.4	<0.1	0.2	7.3	<0.1	<0.6	74.7

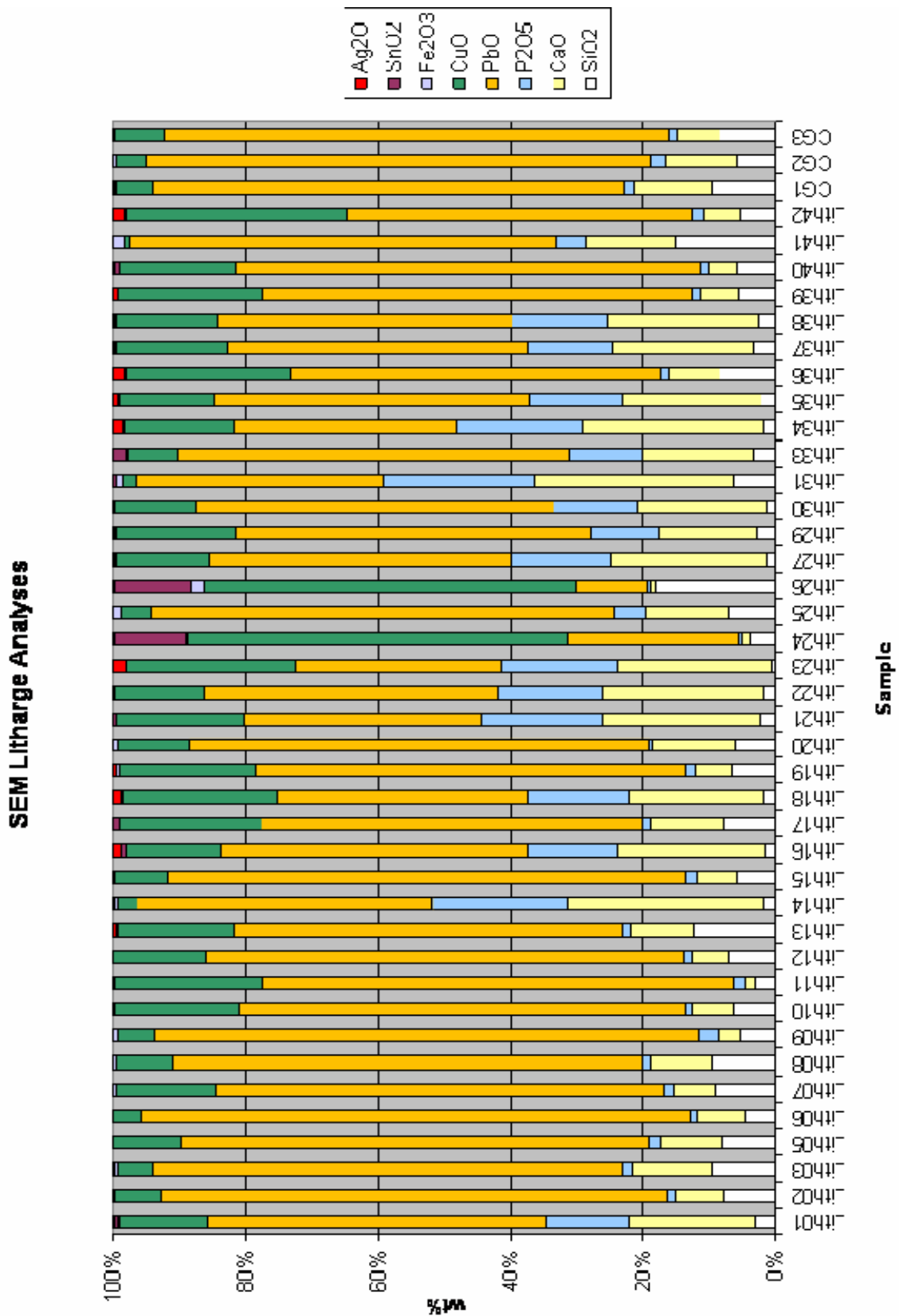


Fig 77. Normalised selected elements SEM analyses of all litharge samples.

The majority of the litharge samples have between 33 and 80wt% PbO (Table 3) which is typical of cupellation hearth linings. The next most abundant metal oxide is Cu_2O with most samples fitting into the 4 to 33wt% bracket. Lith16, lith17, lith24, lith26, lith33 and lith40 all have detectable SnO_2 but both lith24 and lith26 display very high quantities (around 11wt%). Indeed, lith24 and lith26 seem to differ from the other litharge with only 25wt% and 10wt% PbO respectively. They also have very high contents of Cu_2O (~55wt%). Most samples have CaO contents between 5 and 30wt%, P_2O_5 either below 3wt% or within 10 to 22wt% and SiO_2 between 1 and 17wt% but most between 5 and 9wt%. All other elements tend to be below 2wt%.

Cupellation Hearth Lining Compositions

In order to find out the composition of the original cupellation hearth linings all elements heavier than nickel were removed from the compositions and the remaining oxides normalised to 100% (Bayley and Eckstein 2006; Martín-Torres *et al*/2008, 10; 2009, 439). It is clear from the results that there are two major compositional groups (Table 4 and Figs 78 and 79). These seem to fit perfectly with the microstructural observations.

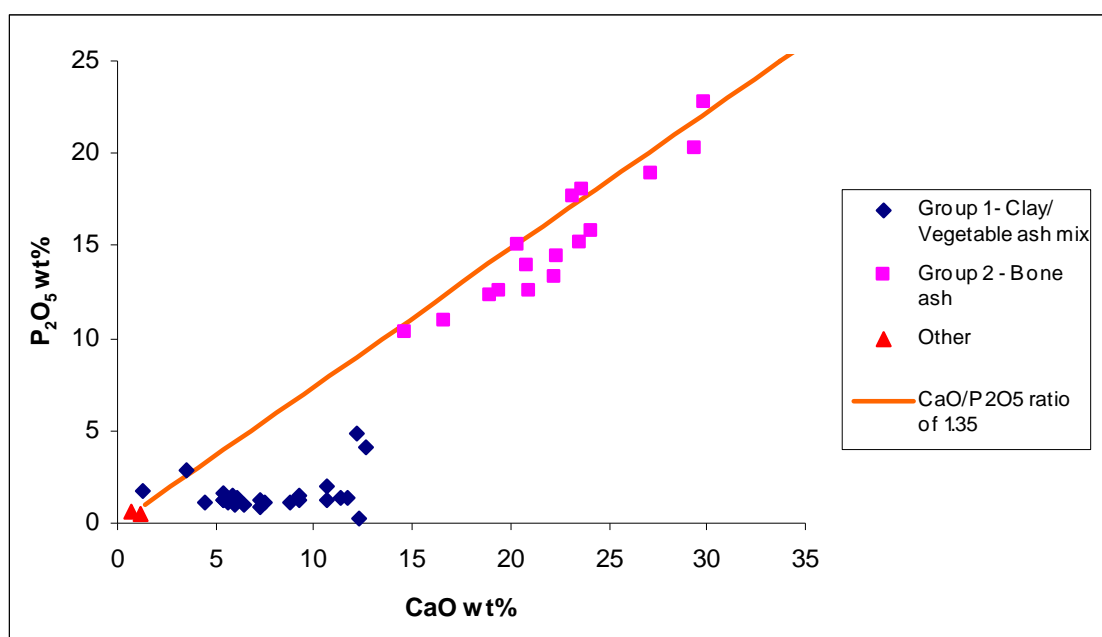


Fig 78. Graph showing the $\text{CaO}/\text{P}_2\text{O}_5$ ratio of all litharge samples; note the two major groupings which fit with the microstructural observations (clay/vegetable ash mix and bone ash hearth linings). The two outliers are lith24 and lith26. The data excludes heavy metals and the remaining oxides were normalised to 100%.

Table 4. The non-metal oxide compositions of the cupellation hearth linings normalised to 100wt%.

	Composition	Group	MgO	Al ₂ O ₃	SiO ₂	P ₂ O ₅	K ₂ O	CaO
Lith01	Bone ash	2	0.8	0.5	8.9	35.2	<0.3	54.6
Lith02	Mix	1	5.9	4.6	40.7	6.8	3.4	38.6
Lith03	Mix	1	5.3	3.9	37.4	5.5	1.5	46.4
Lith05	Mix	1	5.8	1.7	38.0	7.1	2.6	44.8
Lith06	Mix	1	12.1	4.4	29.1	5.8	1.0	47.7
Lith07	Mix	1	5.1	6.7	46.1	7.4	2.9	31.8
Lith08	Mix	1	7.5	5.1	39.4	4.9	5.0	38.0
Lith09	Mix	1	5.3	6.4	39.5	21.9	<0.8	26.8
Lith10	Mix	1	7.8	5.9	37.8	6.3	5.1	37.1
Lith11	Mix	1	0.6	<1.6	49.4	28.8	<1.6	20.3
Lith12	Mix	1	11.1	5.4	41.6	7.7	0.9	33.3
Lith13	Mix	1	8.8	5.2	44.7	4.5	1.7	35.2
Lith14	Bone ash	2	0.3	0.6	3.4	39.1	0.1	56.5
Lith15	Mix	1	10.3	7.8	34.7	9.6	0.9	36.7
Lith16	Bone ash	2	0.5	<0.3	4.1	35.6	<0.3	59.4
Lith17	Mix	1	3.4	6.7	35.1	5.9	<0.5	48.9
Lith18	Bone ash	2	1.5	0.6	4.4	39.6	<0.3	53.8
Lith19	Mix	1	7.5	6.0	39.7	8.1	4.8	33.9
Lith20	Mix	1	4.0	9.7	26.9	1.5	<0.5	57.8
Lith21	Bone ash	2	0.3	0.3	5.2	40.7	0.2	53.4
Lith22	Bone ash	2	0.8	0.2	4.0	37.6	<0.2	57.3
Lith23	Bone ash	2	0.6	<0.2	1.2	42.4	<0.2	55.7
Lith24	Other		1.7	7.2	60.2	8.0	4.3	18.6
Lith25	Mix	1	2.6	5.9	25.8	18.2	1.1	46.4
Lith26	Other		1.0	10.2	81.0	2.8	1.7	3.3
Lith27	Bone ash	2	0.7	<0.2	3.1	37.7	<0.2	58.4
Lith29	Bone ash	2	0.5	1.1	9.9	36.5	0.4	51.6
Lith30	Bone ash	2	0.9	0.8	3.5	37.3	<0.3	57.4
Lith31	Bone ash	2	0.5	1.1	10.3	38.0	0.2	49.9
Lith33	Bone ash	2	0.4	0.5	10.5	35.3	<0.3	53.2
Lith34	Bone ash	2	0.6	0.2	3.6	39.1	<0.2	56.4
Lith35	Bone ash	2	0.7	0.4	5.9	37.2	<0.3	55.7
Lith36	Mix	1	6.0	5.2	40.8	5.6	5.2	37.3
Lith37	Bone ash	2	0.9	0.4	9.0	33.2	1.6	55.0
Lith38	Bone ash	2	0.7	0.5	6.8	35.9	0.5	55.7
Lith39	Mix	1	10.0	4.8	37.8	7.6	1.2	38.5
Lith40	Mix	1	9.1	5.2	41.9	8.5	2.1	33.2
Lith41	Mix	1	3.1	6.9	39.6	11.3	4.0	35.2
Lith42	Mix	1	5.0	3.6	38.8	11.7	1.3	39.6
CG1	Mix	1	3.9	5.9	37.4	5.7	2.2	44.9
CG2	Mix	1	3.7	6.0	26.8	9.7	2.7	51.1
CG3	Mix	1	6.0	5.7	46.4	5.7	<0.6	36.0

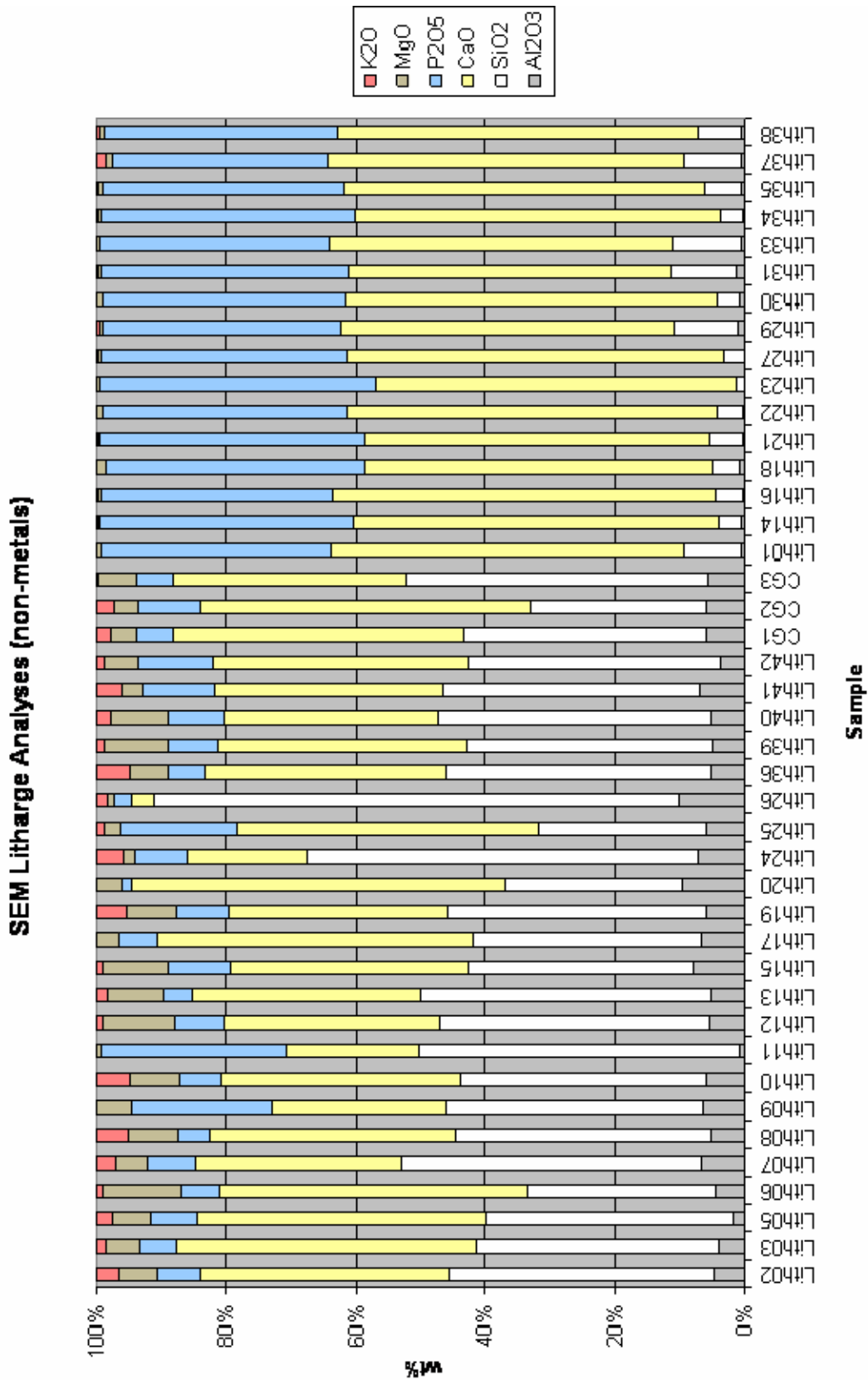


Fig 79. Normalised non-metals SEM analyses of all litharge samples.

One group is composed primarily of SiO_2 (~30–40wt%) and CaO (~35–45wt%) with small amounts of Al_2O_3 (~4–7wt%), MgO (~5–10wt%), P_2O_5 (~5–8wt%) and up to 5wt% K_2O . These belong to microstructural group 1 with complex microstructures and a variety of crystalline mineral phases. The group comprised all three samples from Brook Street, nine out of 10 samples from Saltergate, one out of 13 samples from Flaxengate, the sample from No 1 Poultry, the sample from Grange Farm, the sample from Merida, three out of five samples from Dunkirt Barn, both samples from Dublin and all three samples from Coppergate. Their high SiO_2 , Al_2O_3 and CaO contents suggests that they were partially made of clay marl while the presence of MgO and K_2O indicates a vegetable ash mixture. The presence of some P_2O_5 may be indicative of minor contents of bone ash but some plant ashes also contain small amounts of P_2O_5 (Turner 1956). There are two outliers in this group: both lith09 and lith11 have higher contents of P_2O_5 and lower CaO . It has been noticed that these two samples were different as they both displayed high levels of Cl and S which are undoubtedly post depositional corrosion. As CaO and P_2O_5 are very susceptible to post depositional alteration (Martín-Torres *et al*/2008, 11) it is probable that the differences in composition are due to this. On the other hand, there were traces of broken down apatite in lith09's microstructure so the original hearth lining must have been made with a mixture of clay marl, bone ash and a vegetable ash containing P_2O_5 .

The other group is dominated by CaO (~52–58wt%) and P_2O_5 (35–40wt%) with up to 10wt% SiO_2 . These belong to microstructural group 2 with large apatite grains: the sample from Wolvesey Palace, one out of 10 samples from Saltergate, the sample from Driffield Terrace, 10 out of the 13 samples from Flaxengate, the sample from Swan Lane and two out of five samples from Dunkirt Barn. They seem to be pure bone ash with a $\text{CaO}/\text{P}_2\text{O}_5$ ratio around 1.3. The chemical composition of this group matches almost exactly the pure bone ash experimental cupels discussed by White (2010b, 6). However, some of these samples contain SiO_2 which may suggest the addition of clay marl perhaps as a binding agent. Another possibility is the reaction of the bone ash with the underlying clay hearth. It is possible that the litharge and other metal oxides fully impregnated the ash and started to be absorbed by the clay. All the bone ash samples are very similar in composition and the possibility that some of these are from the same litharge cake cannot be ruled out — specifically regarding the Flaxengate litharge.

There are two major outliers to these two chemical groupings. Lith24 and lith26 have re-normalised SiO_2 contents of 60 and 80wt% respectively and Al_2O_3 contents close to 10wt% (Table 4). Most surprising are the very low levels of CaO ; Lith24 has close to 20wt% but lith26 less than 4wt%. Considering that all the other litharge samples have over 35wt% CaO it would suggest that these two samples were misidentified and are not cupellation hearth linings. Their low PbO but high CuO_2 and SnO_2 contents discussed above also support this. It is not possible at this stage to tell what these two fragments were (perhaps residues from scorification) but it is almost certain that the material was clay rich and the metal a bronze.

Following Martín-Torres *et al*'s (2009) methodology it was possible to remove the bone ash (apatite) contribution from the compositions to work out the amount of excipient. This was done by multiplying the P₂O₅ by 1.3 to get the bone ash's contribution of CaO. Although Martín-Torres *et al* (2009) use a ratio of 1.2, spot analyses on the apatite grains in the litharge analysed in this report gave a CaO/P₂O₅ ratio of 1.3 so this figure was used here. This will be discussed further below. The P₂O₅ and the CaO coming from the apatite was removed from the compositions and the remaining element oxides re-normalised to 100%. The results are displayed in Tables 5 and 6.

Table 5. The calculated excipient composition of the bone ash hearth linings (normalised to 100%) with their overall contribution to the original litharge cakes.

Sample	Na ₂ O	MgO	Al ₂ O ₃	SiO ₂	K ₂ O	CaO	MnO	Fe ₂ O ₃	Overall %
Lith01	<1.4	3.8	2.3	44.0	<1.4	43.2	<1.4	5.7	20.0
Lith14	<1.8	3.0	5.2	30.4	<1.8	50.7	<1.8	8.4	11.0
Lith16	<1.5	2.9	1.3	22.4	<1.5	71.8	<1.5	<1.5	18.2
Lith18	<2.9	15.9	6.8	47.5	<2.9	25.0	<2.9	3.1	9.2
Lith21	<3.5	5.0	3.5	76.2	<3.5	6.5	<3.5	6.2	6.4
Lith22	<1.7	6.1	1.7	29.2	<1.7	61.9	<1.7	<1.7	13.6
Lith23	<9.7	22.4	<9.7	47.7	<9.7	23.1	<9.7	<9.7	2.5
Lith27	<1.9	5.1	<1.9	23.2	<1.9	70.2	<1.9	<1.9	13.2
Lith29	<2.2	3.3	6.6	60.7	2.4	24.9	<2.2	<2.2	16.2
Lith30	<2.0	6.2	5.3	23.8	<2.0	61.2	<2.0	<2.0	14.5
Lith31	1.7	3.4	7.8	70.2	1.5	3.6	<1.2	11.3	14.3
Lith33	<1.7	2.0	2.6	53.7	<1.7	37.3	<1.7	3.6	19.4
Lith34	<2.0	5.9	<2.0	35.4	<2.0	55.0	<2.0	<2.0	10.2
Lith35	<1.8	5.0	2.8	40.0	<1.8	49.9	<1.8	<1.8	14.7
Lith37	<1.1	3.7	1.5	37.2	6.5	49.6	<1.1	<1.1	24.0
Lith38	<1.4	3.9	2.5	37.8	2.6	50.5	<1.4	1.4	17.9

The results in Table 5 clearly show that the bone ash hearth linings were almost pure containing in majority less than 20wt% excipient. Most seem to share a similar excipient composition with approximately 30–50wt% SiO₂ and 40–50wt% CaO. The presence of large proportions of SiO₂ and some Al₂O₃ suggests that the principle excipient was probably clay marl. The lack of any substantial K₂O content rules out tree wood ashes while the high CaO makes grass ashes unlikely (Sanderson and Hunter 1981, 28; Stern and Gerber 2004, 140; Turner 1956, 289). Another possibility would be beech leaves which would also account for the 4 to 6wt% MgO and 2 to 3wt% K₂O found in most samples (Turner 1956, 289). Lith21 and lith31 both have around 70wt% SiO₂, less than 7wt% CaO and reasonably high Fe₂O₃ content which suggests that the primary excipient was clay, perhaps contamination from the hearth. Both lith18 and lith23 have high MgO contents which indicates that some other type of ash was used but what it was cannot be ascertained here. Whatever excipient was added it made only a tiny proportion of the hearth linings; 9wt% of lith18 and 2wt% of lith23. Due to these small proportions, contamination from the burning charcoal or wood during cupellation cannot be ruled out.

Lith37 and lith38 have almost identical compositions and it is likely that they are from the same hearth lining.

Table 6. The excipient composition of the non-bone ash hearth linings (normalised to 100%) with their overall contribution to the original litharge cakes.

Sample	Na ₂ O	MgO	Al ₂ O ₃	SiO ₂	K ₂ O	CaO	MnO	Fe ₂ O ₃	Overall %
Lith02	<0.6	6.8	5.3	47.0	3.9	34.4	0.8	1.8	84.7
Lith03	<0.5	5.9	4.4	41.7	1.7	43.7	0.8	1.9	87.5
Lith05	<0.6	6.9	2.0	45.3	3.0	42.4	<0.6	<0.6	83.7
Lith06	<0.8	13.9	5.0	33.2	1.1	45.9	<0.8	<0.8	86.8
Lith07	<0.6	6.0	7.8	54.4	3.5	26.2	<0.6	1.9	83.3
Lith08	<0.5	8.3	5.7	43.6	5.5	34.9	<0.5	1.5	88.8
Lith09	<1.4	9.3	11.2	68.4	<1.4	<1.4	1.9	9.3	54.2
Lith10	<0.7	9.0	6.9	43.9	6.0	33.7	<0.7	<0.7	85.6
Lith11	<3.1	<3.1	<3.1	96.0	<3.1	<3.1	<3.1	<3.1	51.2
Lith12	<0.7	13.4	6.5	50.0	1.1	28.1	<0.7	<0.7	82.5
Lith13	<0.4	9.6	5.7	48.8	1.8	32.0	0.5	1.6	89.8
Lith15	<0.8	13.0	9.9	44.0	1.2	30.7	<0.8	1.1	78.2
Lith17	<0.5	3.9	7.7	40.2	<0.5	47.3	<0.5	0.8	86.6
Lith19	<0.8	8.8	7.0	46.8	5.6	27.5	1.3	2.9	82.0
Lith20	<0.5	4.1	9.8	27.2	<0.5	56.3	<0.5	2.5	96.6
Lith25	<0.6	4.1	9.4	41.1	1.8	36.3	0.8	6.5	60.1
Lith36	<0.6	6.6	5.8	45.5	5.8	33.5	1.2	1.5	87.5
Lith39	<0.8	12.0	5.8	45.4	1.5	34.4	<0.8	<0.8	82.6
Lith40	<0.9	11.1	6.4	51.3	2.6	27.1	<0.9	<0.9	80.6
Lith41	2.0	3.8	8.5	49.4	5.0	25.6	0.7	4.9	75.5
Lith42	<1.0	6.8	4.9	52.3	1.8	33.0	<1.0	<1.0	73.4
CG1	<0.5	4.4	6.7	42.1	2.4	42.2	0.8	1.4	87.1
CG2	<0.6	4.6	7.5	33.6	3.4	48.2	1.0	1.7	78.2
CG3	<0.6	6.7	6.4	52.5	<0.6	32.3	<0.6	1.4	87.0

Working out the excipient of the non-bone ash litharge cakes (Table 6) is more complicated. It has been assumed that the P₂O₅ contents of the litharge cakes were contributed by bone ash but this is by no means certain. Nevertheless, if this assumption is correct, bone ash would account for a minor proportion (in most cases less than 20wt%) of the original hearth lining. Apart from a few outliers (lith09, lith11, lith20, lith24 and lith26) the excipient compositions in the samples are quite similar with approximately 30–45wt% CaO, 40–50wt% SiO₂, 5–10wt% Al₂O₃, 4–14wt% MgO, <5wt% K₂O and <3wt% Fe₂O₃. This composition is close to that of beech leaves but the CaO content is a bit low and the SiO₂ a bit high (Turner 1956, 289). Another possibility is leached beech wood ash although the SiO₂ is a bit low in the samples (Stern and Gerber 2004, 140). It is likely that the excipient is a mixture of different ingredients, most probably clay marl and several vegetable ashes. As with the bone ash litharge the lack of any substantial K₂O rules out most tree wood ashes while the high CaO make grass ashes unlikely (Sanderson and Hunter 1981, 28; Stern and Gerber 2004, 140; Turner 1956, 289).

The outliers show some differences to the above. Lith09 and lith11 both have around 50wt% excipient. These did not have enough CaO to account for all the P₂O₅. Lith09 was short by 2wt% while lith11 was lacking 11wt%. This could suggest that there was another ingredient present contributing P₂O₅ but no CaO but it could equally be an artefact of corrosion. CaO and P₂O₅ are very susceptible to post depositional alteration and it has been noted above that these two fragments contained Cl and S which are signs of corrosion. As for their excipient, the relatively high percentage of SiO₂, Fe₂O₃ and Al₂O₃ in lith09 points to a clay. The 96wt% SiO₂ in lith11 suggests quartz (sand). Another outlier is lith20 which contains more CaO (56wt%) and less SiO₂ (27wt%). It contains no bone ash and must be entirely composed of clay marl or vegetable/plant ash. A point of interest is that both lith41 and lith42 have lower proportions of excipient (~75wt%) than any other hearth lining. Although the excipient composition does not differ significantly from the other hearth linings, apatite grains found in lith41 prove that there was some bone ash present in these samples. It may not be a coincidence that apart from lith09 and lith11 which may be corroded, the only other samples showing major compositional differences were those found outside England. This may be due to the use of different natural resources or indeed diverging recipes for the manufacture of cupellation hearth linings.

Martinón-Torres *et al* (2008, 10–11) discussed the variability of CaO/P₂O₅ ratios in different animal species. Would it be possible to tell from the CaO/P₂O₅ ratio of the apatite what kind of animal bones were used in the cupellation hearth linings? For this, analyses on two different types of apatite were effectuated. Between 3 and 5 spectra of pure apatite that had not yet broken down and another 3 to 5 spectra of apatite impregnated with lead (breaking down) were taken per bone ash sample. These analyses showed that all the pure bone ash grains that had not been broken down by metal oxides had exactly the same CaO/P₂O₅ ratio — 1.35 +/- 0.03. The CaO/P₂O₅ ratio of the broken-down apatite on the other hand displayed greater variation — 1.28 to 1.57.

The similar CaO/P₂O₅ ratios of the pure apatite grains suggest that one type of animal bone was preferred in the production of hearth linings. If this was the case the different ratios observed on the broken down grains may be attributed to the inclusion of foreign substances (in this case the metal oxides). Another possibility is that because the CaO/P₂O₅ ratio in bone is variable in different parts of one animal the broken down grains represent this phenomenon (Martinón-Torres *et al*/2008, 10–11; Tzaphlidou and Zaichick 2002; Zaichick and Tzaphlidou 2002) while the pure apatite may be from a specific part of the body that is harder to break down explaining their intact nature. If on the other hand Theophilus's descriptions (quoted in the discussion below) are correct, then we may expect variation from the use of differing animal species. Due to this variation of CaO/P₂O₅ ratios in bone, it is hard (if not impossible) at this stage to suggest one possible animal species. Further work would be required to assign specific species to the bone ash used in cupellation hearth linings.

The Nature of the Excipient

It is important to reiterate that the calculation of the weight ratio of CaO to P₂O₅ is based on two assumptions: that the excipient did not contain any significant P (like clay) and that the CaO/P₂O₅ ratio in bone is relatively stable and predictable. However, most vegetable ashes have 4–10wt% P₂O₅ (Stern and Gerber 2004, 140; Turner 1956, 289) which would mean that if most of the samples in group one contained vegetable ashes then they did not contain any bone ash. If the P₂O₅ and CaO taken away to represent bone ash is put back into the equation then the compositions resemble leached beech wood ash or beech leaves (Stern and Gerber 2004, 140; Turner 1956, 289). Unfortunately the precise identification of the excipients or raw materials employed in the cupellation hearth linings cannot be ascertained or pinpointed. This is in part due to the lack of published data concerning vegetable ash or even clay marl compositions. Furthermore, experimental studies on vegetable ashes have revealed that the compositions vary significantly even in the same plant species depending on the underlying geology on which they grew, time of year they were harvested and preparation methodology (Jackson *et al*/2005; Sanderson and Gerber 1981; Stern and Gerber 2004; Turner 1956). Nevertheless, as a comparative tool it is very informative and the compositional similarities in most samples may not be a coincidence.

The compositions reveal that aside from bone ash the other most probable raw material employed would have been leached beech wood ash or beech leaves. This fits in with Theophilus's descriptions of hearth lining manufacture,

“Take the bone of any kind of animal that you may have found in the street and burn them; when they are cold, grind them very fine and mix them a third part of beechwood ashes and make dishes...” (Hawthorne and Smith 1079, 146).

Compositional Variability in Litharge Cakes

An important consideration in the scientific analysis of archaeological materials is the sampling methodology employed. Litharge in the archaeological record is often very fragmentary which raises questions of how representative these fragments are of complete litharge cakes. The following section will deal with the compositional variability within litharge cakes. It is hoped this will shed light on the behaviour of certain elements as well as perhaps reveal technological choices employed by these ancient artisans.

Ideally complete litharge cakes would be required to assess variability throughout the length and thickness. Unfortunately, no complete cake was present in the assemblage but there were a few larger diagnostic pieces. Two large fragments were selected for analysis, a clay/vegetable ash (lith19) and a bone ash sample (EL4). These were cut into three smaller fragments to investigate the compositional variability along their length (Figs 80 and 81). Sample EL4 from Thetford, Norfolk was not part of this study but was one of

the six fragments analysed by Bayley and Eckstein (2006) and chosen for this investigation as it is was the most complete fragment available. The three fragments from each larger piece were treated as separate samples and analysed by SEM-EDS. The results are displayed in Table 7. In addition to these analyses the two large fragments were analysed by EDXRF (Eagle II) using the mapping programme on the Vison32 software. This showed the compositional intensities/concentrations of PbO, Cu₂O, CaO, AgO, Al₂O₃, K₂O, P₂O₅ and MgO within the fragments analysed.

Table 7. The average compositions (14 to 19 analyses) of the cut fragments from lith19 and EL4.

Sample	MgO	Al ₂ O ₃	SiO ₂	P ₂ O ₅	K ₂ O	CaO	MnO	Fe ₂ O ₃	Cu ₂ O	AgO	PbO
Lith19.1	1.4	1.5	6.5	1.0	1.3	5.8	0.1	0.2	23.7	0.6	57.9
Lith19.2	1.2	0.9	6.3	1.3	0.8	5.4	0.2	0.4	19.9	0.5	63.1
Lith19.3	1.1	0.9	5.7	1.3	0.8	5.1	0.1	0.3	22.6	0.8	61.1
EL4.1	0.3	<0.1	1.3	11.4	<0.1	20.4	<0.1	<0.1	6.4	<0.1	60.1
EL4.2	0.3	<0.1	1.1	10.6	<0.1	18.4	<0.1	<0.1	6.9	<0.1	62.6
EL4.3	0.3	<0.1	1.0	12.7	<0.1	22.6	<0.1	<0.1	6.3	<0.1	56.9



Fig 80. Section through lith 19.



Fig 81. Section through EL4.

The results in Table 7 show that the cut samples were almost identical in composition. This suggests that there was little compositional variation along the length of the litharge cakes. The EDXRF images also show very little variation in composition (Figs 82 and 83).

These results show that there is little compositional variation in a horizontal plane (length) but it does not assess the variation in a vertical plane (depth). To do this the most complete samples in terms of section depth were analysed. This comprised 19 litharge samples: lith2, lith3, lith5, lith6, lith7, lith8, lith10, lith13, lith16, lith17, lith18, lith19, lith22, lith23, lith27, lith35, lith36, lith37 and lith38. Only samples with known orientation and at least one surviving top or bottom edge were chosen for analysis. Bulk analyses at 250x (1.2mm²) were effectuated every 0.8mm from the top to the bottom of the samples. The results for every individual sample are given in Appendix 4.

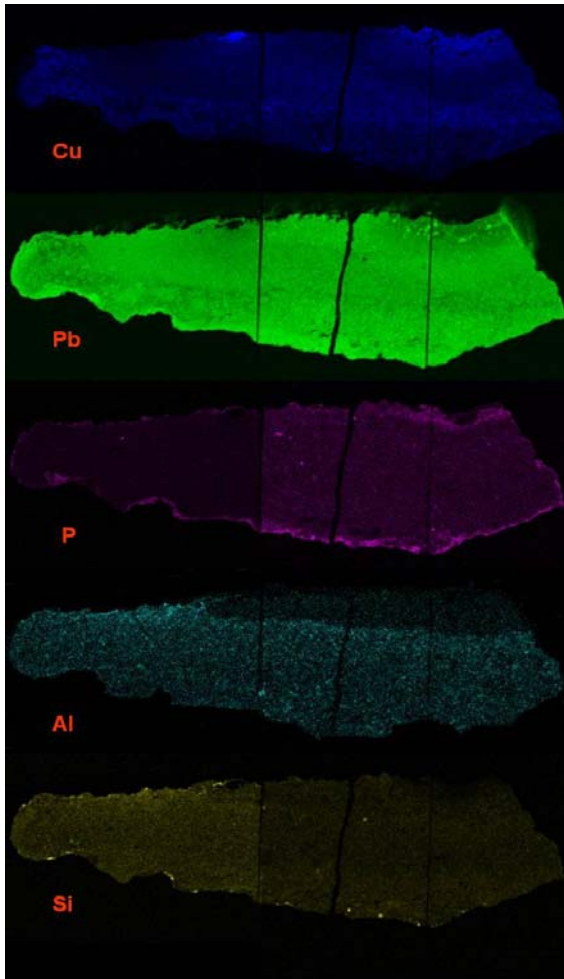


Fig 82. XRF mapping of selected element concentrations in lith19 (clay/vegetable ash).

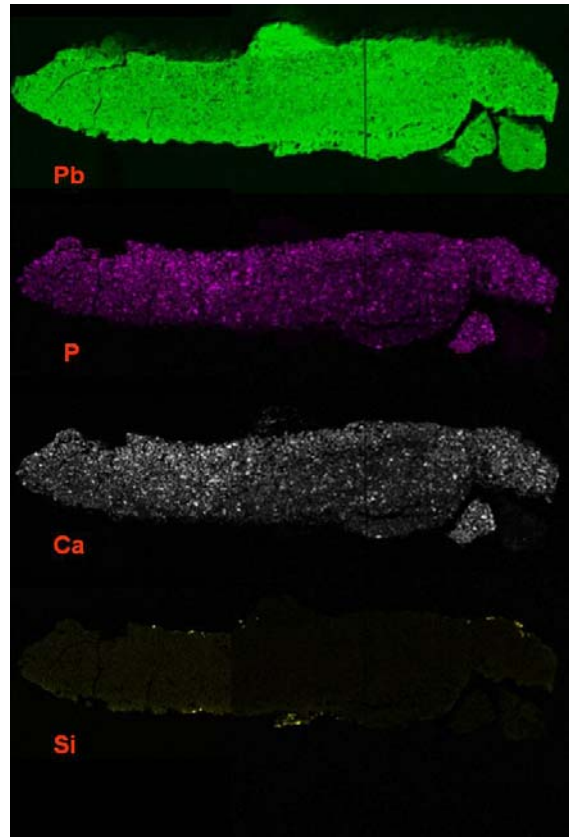


Fig 83. XRF mapping of selected element concentrations in EL4 (bone ash).

In a similar fashion to the above, the results were separated into the original hearth lining element oxides and the metal oxides. In each case they were re-normalized to 100% facilitating comparisons and discussion. Each element was then plotted on a line graph showing how its content varied through the litharge cake (every 0.8mm bulk reading — Figs 84 and 85). The results show that in all samples the original hearth composition does not vary significantly, in turn suggesting that the linings were made to one recipe and not layered. Slight changes on the top and bottom (about 1mm) of the samples were noticed — for example, the increase in the concentration of SiO_2 or CaO which may be due to the inclusion of adhering clay on the edges or post depositional alteration. In lith05 and lith18 the SiO_2 and Al_2O_3 rise significantly in the bottom quarter which may be attributed to contamination from the clay hearth on which the calcareous lining was resting. The metal oxides on the other hand do show variation in the vertical plane. It is evident that the majority of the Ag concentrates near the top edge of the samples and decreases dramatically a few mm away from the surface to nothing in the centre and bottom of the samples. It is also clear that the $\text{PbO}/\text{Cu}_2\text{O}$ ratio increases in the bottom half of the samples (Figs 86 and 87). It seems that the Cu_2O does not penetrate the hearth lining as far as the PbO .

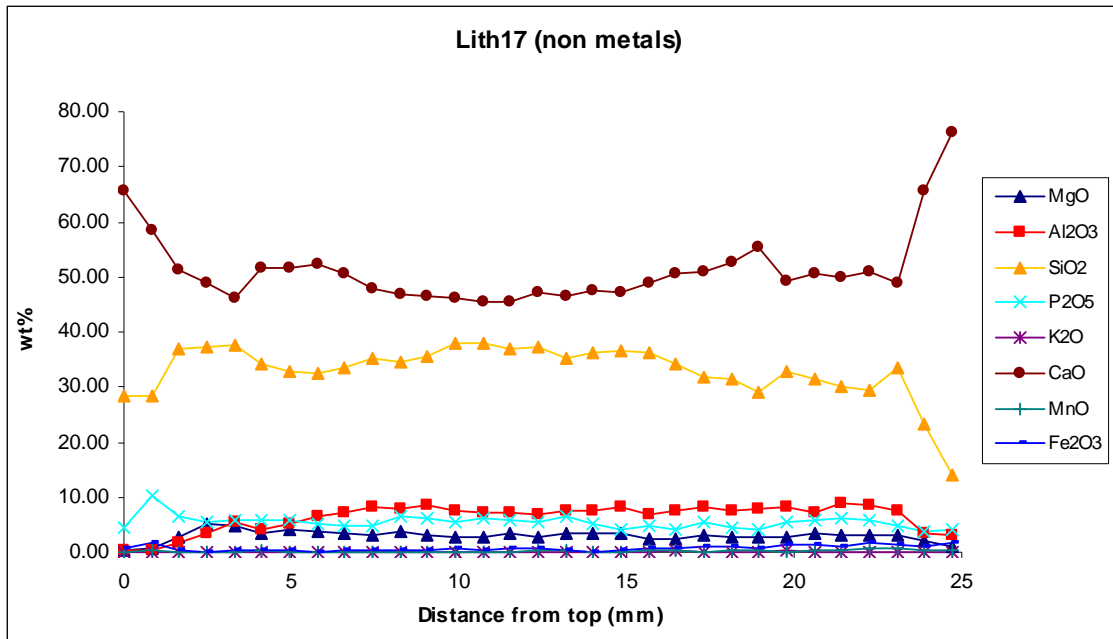


Fig 84. Graph showing the concentration of non-metallic element oxides through lith 17's depth.

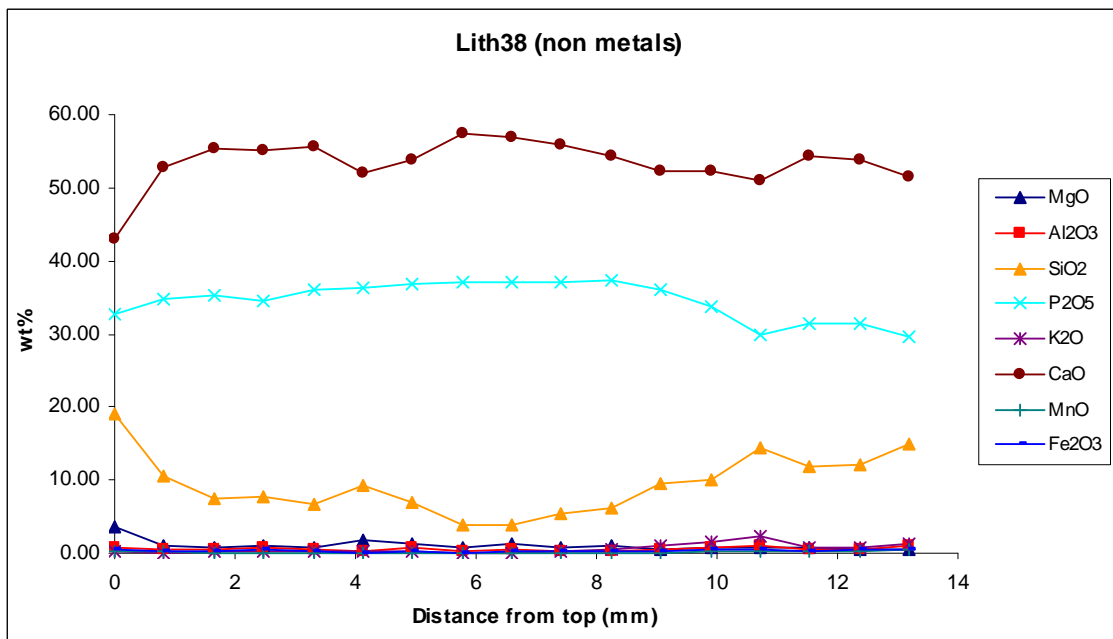


Fig 85. Graph showing the concentration of non-metallic element oxides through lith 38's depth.

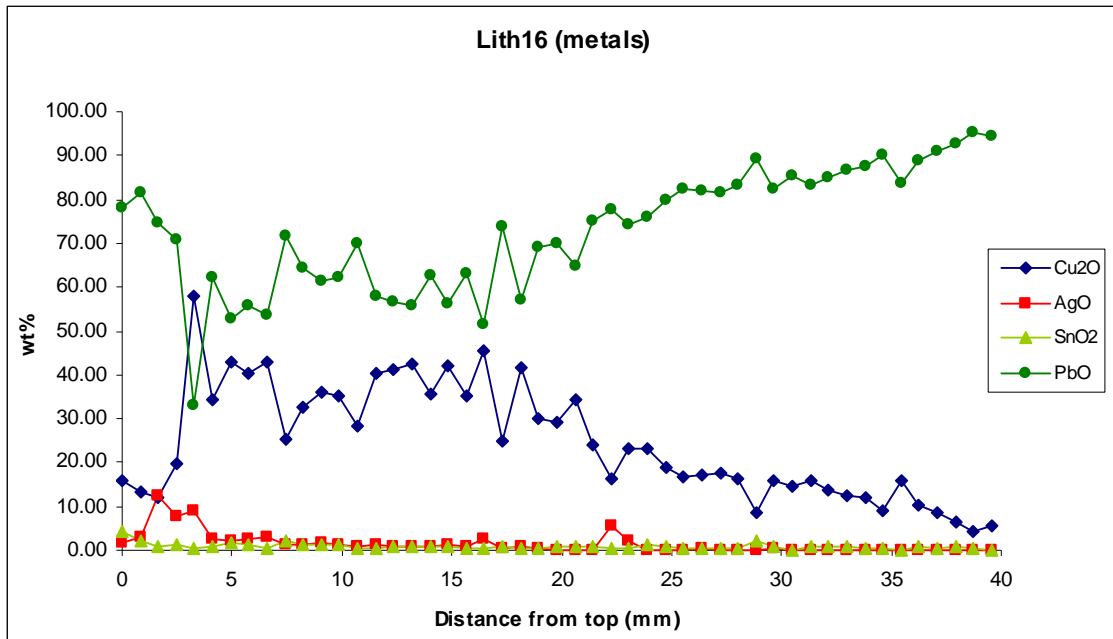


Fig 86. Graph showing the concentration of metallic element oxides through lith 16's depth.

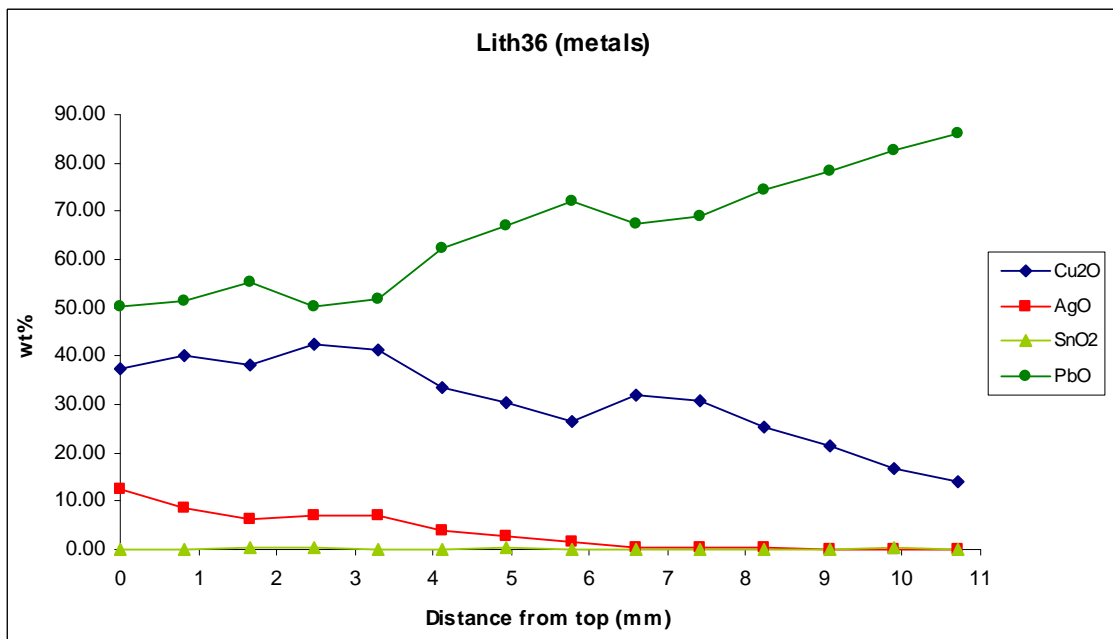


Fig 87. Graph showing the concentration of metallic element oxides through lith 36's depth.

This pattern is in direct contradiction to the findings on experimental cupels (Tereygeol and Thomas 2003, 179). In the two experimental cupels analysed, the Cu_2O concentrated on the bottom and stabilised around 9–12mm from the top of the cupels. Tereygeol and Thomas (2003, 176) let the metal intended for refinement melt in the cupel before

adding the required lead. Therefore, a reason for this phenomenon may be due to the preferential absorption of Cu_2O at the start of the cupellation process before the lead was added. In the case of the litharge cakes historical sources, in particular Theophilus's account seems to suggest that the lead was added with the metal intended for refining at the start of the cupellation process:

“Then put the silver onto it [the dish with calcareous lining], add a little lead on top, heap charcoal over it, and melt it” (Hawthorne and Smith 1079, 96–97)

Biringuccio states that the lead is melted first in the hearth and when it becomes “clear and shining like a star” the metal to be refined can be added (Smith and Gnudi 1990, 164). This may explain the higher $\text{PbO}/\text{Cu}_2\text{O}$ ratios at the bottom of the litharge cakes. Lead is more readily oxidised than copper meaning that it would have oxidised first and been preferentially absorbed by the calcareous lining (Dungworth 2000, 84–85). In addition, the aggressive (amphoteric) nature of PbO would explain its deeper penetration in the lining material.

The metal/non-metal ratio was also examined. Two patterns were noticed. Some of the samples (lith02, lith03, lith06, lith07, lith08, lith10, lith18 and lith38) show that the metal/non-metal ratio decreases from top to bottom (Fig 88). This means that the metal oxides did not penetrate as deep into the hearth lining. The other samples (lith16, lith17, lith19, lith22, lith23, lith27, lith35, lith36 and lith37) have a constant metal/non-metal ratio throughout the depth of the hearth lining (Fig 89); in those cases the metal oxides penetrated the hearth lining evenly. There does not seem to be any correlation between the original composition or date of the hearth lining and the metal/non-metal ratio through their depth.

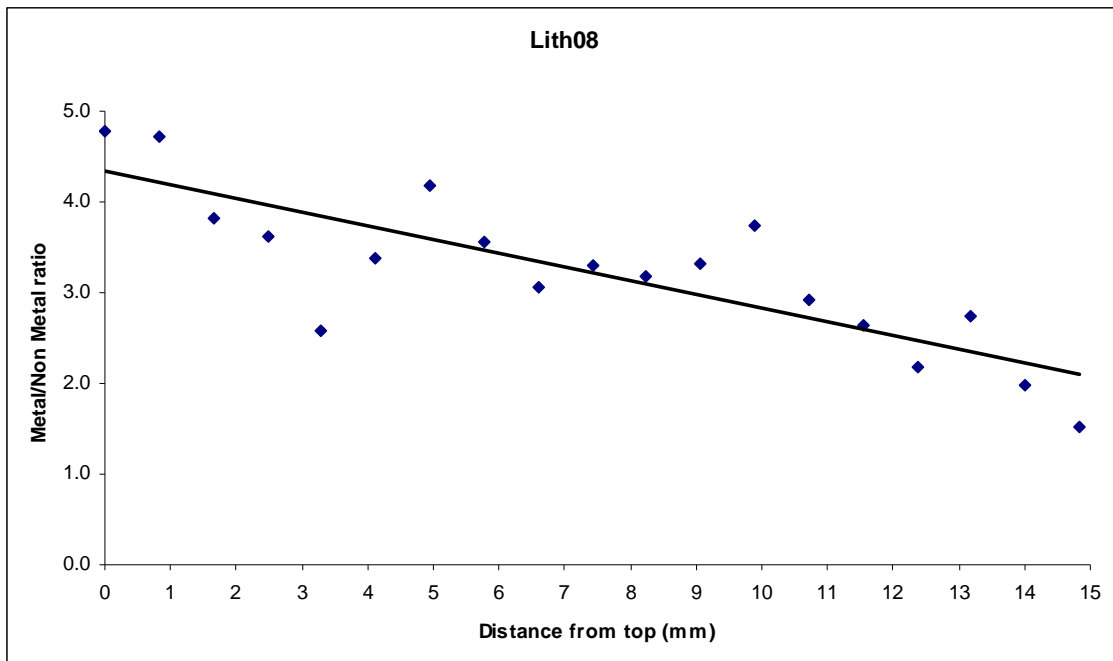


Fig 88. The metal/non metal ratio through lith08's depth.

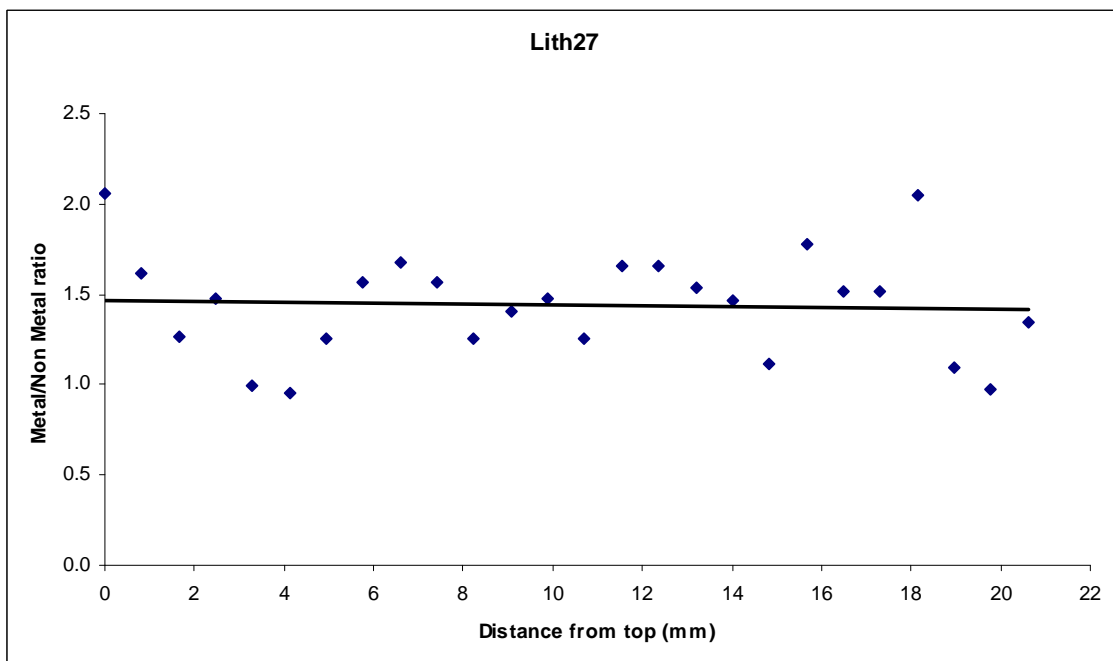


Fig 89. The metal/non metal ratio through lith27's depth.

DISCUSSION

Efficiency and Date

Bayley and Eckstein (2006) and Bayley (2009) have argued that the efficiency of the cupellation process could be represented by the PbO/Cu₂O ratio in the litharge cakes. This study supports this as it is apparent that samples with lower PbO/Cu₂O ratios tended to also contain more silver (Fig 90). Their analyses on nine litharge cakes seemed to indicate low PbO/Cu₂O ratios in Roman litharge and higher PbO/Cu₂O ratios in later medieval litharge. Based on the above assumption it was suggested that medieval cupellation methods were more efficient than those used by their Roman predecessors (Bayley and Eckstein 2006; Bayley 2009). The analysis of 45 Roman and medieval litharge cakes in this study has proved that there is no correlation between date and the PbO/Cu₂O ratio (Fig 90). The medieval PbO/Cu₂O ratio average was 8.8 (±5.2) with 0.2wt% (±0.6) AgO and the Roman 5.7 (±5.2) with 0.4wt% (±0.5) AgO. Although on average the ratio is greater with the medieval litharge the standard deviations are too large to show two distinct groupings. This means that medieval cupellation cannot be proven to have been more effective than Roman litharge. However, there are several problems associated with these studies and more specifically the sampling methodology.

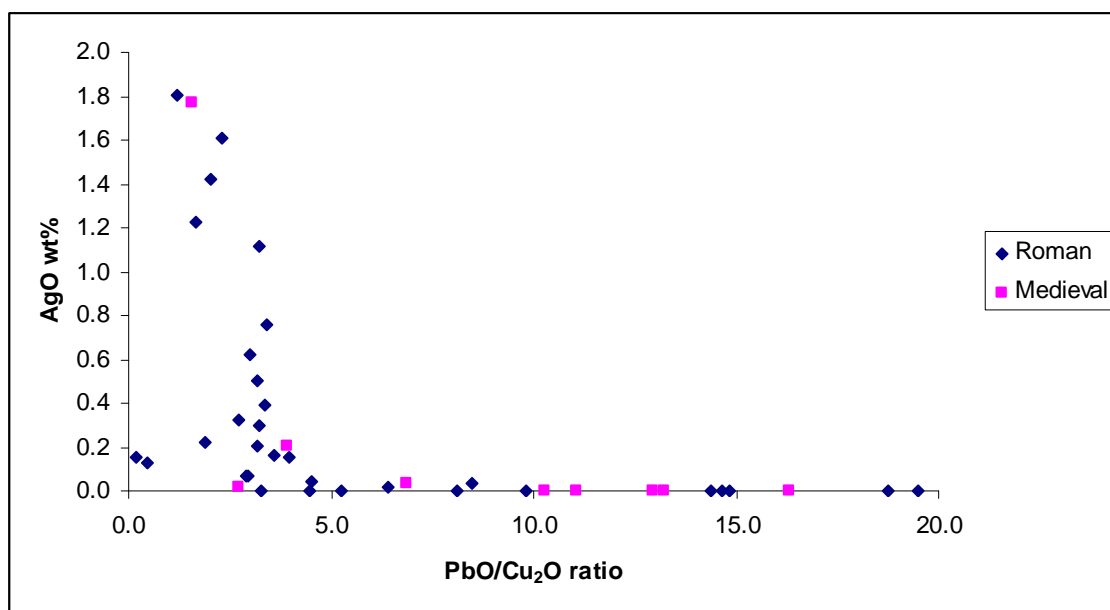


Fig 90. Graph showing the AgO wt% content of all samples against their PbO/Cu₂O ratio.

Firstly, it is important to state that the dating for some of the litharge cakes is uncertain. Many of the fragments (especially the ones from Lincoln) were found in medieval contexts but have been dated as Roman (Bayley 2008b). Although there is no evidence to dispute this date, it cannot be proven. On the other hand, the finds from Dunkirt Barn were found in Roman contexts and are more convincing while the Winchester, London,

York and Dublin litharge cakes are almost definitely medieval in date (although since there was Roman occupation in Winchester, London and York it cannot be totally definite). These better dated hearth linings are sufficient to prove the lack of correlation between efficiency and date (Fig 91).

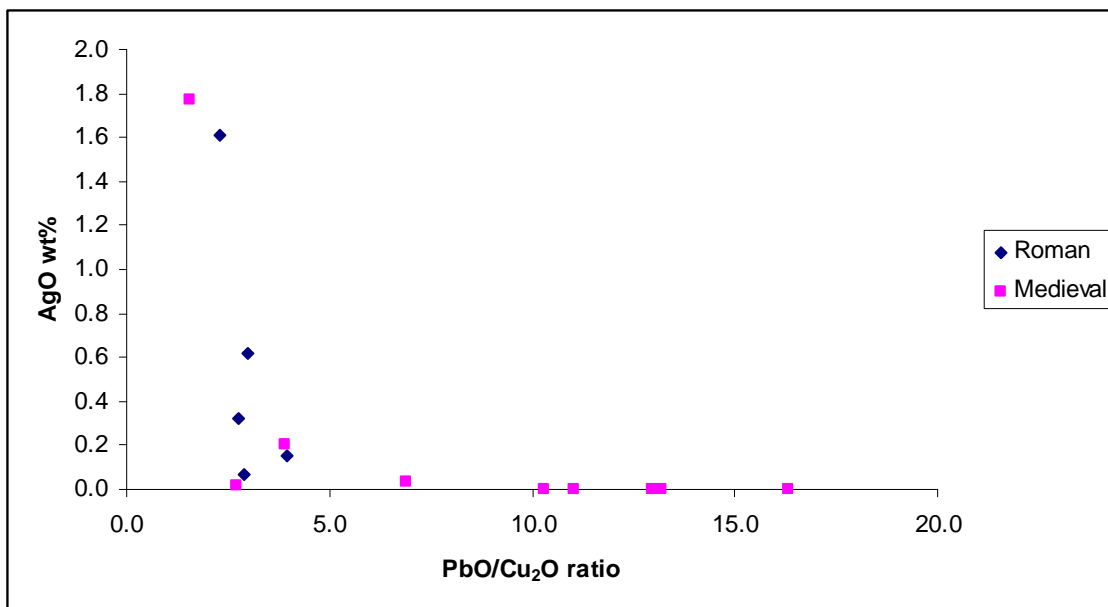


Fig 91. Graph showing the AgO wt% content of each better dated sample against their PbO/Cu₂O ratio.

The second problem is the sampling methodology. It has been proved that although the composition of litharge cakes does not vary on a horizontal plane, through their length, the metal oxides did show variation in a vertical plane, through their depth. In the 19 samples investigated the PbO/Cu₂O ratio increased the further away from the top. This would mean the PbO/Cu₂O ratio would vary depending on where the samples were taken (depth wise). As this ratio is the principal supporting evidence in Bayley and Eckstein's (2006) efficiency theory it would be crucial to have the whole or most of the litharge cake depth for suitable comparisons to be made. Unfortunately the majority of the samples in this study were very fragmentary and their orientation unknown. Therefore, it is important to recognize that the lack of correlation may be due to this sampling inconsistency. However, by re-plotting only the samples with the most complete depth (Fig 92) they also show that there is no clear correlation between date and the PbO/Cu₂O ratio but the majority of the Roman litharge cakes show greater contents of AgO. Unfortunately AgO by itself cannot be used to assess efficiency as the original Ag content of the metal refined cannot be known (Martín-Torres *et al*/2009, 438).

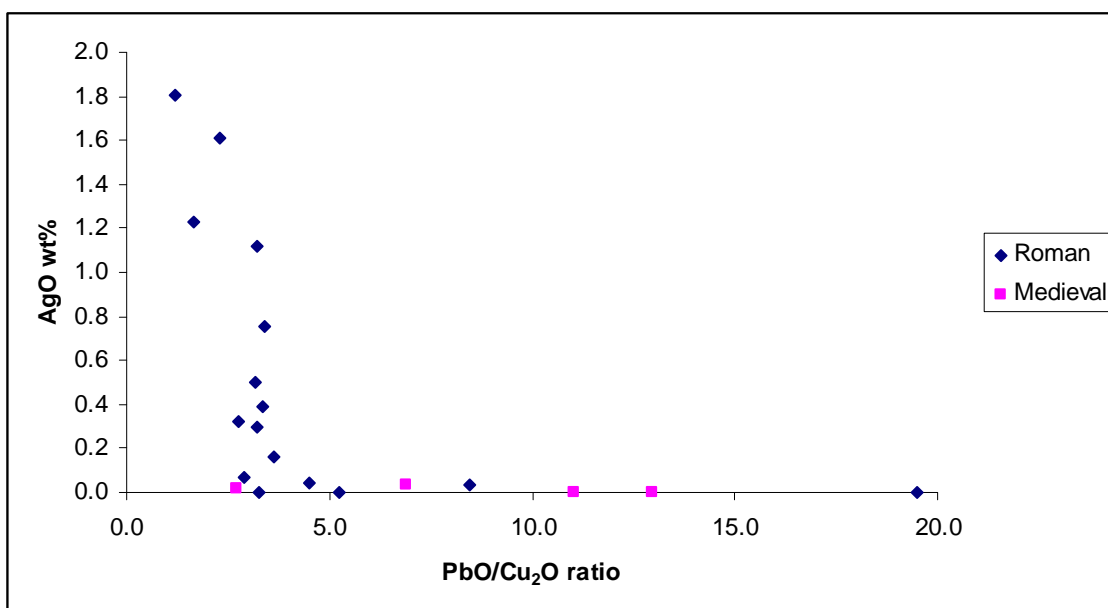


Fig 92. Graph showing the AgO wt% content of the samples with most surviving depth against their PbO/Cu₂O ratio.

Efficiency and Hearth Composition

Another point of discussion is the original hearth lining composition and efficiency. Is there a correlation between cupellation hearth lining composition and effectiveness of process? Bayley and Eckstein's (2006) and Bayley's (2009) analyses of nine litharge cakes suggested that there was no correlation and the examination of a further 45 fragments supports this supposition (Fig 93.). The clay/vegetable ash mixture PbO/Cu₂O average ratio was 7.3 (± 5.5) with 0.2wt% (± 0.5 wt%) AgO and the bone ash had an average of 4.9 (± 4.9) with 0.5wt% (± 0.6 wt%) AgO. This proves (assuming that the PbO/Cu₂O ratio is a true reflection of efficiency) that there is no correlation between cupellation efficiency and the cupellation hearth lining composition. However, out of 17 samples with PbO/Cu₂O ratios above 5, 14 are clay/vegetable ash while only three are bone ash. This may be a phenomenon created by the uneven number of samples in each group; there are more clay/vegetable ash fragments than bone ash.

Martinón-Torres *et al* (2009, 442–443) state that “from a present-day analytical perspective, it appears that wood-containing cupels have a slightly lower capacity to absorb lead oxide than their pure bone counterparts. This is due to the fact that the presence of silica from the wood ash triggers the formation of calcium phosphate silicates, which are impervious to the absorption of metal oxides”. However, this does not appear to have been the case for the litharge cakes analysed in this study. Although calcium silicate phosphates formed they did not appear to have inhibited absorption. It is evident that the bone ash litharge cakes contain less metal oxides (averaging at 60wt% ± 8 wt%) than the clay/vegetable ash litharge (averaging at 81wt% ± 6 wt%) (Fig 94). It is also

apparent that the pure bone ash cakes contain less PbO than their clay/vegetable ash counterparts (Fig 95). This is interesting because contrary to previous assumptions it suggests that the pure bone ash litharge was not as efficient in absorbing oxidised metal as the clay/vegetable ash litharge.

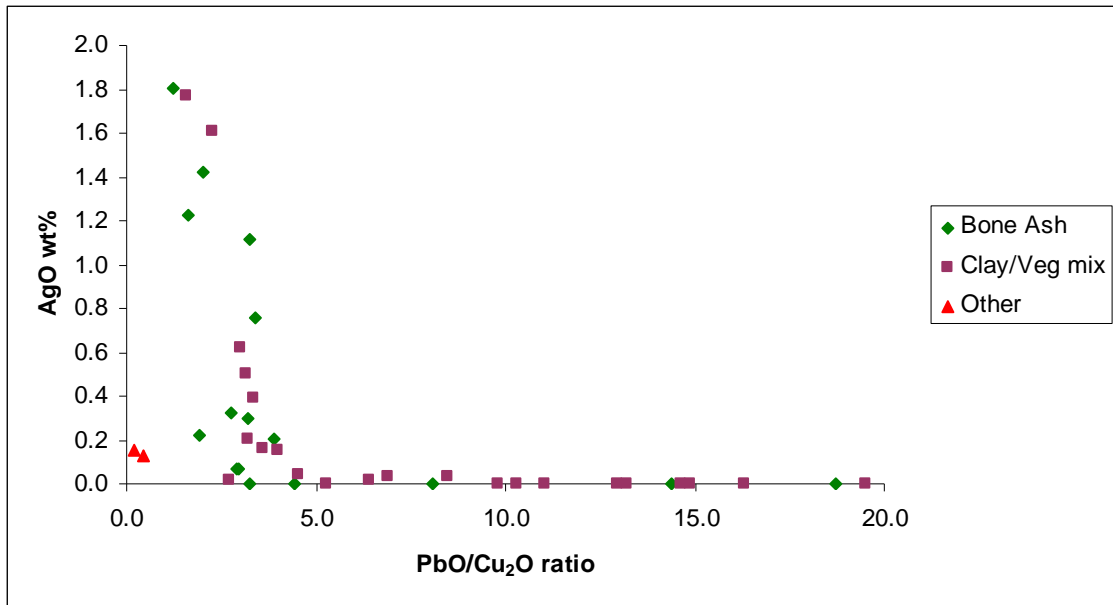


Fig 93. Graph showing the AgO wt% content of the samples categorised by original hearth lining composition against their PbO/Cu₂O ratio.

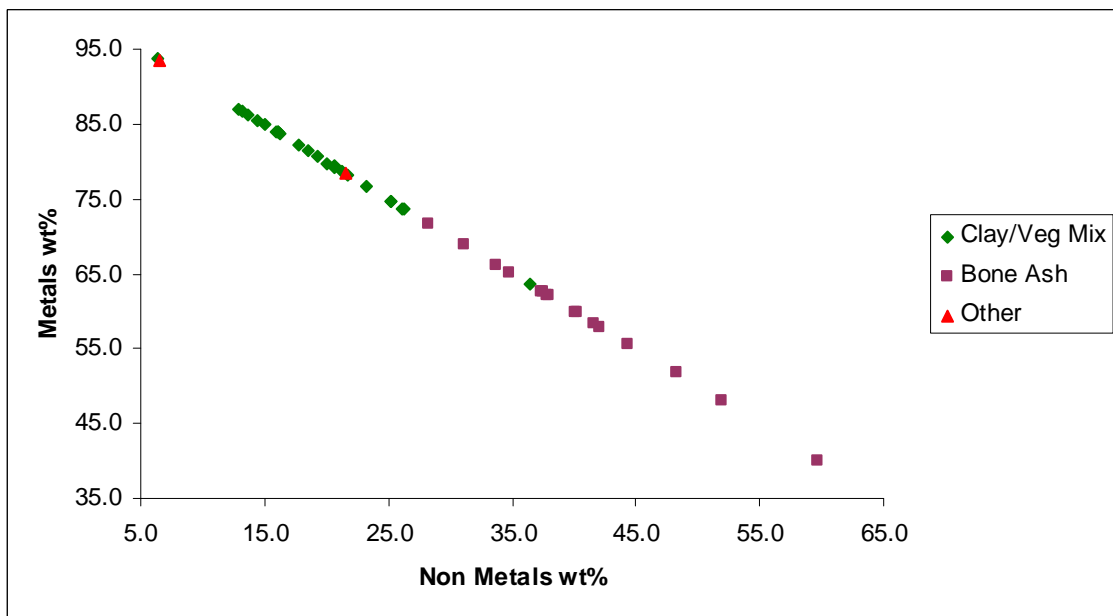


Fig 94. Graph showing the metal/non metal ratio of each sample categorised by original hearth lining composition.

natural resources. Perhaps bone ash was used in places where it was more readily available than a particular type of wood. It was noticed that the major compositional variations were seen in the litharge cakes found outside England. This may be due to different cultural traditions or availability of different natural resources.

Of course it is important not to over-interpret; it is possible that the choice of materials may have been totally random and any 'suitable' resources readily available would have been used. The lack of compositional variation in the clay/vegetable ash samples as opposed to the greater variation in excipient composition in the bone ash samples would suggest that a stricter recipe was used for clay/vegetable ash than bone ash. Perhaps any material was used to supplement the bone ash litharge to act as a binding agent as opposed to a deliberate effort to make the lining more absorbent.

It is easy to interpret data to suit/create numerous and wonderful hypotheses but rarely can they be fully proven. There may be numerous reasons for the patterns and anomalies extrapolated from the data and by trying to fit them into our obsession for 'common sense' we may forget that there may not be a well fitting theory or that our modern view on the subject/technology puts certain past human choices and actions out of our reach/understanding. To a further extent our greater scientific knowledge on material properties may put us at a disadvantage overshadowing other, less scientifically obvious factors.

CONCLUSION

Studies conducted by Bayley and Eckstein (2006) and Bayley (2009) pointed to differences between the efficiency of Roman and medieval cupellation. It was suggested that the PbO/Cu_2O ratio in litharge cakes directly reflected the efficiency of the process and the analyses of nine litharge cake fragments revealed higher PbO/Cu_2O ratios in medieval than Roman examples. This led to the hypothesis that cupellation in the medieval period was more successful/advanced than in Roman times.

Microstructural and chemical analyses were conducted on 45 Roman and medieval litharge cake fragments. This study has found no correlation between date and efficiency, relating to the PbO/Cu_2O ratios. The Roman and medieval litharge analysed displayed varying PbO/Cu_2O ratios. The chemical analyses revealed two major original hearth lining compositional groups; a clay/vegetable ash mixture and pure bone ash. The results also found no correlation between efficiency and original hearth lining composition. However, in contradiction to previous studies (based on cupels) it is apparent that the clay/vegetable ash hearth lining was more absorbent than the pure bone ash.

Another point of interest is the fact that the majority of the medieval litharge cakes seem to be composed of clay/vegetable ash while their Roman counterparts comprise of a mixture of the two main compositions. It has been suggested here that this may have

been due in part to cultural traditions or that the hearth lining material was chosen for specific tasks exploiting the benefits of the raw materials. For example, the seemingly more absorbent and easier to produce clay/vegetable ash may have been preferred for larger scale cupellation. The chosen materials may have offered better benefits to specific metals refined. It is also possible that the materials employed were chosen purely on availability as opposed to any beneficial properties of specific recipes. Unfortunately the fragmentary nature of the archaeological material and unreliability of contextual information does not permit further interpretation.

The study highlighted the importance of suitable sampling. The compositional variation within litharge cakes was examined on a horizontal (length) and vertical (depth) plane. Although no major variation was noticed on the horizontal plane the PbO/Cu₂O ratio did vary dramatically on the vertical plane. This means that to get a representative PbO/Cu₂O ratio, sampling must comprise the majority of the litharge cake's depth. These analyses also revealed that the litharge cakes were made to one recipe and not layered with different materials.

Future studies should include the comparison of these findings to other published litharge cake analyses. The analysis of more, well dated litharge cakes would be very useful and would permit reassessment of the differences or similarities of Roman and medieval cupellation. One aspect of further interest could be pinpointing the exact recipes used for hearth linings which may involve expanding the chemical datasets currently available for vegetable ashes. Experimental studies should be undertaken in future to examine the behaviour of metals and oxides within litharge cakes. Comparative studies of the experimental work and archaeological litharge cakes may advance our understanding of large scale cupellation and provide information on the material and technological choices and practices of past artisans.

REFERENCES

- Bayley, J 2008a 'Medieval precious metal refining: archaeology and contemporary texts compared', in Martín-Torres, M and Rehren, T (eds), *Archaeology, History and Science: Integrating Approaches to Ancient Materials*. London: Institute of Archaeology Press UCL, 131–150
- Bayley, J 2008b *Lincoln: Evidence for Metalworking on Flaxengate and Other Sites in the City*. Research Department Report 67-2008. Portsmouth: English Heritage
- Bayley, J 2009 'Understanding litharge cakes', paper presented at the HMS Archaeometallurgy conference, University of Bradford, 10-12th November 2009

Bayley, J and Eckstein, K 1997 'Silver refining - production, recycling, assaying', in Sinclair, A Slater, E and Gowlett, J (eds), *Archaeological Sciences 1995*. Oxford: Oxbow Monograph 64, 107–11

Bayley, J and Eckstein, K 2006 'Roman and medieval litharge cakes: structure and composition', in Pérez-Arantegui, J (ed), *34th International Symposium on Archaeometry, 3-7 May 2004, Zaragoza, Spain*. Zaragoza: Institución "Fernando el Católico", 145–153

Cau Ontiveros, M A, Day, P M and Montana, G 2002 'Secondary calcite in archaeological ceramics: evaluation of alteration and contamination processes by thin section study', in Kilikogiou, V Maniatis, A and Hein, A (eds), *Modern Trends in Scientific Studies on Ancient Ceramics: EMAC 99 Proceedings of the European meeting on Ancient Ceramics, Athens*. Oxford: BAR 1011, 9–18

Cunliffe, B and Poole, C 2008 *The Danebury Environs Roman Programme. A Wessex Landscape During the Roman Era*. Vol. 2 - Part 7: Dunkirt Barn, Abbots Ann, Hants, 2005 and 2006. English heritage and Oxford University School of Archaeology Monograph 7. Oxford: Oxford University School of Archaeology

Dungworth, D 2000 'A note on the analysis of crucibles and moulds'. *Historical Metallurgy* 34, 83–86

Hawthorne, J G and Smith, C S 1979 *Theophilus: On Divers Arts*. New York: Dover

Hoover, H C and Hoover, L H 1950 *Georgius Agricola: De re metallica*. New York: Dover

Jackson, C M and Booth, CA and Smedley, J W 2005 'Glass by design? Raw materials, recipes and compositional data'. *Archaeometry* 47, 781–795

Kassianidou, V 2003 'Early extraction of silver ores from complex polymetallic ores', in Craddock, P and Lang, J (eds) *Mining and Metal Production Through the Ages*. London: The British Museum Press, 198–206

Martinón-Torres, M, Thomas, N, Rehren, T and Mongiatti, A 2008 'Some problems and potentials of the study of cupellation remains: the case of early modern Montbéliard, France'. *Archaeoscience: Revue d'Archeometrie* 32, 59–70

Martinón-Torres, M, Thomas, N, Rehren, T and Mongiatti, A 2009 'Identifying materials, recipes and choices: some suggestions for the study of archaeological cupels', in Giunliamair, A, Craddock, P, Hauptmann, A, Bayley, J, Cavallini, M, Garagnani, G, Gilmour, B, La Niece, S, Nicodemi, W and Rehren, T (eds) *Archaeometallurgy in Europe 2007: Selected Papers from 2nd International Conference, Aquileia, Italy, 17–21 June*. Milano: Associazione Italiana di Metallurgia, 435–445

Nriagu, J O 1985 'Cupellation: the oldest quantitative chemical process'. *Journal Chemical Education* 62, 668–674

Riche, A and Gelis, E 1888 *L'art de l'essayeur*. Paris: Bailliere et fils

Sanderson, D C W and Hunter, J R 1981 'Composition variability in vegetable ash'. *Science and Archaeology* 23, 27–30

Smith, C S and Gnudi, M T 1990 *The Pirotechnia of Vannoccio Biringuccio: The Classic Sixteenth-Century Treatise on Metals and Metallurgy*. New York: Dover Publications

Stem, W B and Gerber, Y 2004 'Potassium-calcium glass: new data and experiments'. *Archaeometry* 46.1, 137–156

Tereygeol, F and Thomas, N 2003 'La coupellation des alliage cuivre-argent: approche experimentale de l'essai d'argent par voie seche'. *Revue d'Archeometrie* 27, 171–181

Turner, W E S 1956 'Studies in ancient glasses and glassmaking processes. Part V. Raw materials and melting processes'. *Journal of the Society of Glass Technology*, 277–300

Tzaphlidou, M and Zaichick, V 2002 'Neutron activation analysis of calcium/phosphorous ratio in rib bone of healthy humans'. *Applied Radiation and Isotopes* 57, 779–783

White, H 2010a *Grange Road, Bermondsey, London: Scientific Examination of the Cupels*. Research Department Report 91-2010, Portsmouth: English Heritage

White, H 2010b *Legge's Mount, The Tower of London, London: Scientific Examination of the Cupels*. Research Department Report 57-2010, Portsmouth: English Heritage

Zaichick, V and Tzaphlidou, M 2002 'Determination of calcium, phosphorous, and the calcium/phosphorous ratio in cortical bone from the human femoral neck by neutron activation analysis'. *Applied Radiation and Isotopes* 56, 781–786

APPENDIX I. LITHARGE FRAGMENT PHOTOGRAPHS

Photographs taken by Roger Wilkes.



Lith01



Lith01



Lith02



Lith02



Lith03



Lith03



Lith04



Lith04



Lith05



Lith05



Lith06



Lith06



Lith07



Lith07



Lith08



Lith08



Lith09



Lith09



Lith 10



Lith 10



Lith 11



Lith 11



Lith 12



Lith 12



Lith 13



Lith 13



Lith 14



Lith 14



Lith 15



Lith 15



Lith 16



Lith 16



Lith 17



Lith 18



Lith 18



Lith19



Lith20



Lith20



Lith21



Lith21



Lith22



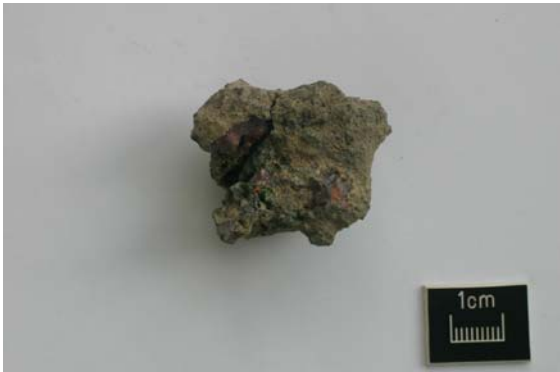
Lith22



Lith23



Lith23



Lith24



Lith24



Lith25



Lith25



Lith26



Lith26



Lith27



Lith27



Lith28



Lith28



Lith29



Lith29



Lith30



Lith30



Lith32



Lith32



Lith33



Lith33



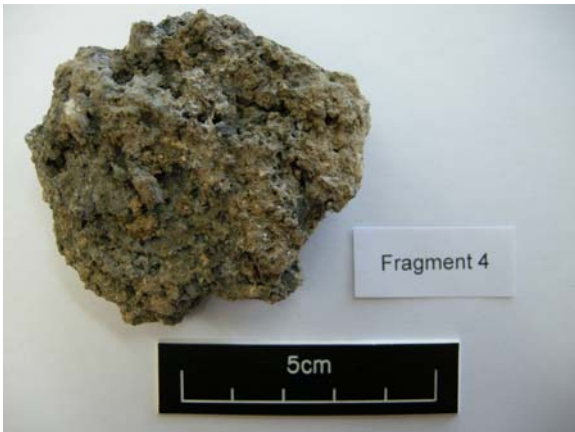
Lith34



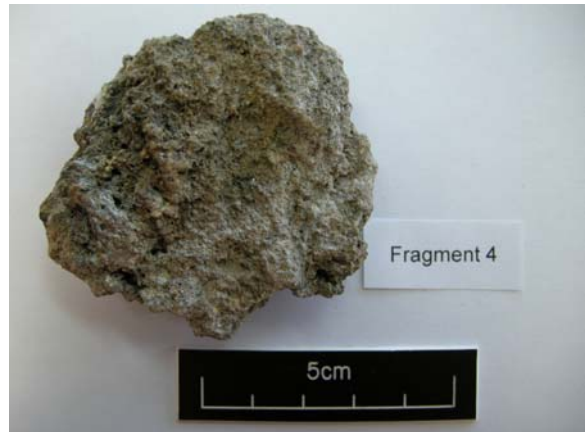
Lith36



Lith36



Lith37



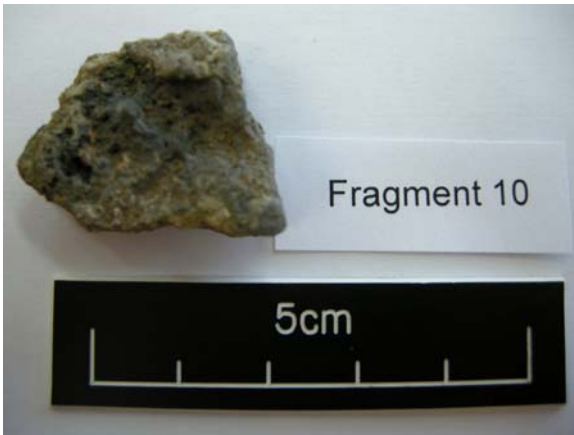
Lith37



Lith38



Lith38



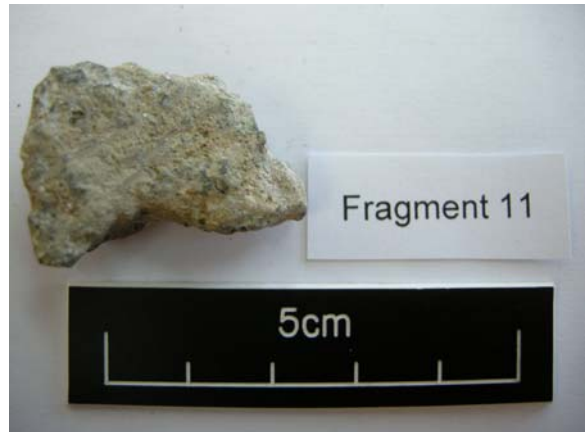
Lith39



Lith39



Lith40



Lith40

APPENDIX 2. LOW MAGNIFICATION MACROSCOPIC LITHARGE SAMPLE PHOTOGRAPHS

All sample mounts are 30mm unless otherwise stated. For the large rectangular samples the length of the fragment section is given. All photographs taken by Roger Wilkes.



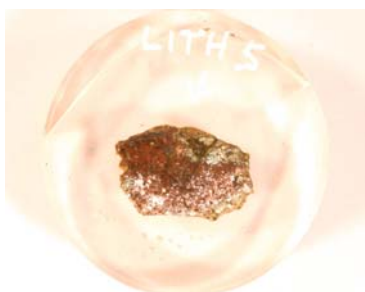
Lith01



Lith02



Lith03



Lith05



Lith06 – 64mm



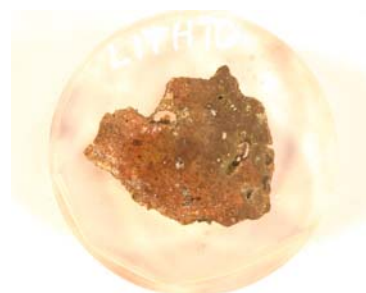
Lith07



Lith08



Lith09



Lith10



Lith11



Lith12



Lith13



Lith14



Lith15



Lith16 – 69mm



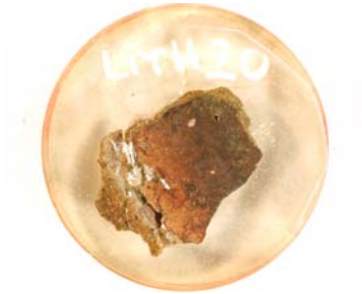
Lith17 – 55mm



Lith18



Lith19 – 78mm



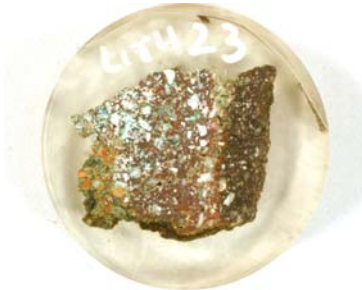
Lith20



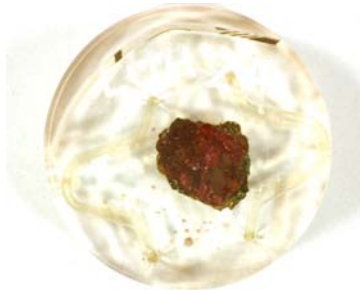
Lith21



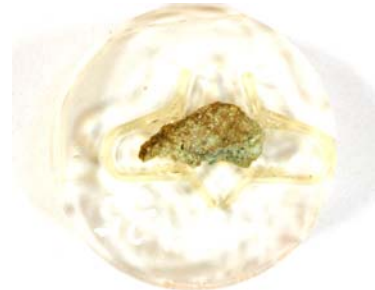
Lith22



Lith23



Lith24



Lith25



Lith26



Lith27



Lith29



Lith30



Lith31



Lith33



Lith34



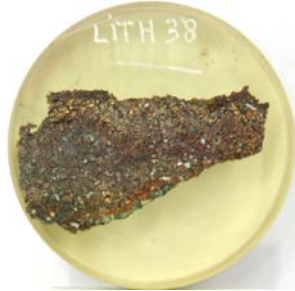
Lith35



Lith36



Lith37 – 40mm



Lith38 – 40mm



Lith39



Lith40



Lith41



Lith42



CGI, 2 and 3

APPENDIX 3. STANDARD DATA

Standard DLH1

Spectra	Na ₂ O	MgO	Al ₂ O ₃	SiO ₂	K ₂ O	CaO	Fe ₂ O ₃	PbO
1	0.96	0.37	3.87	24.70	0.97	1.01	0.94	67.20
2	1.13	0.26	3.99	24.67	0.97	1.09	0.92	66.97
3	1.00	0.35	3.94	24.50	1.06	1.02	0.97	67.16
4	0.99	0.26	4.04	24.66	0.89	1.05	1.00	67.12
5	1.10	0.21	3.99	24.71	0.97	1.04	0.93	67.05
6	1.10	0.28	3.93	24.72	0.99	0.98	0.88	67.11
7	1.13	0.20	4.09	24.68	0.96	1.04	0.83	67.06
8	1.05	0.25	4.04	24.63	0.96	1.04	0.93	67.09
9	1.13	0.18	4.06	24.58	0.97	1.05	0.95	67.07
10	1.18	0.28	4.07	24.73	0.98	1.05	0.96	66.75
Mean	1.08	0.27	4.00	24.66	0.97	1.04	0.93	67.06
Reported	1.01	0.33	3.98	24.96	0.96	1.04	0.98	67.04

Standard DLH2

Spectra	Na ₂ O	MgO	Al ₂ O ₃	SiO ₂	K ₂ O	CaO	Fe ₂ O ₃	CoO	SnO ₂	PbO
1	7.75	0.87	3.96	39.35	2.85	3.01	0.87	0.41	3.77	37.17
2	7.64	0.88	3.98	39.33	2.95	2.96	0.89	0.41	4.03	36.92
3	7.71	0.85	4.40	39.35	2.85	2.91	0.98	0.39	3.95	36.60
4	7.69	0.92	3.88	39.45	2.86	2.99	1.01	0.45	3.86	36.89
5	7.70	0.96	3.97	39.25	2.90	2.93	0.94	0.46	3.98	36.90
6	7.76	0.96	4.23	39.25	2.92	2.85	0.85	0.40	3.97	36.80
7	7.68	0.79	4.41	39.22	2.94	2.91	0.94	0.42	4.04	36.64
8	7.65	0.86	4.07	39.40	2.86	3.03	0.94	0.42	3.85	36.93
9	7.62	0.91	3.83	39.48	2.85	2.99	0.91	0.40	4.15	36.84
10	7.55	0.96	3.86	39.49	2.90	2.95	0.87	0.43	3.87	37.14
Mean	7.68	0.90	4.06	39.36	2.89	2.95	0.92	0.42	3.95	36.88
Reported	7.34	0.89	4.15	40.05	2.79	2.88	0.91	0.39	4.06	36.36

Standard Apatite (1379 MAC)

Spectra	Na ₂ O	MgO	Al ₂ O ₃	Si ₂ O	P ₂ O ₅	CaO	MnO	FeO	La ₂ O ₃	Ce ₂ O ₃	PbO	F
1	0.30	0.07	0.03	0.43	40.84	53.47	0.00	0.13	0.31	0.48	0.11	4.30
2	0.32	0.02	0.06	0.35	40.65	53.43	0.00	0.02	0.53	0.55	0.24	4.35
3	0.33	0.02	0.02	0.40	40.87	53.44	0.00	0.01	0.33	0.57	0.19	4.13
4	0.35	0.00	0.04	0.42	40.56	53.75	0.03	0.02	0.41	0.44	0.16	3.73
5	0.27	0.07	0.05	0.41	40.84	53.36	0.01	0.03	0.45	0.42	0.25	5.09
6	0.37	0.09	0.00	0.48	41.19	52.96	0.02	0.04	0.33	0.50	0.20	4.86
7	0.37	0.05	0.09	0.43	40.40	53.71	0.00	0.04	0.43	0.47	0.19	3.80
Mean	0.33	BDL	BDL	0.42	40.76	53.45	BDL	BDL	0.40	0.49	0.19	4.32
Reported	0.29	0.01	0.02	0.26	42.24	53.90	0.01	0.02	0.53	0.60	0.24	3.75

APPENDIX 4. STRATIGRAPHIC BULK DATA

Bulk data taken from top to bottom in the most complete litharge cake samples.

Lith02

(mm)	MgO	Al ₂ O ₃	SiO ₂	P ₂ O ₅	K ₂ O	CaO	MnO	Fe ₂ O ₃	Cu ₂ O	AgO	SnO ₂	PbO
0.0	0.9	0.1	5.1	1.3	0.1	7.7	0.0	0.0	6.7	<0.1	0.1	78.0
0.8	1.1	0.1	5.3	1.1	0.1	7.8	0.0	0.0	10.1	<0.1	<0.1	74.3
1.6	1.1	0.2	4.5	0.6	0.1	5.1	0.0	0.0	12.0	<0.1	<0.1	76.5
2.5	1.0	0.6	5.1	1.2	0.3	4.7	0.0	0.0	9.6	<0.1	<0.1	77.6
3.3	1.3	1.2	5.8	1.1	0.8	5.6	0.0	0.1	6.6	<0.1	<0.1	77.5
4.1	1.2	1.1	6.3	1.3	0.7	5.5	0.1	0.1	6.8	<0.1	<0.1	76.9
4.9	0.8	1.1	9.2	1.1	0.9	6.3	0.2	0.2	4.2	<0.1	<0.1	76.0
5.8	0.9	1.2	10.0	1.0	0.9	6.6	0.1	0.4	3.7	<0.1	<0.1	75.1
6.6	0.9	0.9	9.9	0.9	0.8	12.2	0.2	0.4	4.1	<0.1	<0.1	69.7
7.4	1.1	1.0	11.2	0.7	0.8	9.6	0.1	0.3	4.2	0.1	0.1	70.8
8.2	1.2	1.1	10.3	1.2	0.9	9.1	0.3	0.5	3.7	<0.1	<0.1	71.6
9.1	0.9	1.3	8.1	3.7	1.0	5.6	0.1	1.0	2.9	<0.1	<0.1	75.4

Lith03

(mm)	MgO	Al ₂ O ₃	SiO ₂	P ₂ O ₅	K ₂ O	CaO	MnO	Fe ₂ O ₃	Cu ₂ O	AgO	SnO ₂	PbO
0.0	0.6	0.1	5.0	1.1	<0.1	3.7	<0.1	<0.1	8.0	<0.1	<0.1	81.6
0.8	0.9	0.4	9.0	1.0	0.6	10.7	0.1	0.1	7.6	0.1	<0.1	69.8
1.6	0.9	0.9	9.5	0.9	1.2	9.3	0.1	0.1	7.0	<0.1	0.1	70.0
2.5	1.5	2.1	11.8	0.9	1.7	7.1	0.2	0.3	5.4	<0.1	0.2	68.8
3.3	1.7	1.3	9.0	0.9	0.6	15.1	0.1	0.2	6.0	<0.1	0.4	64.7
4.1	1.9	1.0	7.2	1.3	0.2	23.5	0.2	0.1	4.3	<0.1	0.3	60.1
4.9	1.7	1.1	6.8	1.0	0.1	22.1	0.2	0.5	4.2	<0.1	0.2	62.1
5.8	1.7	1.0	6.1	1.2	0.1	25.4	0.3	0.3	4.3	<0.1	0.3	59.3
6.6	1.7	1.3	7.6	1.7	0.2	24.2	0.3	0.8	2.7	<0.1	0.2	59.2
7.4	1.4	1.6	11.6	5.7	0.3	30.1	0.5	1.3	1.8	<0.1	0.1	45.6
8.2	1.6	2.2	19.9	8.3	0.5	43.0	0.6	1.6	1.2	<0.1	<0.1	21.2

Lith05

(mm)	MgO	Al ₂ O ₃	SiO ₂	P ₂ O ₅	K ₂ O	CaO	MnO	Fe ₂ O ₃	Cu ₂ O	AgO	SnO ₂	PbO
0.0	<0.1	0.1	2.7	0.7	0.1	3.5	<0.1	0.1	9.7	<0.1	<0.1	83.0
0.8	0.6	0.1	6.5	1.4	0.7	10.2	<0.1	0.1	8.8	<0.1	<0.1	71.7
1.6	0.7	<0.1	6.9	1.1	0.8	13.2	<0.1	<0.1	8.7	0.1	<0.1	68.4
2.5	1.4	0.1	7.9	1.5	1.2	14.9	0.1	0.1	12.0	0.3	0.1	60.6
3.3	0.7	0.2	6.1	1.0	0.9	11.0	<0.1	<0.1	21.9	0.8	<0.1	57.4
4.1	1.3	0.2	7.3	1.1	1.1	13.3	<0.1	<0.1	15.2	0.4	0.1	60.0
4.9	1.3	0.1	7.7	1.2	0.8	11.4	<0.1	<0.1	14.7	<0.1	<0.1	62.7
5.8	1.7	0.2	8.6	1.4	0.1	4.3	<0.1	0.1	12.1	<0.1	<0.1	71.4
6.6	1.1	0.6	7.7	1.0	0.2	1.9	0.1	0.1	9.7	<0.1	<0.1	77.7
7.4	1.2	0.8	7.2	1.2	0.3	2.3	0.1	0.1	7.5	0.1	<0.1	79.3
8.2	1.5	1.0	7.1	1.1	0.2	2.2	0.1	<0.1	4.9	<0.1	<0.1	81.8

Lith06

(mm)	MgO	Al ₂ O ₃	SiO ₂	P ₂ O ₅	K ₂ O	CaO	MnO	Fe ₂ O ₃	Cu ₂ O	AgO	SnO ₂	PbO
0.0	0.5	<0.1	1.7	0.7	0.1	2.8	<0.1	<0.1	4.7	<0.1	<0.1	89.4
0.8	0.6	0.1	2.0	0.7	<0.1	3.1	<0.1	0.1	4.4	<0.1	<0.1	89.1
1.6	0.1	0.1	0.8	0.5	<0.1	1.3	<0.1	<0.1	4.6	0.1	0.1	92.4
2.5	<0.1	0.1	0.6	0.4	<0.1	1.2	<0.1	0.1	4.6	<0.1	<0.1	92.9
3.3	<0.1	<0.1	0.7	0.4	<0.1	1.0	0.1	<0.1	3.3	<0.1	<0.1	94.5
4.1	<0.1	<0.1	0.7	0.4	<0.1	0.8	<0.1	<0.1	3.5	<0.1	<0.1	94.6
4.9	<0.1	0.1	0.7	0.5	<0.1	0.7	<0.1	<0.1	3.5	<0.1	<0.1	94.5
5.8	0.1	0.1	0.7	0.5	<0.1	0.9	<0.1	<0.1	1.9	<0.1	<0.1	95.7
6.6	0.1	<0.1	0.8	0.4	<0.1	0.7	<0.1	<0.1	2.3	<0.1	<0.1	95.7
7.4	0.6	0.2	3.8	0.8	0.1	6.8	<0.1	<0.1	2.7	0.1	<0.1	84.9
8.2	2.4	<0.1	6.8	0.9	0.2	11.6	<0.1	0.1	4.4	<0.1	<0.1	73.5
9.1	1.8	0.1	5.9	0.9	0.2	10.5	<0.1	<0.1	4.0	0.1	<0.1	76.5
9.9	1.9	<0.1	5.4	1.5	0.2	10.2	<0.1	<0.1	3.9	<0.1	<0.1	76.9
10.7	1.4	<0.1	5.4	1.1	0.1	8.5	<0.1	0.1	2.9	0.1	<0.1	80.4
11.5	1.7	0.1	4.9	2.0	0.2	10.1	<0.1	<0.1	3.7	<0.1	0.1	77.2
12.4	2.4	<0.1	5.6	0.9	0.1	8.3	<0.1	<0.1	4.8	<0.1	<0.1	77.9
13.2	1.5	<0.1	5.4	0.9	<0.1	10.0	0.1	<0.1	5.5	<0.1	<0.1	76.6
14.0	1.8	0.1	5.4	0.8	0.1	12.2	<0.1	<0.1	4.1	<0.1	<0.1	75.4
14.8	3.2	<0.1	5.7	1.3	0.2	9.4	<0.1	<0.1	4.7	<0.1	<0.1	75.5
15.7	2.2	0.2	4.9	1.0	0.3	15.4	<0.1	<0.1	4.8	0.1	<0.1	71.2
16.5	1.4	0.1	4.8	0.9	<0.1	12.6	<0.1	<0.1	4.3	<0.1	<0.1	75.7
17.3	1.6	0.2	5.1	1.1	0.2	8.6	<0.1	0.1	4.3	<0.1	<0.1	78.9
18.1	1.5	0.2	4.8	0.8	<0.1	6.1	<0.1	<0.1	4.4	<0.1	<0.1	82.2
19.0	1.8	0.2	5.0	0.9	<0.1	6.2	<0.1	<0.1	4.9	<0.1	<0.1	80.8
19.8	1.8	0.7	5.3	0.7	<0.1	6.9	<0.1	<0.1	4.6	<0.1	0.1	79.9
20.6	1.5	1.5	5.1	0.8	<0.1	7.8	<0.1	0.1	3.3	<0.1	<0.1	79.9
21.4	2.1	1.6	5.4	1.0	0.1	8.4	<0.1	0.1	3.5	<0.1	<0.1	77.6
22.3	1.9	1.0	5.4	0.7	<0.1	5.5	<0.1	<0.1	4.5	<0.1	<0.1	80.9
23.1	1.5	1.0	5.0	1.0	<0.1	5.2	<0.1	0.1	3.7	<0.1	<0.1	82.6
23.9	1.6	1.4	4.6	0.8	<0.1	5.7	<0.1	<0.1	3.4	<0.1	<0.1	82.5
24.7	1.4	1.2	4.8	0.6	0.1	6.9	<0.1	<0.1	3.7	<0.1	<0.1	81.3
25.6	1.9	1.2	5.1	0.9	0.1	8.0	0.1	<0.1	3.6	0.1	<0.1	79.0
26.4	2.3	1.0	5.0	1.1	<0.1	7.9	<0.1	0.1	3.9	<0.1	<0.1	78.7
27.2	3.0	1.3	6.0	0.8	0.1	12.5	0.1	<0.1	3.1	<0.1	<0.1	73.1
28.0	1.3	0.6	2.8	0.5	<0.1	6.6	<0.1	<0.1	2.1	0.3	<0.1	85.8
28.8	<0.1	<0.1	0.7	0.4	<0.1	0.8	<0.1	<0.1	0.8	0.8	<0.1	96.4
29.7	0.4	0.2	1.6	0.5	<0.1	5.3	<0.1	<0.1	2.0	0.3	<0.1	89.7
30.5	1.3	0.9	4.2	1.2	0.3	10.8	0.1	0.2	2.6	<0.1	<0.1	78.5
31.3	0.6	0.7	3.7	0.7	0.1	8.8	0.1	<0.1	4.2	0.3	<0.1	80.7
32.1	0.2	0.3	1.7	0.4	0.3	4.1	<0.1	<0.1	3.0	0.4	0.1	89.4
33.0	1.0	0.7	4.4	0.8	0.3	6.7	0.1	0.1	2.8	0.2	<0.1	82.9
33.8	2.2	1.7	7.0	0.9	1.4	10.7	0.3	0.2	3.6	<0.1	0.2	71.8
34.6	2.0	1.9	8.9	0.9	1.3	10.2	0.2	0.3	2.9	<0.1	<0.1	71.3
35.4	1.0	2.0	5.5	0.9	1.2	5.5	<0.1	0.1	3.5	0.1	<0.1	80.3

Lith07

(mm)	MgO	Al ₂ O ₃	SiO ₂	P ₂ O ₅	K ₂ O	CaO	MnO	Fe ₂ O ₃	Cu ₂ O	AgO	SnO ₂	PbO
0.0	0.5	0.4	5.6	0.7	0.2	1.5	<0.1	<0.1	23.9	0.5	<0.1	66.6
0.8	0.7	1.0	6.4	1.1	0.4	3.0	0.1	0.1	17.2	0.1	<0.1	69.9
1.6	0.8	1.0	6.7	1.0	0.5	4.3	0.1	0.2	16.2	<0.1	0.2	69.0
2.5	0.9	1.0	7.8	0.9	0.3	3.7	<0.1	0.2	18.2	<0.1	<0.1	66.8
3.3	0.9	1.1	9.0	1.3	0.5	5.4	0.1	0.4	17.9	<0.1	<0.1	63.5
4.1	1.1	1.6	11.4	1.2	0.8	7.3	<0.1	0.3	11.6	<0.1	<0.1	64.7
4.9	1.0	1.5	15.5	2.9	0.7	9.8	0.1	0.8	4.5	<0.1	0.1	63.0
5.8	1.0	2.8	23.5	4.6	1.3	10.9	0.1	1.9	1.2	<0.1	0.1	52.7

Lith08

(mm)	MgO	Al ₂ O ₃	SiO ₂	P ₂ O ₅	K ₂ O	CaO	MnO	Fe ₂ O ₃	Cu ₂ O	AgO	SnO ₂	PbO
0.0	1.2	<0.1	6.2	1.3	0.2	8.2	<0.1	0.1	12.2	0.2	<0.1	70.4
0.8	1.5	<0.1	6.0	1.2	0.3	8.4	<0.1	<0.1	12.8	0.7	<0.1	68.9
1.6	2.0	1.0	7.4	1.0	0.8	8.5	0.1	0.1	17.4	0.2	<0.1	61.7
2.5	1.6	2.1	7.5	0.8	1.4	8.3	<0.1	<0.1	20.0	0.2	<0.1	58.1
3.3	2.3	1.6	9.2	1.3	1.8	11.5	<0.1	0.1	16.5	0.1	<0.1	55.5
4.1	1.9	1.4	8.2	1.0	1.4	8.8	0.1	0.1	18.2	0.1	<0.1	58.9
4.9	1.3	1.2	8.1	0.8	0.9	6.9	0.1	<0.1	18.9	0.2	0.1	61.5
5.8	1.4	1.0	8.6	1.2	0.9	8.6	0.1	0.1	13.9	0.2	<0.1	64.1
6.6	1.7	1.5	9.7	1.2	1.6	8.6	0.2	0.3	8.9	<0.1	<0.1	66.4
7.4	1.3	1.7	9.7	1.6	1.7	7.0	0.1	0.2	6.1	<0.1	<0.1	70.6
8.2	1.3	1.6	9.6	1.5	1.7	7.9	0.1	0.3	4.9	<0.1	0.1	71.1
9.1	1.3	1.0	8.9	1.5	1.1	9.1	0.1	0.2	3.5	0.1	<0.1	73.2
9.9	1.1	1.1	8.0	0.9	1.1	8.6	0.1	0.3	4.4	<0.1	<0.1	74.4
10.7	1.3	1.4	8.4	0.7	1.3	11.9	0.2	0.5	5.0	0.1	<0.1	69.4
11.5	1.6	1.1	10.6	0.9	1.2	11.4	0.2	0.6	3.9	<0.1	0.2	68.4
12.4	2.1	1.1	14.0	1.2	1.3	10.7	0.2	0.8	2.8	<0.1	0.2	65.6
13.2	2.3	1.0	12.1	1.3	1.0	8.1	0.2	0.9	2.8	<0.1	0.1	70.3
14.0	0.9	0.7	8.1	1.3	0.6	21.3	0.2	0.5	3.2	<0.1	0.1	63.1
14.8	0.7	0.9	7.0	6.5	0.5	22.8	0.2	1.3	2.0	0.1	0.1	58.0

Lith10

(mm)	MgO	Al ₂ O ₃	SiO ₂	P ₂ O ₅	K ₂ O	CaO	MnO	Fe ₂ O ₃	Cu ₂ O	AgO	SnO ₂	PbO
0.0	0.2	0.3	4.2	3.2	<0.1	4.0	<0.1	0.2	10.1	<0.1	<0.1	77.8
0.8	0.5	0.4	7.4	1.4	0.1	2.8	<0.1	0.1	14.1	0.2	0.1	73.1
1.6	0.7	0.1	5.5	0.9	0.3	4.9	<0.1	<0.1	18.3	0.3	<0.1	68.9
2.5	0.2	0.1	3.1	1.2	0.1	2.9	<0.1	0.1	18.2	0.3	<0.1	74.0
3.3	0.3	<0.1	3.6	3.4	<0.1	2.7	<0.1	0.3	11.9	<0.1	<0.1	77.9
4.1	<0.1	0.2	3.6	2.0	<0.1	3.1	<0.1	0.2	15.5	0.2	0.3	74.9
4.9	0.4	0.1	4.4	1.0	0.1	2.5	<0.1	<0.1	18.9	0.2	<0.1	72.4
5.8	1.6	0.5	5.0	0.9	0.3	5.5	0.1	<0.1	21.4	0.3	0.3	64.1
6.6	1.8	0.9	6.2	0.9	0.6	7.0	<0.1	<0.1	20.8	0.2	0.1	61.6
7.4	1.4	1.5	6.6	0.8	1.1	7.0	<0.1	<0.1	18.3	0.3	0.1	62.9
8.2	0.8	0.2	2.7	0.5	<0.1	2.5	<0.1	<0.1	47.1	0.6	<0.1	45.6
9.1	0.8	0.1	2.5	0.5	<0.1	2.4	<0.1	<0.1	43.5	0.1	<0.1	50.0
9.9	1.1	0.8	4.1	0.7	0.4	4.0	<0.1	<0.1	26.7	<0.1	<0.1	62.2
10.7	0.9	1.3	4.1	0.6	0.7	4.0	<0.1	<0.1	24.1	0.1	0.1	64.0
11.5	1.6	1.4	6.5	0.8	1.1	7.3	0.1	0.1	19.3	<0.1	<0.1	61.9
12.4	1.7	1.4	6.9	0.9	1.2	7.8	0.1	<0.1	15.6	<0.1	0.1	64.3
13.2	1.6	1.4	7.1	1.0	1.4	8.2	0.1	0.1	13.3	<0.1	0.2	65.6
14.0	1.6	1.5	7.7	1.0	1.8	9.3	0.2	0.1	9.5	<0.1	0.1	67.2
14.8	1.3	1.8	6.9	0.9	1.8	6.7	0.2	0.1	9.7	<0.1	<0.1	70.6
15.7	1.0	1.6	6.9	1.2	1.4	5.2	0.1	0.1	7.8	<0.1	<0.1	74.7
16.5	0.4	1.7	7.4	1.2	1.3	2.3	0.1	0.1	7.0	0.1	0.2	78.2
17.3	0.9	1.2	7.1	1.5	0.7	4.0	<0.1	0.1	5.7	<0.1	0.1	78.7
18.1	1.1	1.2	7.2	1.7	0.4	3.9	0.1	0.2	4.7	<0.1	<0.1	79.6

Lith13

(mm)	MgO	Al ₂ O ₃	SiO ₂	P ₂ O ₅	K ₂ O	CaO	MnO	Fe ₂ O ₃	Cu ₂ O	AgO	SnO ₂	PbO
0.0	1.6	2.3	14.3	5.0	1.6	16.3	<0.1	0.8	13.9	2.6	<0.1	41.5
0.8	1.4	1.2	13.4	1.3	1.0	21.8	<0.1	0.2	17.1	1.3	0.2	41.1
1.6	3.3	0.4	11.1	2.7	0.2	19.7	0.1	0.3	15.0	1.3	0.2	45.7
2.5	2.2	0.5	10.8	2.4	0.2	18.4	0.1	0.3	14.9	0.8	<0.1	49.4
3.3	1.4	0.6	9.2	1.0	0.1	14.5	0.1	0.3	14.0	0.8	<0.1	58.0
4.1	2.2	1.3	11.0	1.0	0.1	4.9	0.1	0.1	27.4	0.8	<0.1	51.2
4.9	2.2	1.4	10.9	1.2	0.3	3.5	0.1	0.2	16.9	0.4	<0.1	63.1
5.8	2.5	1.8	12.2	1.1	0.8	4.3	0.1	0.4	10.2	0.2	0.2	66.2
6.6	2.5	2.1	12.6	1.3	0.7	13.2	0.1	0.6	9.3	<0.1	<0.1	57.6
7.4	2.2	2.2	11.4	1.0	0.9	10.6	0.1	0.5	13.5	<0.1	<0.1	57.4
8.2	2.2	2.0	13.3	0.9	0.7	2.1	0.1	0.5	18.9	0.2	<0.1	59.1
9.1	2.6	1.9	14.4	1.1	0.5	2.7	0.1	0.7	16.3	0.1	<0.1	59.8
9.9	1.9	2.2	10.2	1.2	0.4	4.8	0.2	0.3	12.8	<0.1	<0.1	66.0

Lith16

(mm)	MgO	Al ₂ O ₃	SiO ₂	P ₂ O ₅	K ₂ O	CaO	MnO	Fe ₂ O ₃	Cu ₂ O	AgO	SnO ₂	PbO
0.0	0.2	<0.1	0.7	12.9	<0.1	20.4	0.1	<0.1	10.4	1.1	2.8	51.3
0.8	0.2	0.1	0.8	11.6	0.1	19.6	0.1	<0.1	9.1	2.0	1.5	54.9
1.6	0.3	0.1	0.7	15.9	<0.1	25.9	<0.1	0.1	6.9	7.1	0.4	42.7
2.5	0.3	<0.1	0.8	14.4	<0.1	22.7	<0.1	<0.1	12.3	4.8	0.9	43.7
3.3	0.2	0.1	0.7	14.5	<0.1	17.9	<0.1	<0.1	38.6	5.9	0.2	21.9
4.1	0.2	0.1	0.7	13.4	0.1	20.0	0.1	<0.1	22.5	1.7	0.5	41.0
4.9	0.2	<0.1	0.7	17.6	0.2	24.7	<0.1	<0.1	24.3	1.3	1.0	29.9
5.8	0.2	<0.1	0.8	13.7	0.2	19.7	<0.1	<0.1	26.3	1.8	0.7	36.5
6.6	0.2	<0.1	0.7	9.0	0.2	12.7	<0.1	<0.1	33.2	2.2	0.4	41.5
7.4	0.3	<0.1	0.9	14.6	0.2	23.3	<0.1	<0.1	15.3	0.7	1.2	43.3
8.2	0.3	<0.1	1.0	12.6	0.3	19.3	<0.1	<0.1	21.8	0.9	1.0	42.8
9.1	0.4	<0.1	0.7	15.6	0.2	23.4	<0.1	0.1	21.5	0.9	0.7	36.5
9.9	0.3	<0.1	1.2	15.7	0.3	23.7	<0.1	<0.1	20.7	0.7	0.8	36.6
10.7	0.3	0.1	1.8	14.0	0.5	22.4	<0.1	<0.1	17.4	0.5	0.4	42.8
11.5	0.4	<0.1	1.6	12.4	0.3	18.7	<0.1	<0.1	26.7	0.9	0.2	38.7
12.4	0.3	<0.1	1.6	16.4	0.4	24.1	<0.1	<0.1	23.6	0.5	0.6	32.5
13.2	0.3	<0.1	0.7	23.7	0.1	34.0	0.1	0.1	17.4	0.4	0.4	22.9
14.0	0.3	0.1	1.0	19.2	0.2	28.3	<0.1	<0.1	18.1	0.4	0.5	31.9
14.8	0.3	<0.1	0.9	13.1	0.1	19.0	<0.1	<0.1	28.0	0.8	0.4	37.3
15.7	0.2	0.1	1.1	12.2	<0.1	23.8	0.1	<0.1	22.1	0.7	0.2	39.5
16.5	0.1	0.1	2.0	8.3	<0.1	21.3	<0.1	<0.1	31.1	1.8	0.2	35.1
17.3	0.2	<0.1	1.6	15.2	<0.1	27.0	<0.1	<0.1	13.9	0.3	0.4	41.4
18.1	0.2	0.1	1.1	14.9	<0.1	21.2	0.1	<0.1	25.8	0.7	0.3	35.6
19.0	<0.1	0.1	2.7	14.1	0.1	30.1	<0.1	<0.1	15.8	0.2	0.3	36.4
19.8	0.2	<0.1	1.2	12.6	0.1	38.6	<0.1	<0.1	13.8	<0.1	0.4	33.0
20.6	0.2	0.1	2.4	12.2	<0.1	27.1	<0.1	<0.1	19.8	0.1	0.5	37.6
21.4	<0.1	<0.1	2.2	13.7	<0.1	24.3	<0.1	<0.1	14.4	<0.1	0.4	44.9
22.3	0.1	0.1	1.6	19.2	<0.1	31.9	0.1	0.1	7.7	2.6	0.3	36.4
23.1	0.4	0.1	2.6	13.8	<0.1	23.4	<0.1	<0.1	13.9	1.4	0.2	44.3
23.9	0.2	<0.1	2.2	8.2	<0.1	17.6	<0.1	0.1	16.5	<0.1	0.8	54.4
24.7	0.1	0.1	1.3	11.4	<0.1	24.1	<0.1	0.1	11.9	0.1	0.6	50.2
25.6	0.1	0.1	1.2	10.3	<0.1	22.0	0.1	<0.1	11.2	0.1	0.2	54.8
26.4	0.3	<0.1	1.4	18.5	<0.1	33.3	<0.1	<0.1	8.0	0.1	0.3	38.1
27.2	0.2	0.1	1.2	20.2	<0.1	33.4	<0.1	<0.1	7.9	<0.1	0.2	36.6
28.0	0.2	0.1	1.9	16.1	<0.1	28.2	<0.1	<0.1	8.7	<0.1	0.2	44.5
28.8	0.1	0.2	1.0	21.3	0.1	36.3	<0.1	0.1	3.4	<0.1	1.0	36.4
29.7	0.3	0.2	1.9	16.6	<0.1	27.5	<0.1	0.2	8.5	0.2	0.5	43.9
30.5	0.1	0.1	1.6	13.1	<0.1	22.0	<0.1	<0.1	9.3	<0.1	<0.1	53.8
31.3	0.1	0.2	1.7	14.1	0.1	28.7	<0.1	<0.1	8.8	0.1	0.4	45.7
32.1	0.3	<0.1	1.6	16.6	0.1	31.1	0.1	<0.1	7.0	<0.1	0.5	42.8
33.0	0.3	0.1	1.8	15.9	<0.1	30.0	0.1	<0.1	6.4	0.1	0.4	45.0
33.8	0.3	0.2	1.7	15.8	<0.1	32.9	<0.1	<0.1	6.0	<0.1	0.2	42.9
34.6	0.4	0.2	2.2	11.4	<0.1	22.8	<0.1	0.1	5.6	0.1	0.4	56.8
35.4	0.3	0.2	1.7	12.2	<0.1	23.0	0.1	<0.1	10.0	<0.1	0.1	52.4
36.3	0.4	0.2	2.4	11.0	<0.1	20.5	<0.1	0.1	6.8	<0.1	0.4	58.4
37.1	0.2	0.1	1.2	10.8	<0.1	19.1	<0.1	0.1	5.7	0.1	0.4	62.2
37.9	0.1	0.1	1.2	7.1	0.1	12.6	<0.1	<0.1	5.0	<0.1	0.8	72.9
38.7	0.2	0.1	1.4	6.7	<0.1	10.0	0.1	<0.1	3.7	<0.1	0.2	77.7
39.6	0.4	0.5	2.9	8.3	<0.1	9.2	<0.1	0.1	4.5	<0.1	<0.1	74.2

Lith17

(mm)	MgO	Al ₂ O ₃	SiO ₂	P ₂ O ₅	K ₂ O	CaO	MnO	Fe ₂ O ₃	Cu ₂ O	AgO	SnO ₂	PbO
0.0	0.1	0.1	7.5	1.2	<0.1	17.3	<0.1	0.2	16.2	<0.1	1.2	56.2
0.8	0.1	<0.1	2.9	1.0	<0.1	5.9	<0.1	0.2	5.4	0.1	0.2	84.1
1.6	0.5	0.3	5.8	1.0	<0.1	8.1	<0.1	0.1	16.3	<0.1	0.8	67.2
2.5	1.2	0.8	8.6	1.3	<0.1	11.3	<0.1	<0.1	25.7	<0.1	1.7	49.6
3.3	1.2	1.3	9.1	1.4	<0.1	11.2	<0.1	0.1	26.6	<0.1	2.2	46.8
4.1	1.0	1.1	9.3	1.6	<0.1	14.0	0.1	0.1	23.4	0.1	2.1	47.1
4.9	1.1	1.4	8.7	1.6	<0.1	13.6	<0.1	0.1	18.8	<0.1	1.7	53.2
5.8	1.0	1.7	8.7	1.4	<0.1	13.9	<0.1	<0.1	20.7	<0.1	2.2	50.5
6.6	0.8	1.7	8.0	1.1	<0.1	12.0	<0.1	0.1	20.6	<0.1	1.5	54.2
7.4	0.8	2.1	8.9	1.2	<0.1	12.1	<0.1	0.1	27.9	<0.1	1.8	45.1
8.2	0.8	1.9	8.0	1.5	<0.1	10.9	<0.1	0.1	28.5	0.1	1.8	46.3
9.1	0.7	1.9	8.0	1.4	<0.1	10.5	<0.1	<0.1	25.5	<0.1	1.8	50.3
9.9	0.6	1.7	8.6	1.2	<0.1	10.4	<0.1	0.1	24.9	<0.1	1.2	51.2
10.7	0.6	1.6	8.5	1.3	<0.1	10.1	<0.1	0.1	27.0	0.1	1.0	49.6
11.5	0.8	1.5	8.0	1.3	<0.1	9.8	<0.1	0.2	25.4	<0.1	1.5	51.6
12.4	0.5	1.2	6.4	0.9	<0.1	8.1	0.1	0.1	19.4	<0.1	0.7	62.6
13.2	0.8	1.8	8.3	1.5	<0.1	10.9	0.1	0.1	21.5	<0.1	1.3	53.8
14.0	0.8	1.7	8.1	1.1	<0.1	10.6	<0.1	<0.1	24.2	<0.1	0.8	52.6
14.8	0.9	2.1	9.5	1.0	<0.1	12.3	<0.1	0.1	26.2	<0.1	0.6	47.2
15.7	0.7	1.9	10.0	1.3	<0.1	13.6	0.1	0.2	16.4	<0.1	0.3	55.5
16.5	0.7	2.2	10.0	1.2	0.1	14.9	0.1	0.2	16.1	<0.1	0.4	54.2
17.3	0.7	1.9	7.2	1.2	<0.1	11.7	<0.1	0.2	17.7	0.1	0.2	59.2
18.1	0.7	1.9	8.0	1.1	<0.1	13.3	0.1	0.2	17.4	<0.1	0.5	56.8
19.0	0.7	2.0	7.5	1.1	<0.1	14.2	0.1	0.2	16.3	<0.1	<0.1	57.9
19.8	0.7	2.0	8.2	1.4	0.1	12.4	<0.1	0.4	15.3	<0.1	0.5	59.1
20.6	0.6	1.2	5.5	1.0	<0.1	8.7	0.1	0.2	7.9	0.1	0.1	74.7
21.4	0.6	1.9	6.3	1.3	<0.1	10.4	0.1	0.2	7.3	0.1	0.3	71.5
22.3	0.6	1.7	5.8	1.1	<0.1	10.1	0.1	0.3	5.3	0.1	0.2	74.6
23.1	0.6	1.5	6.7	1.0	<0.1	9.9	0.1	0.3	4.6	<0.1	<0.1	75.2
23.9	0.6	0.9	6.2	1.0	<0.1	17.4	0.1	0.3	4.9	<0.1	0.2	68.4
24.7	0.4	1.0	4.4	1.2	<0.1	24.0	0.1	0.5	4.0	<0.1	0.8	63.8

Lith18

(mm)	MgO	Al ₂ O ₃	SiO ₂	P ₂ O ₅	K ₂ O	CaO	MnO	Fe ₂ O ₃	Cu ₂ O	AgO	SnO ₂	PbO
0.0	0.4	<0.1	1.1	8.7	<0.1	11.5	<0.1	<0.1	31.9	2.8	<0.1	43.4
0.8	0.6	0.1	1.0	8.9	<0.1	12.2	<0.1	<0.1	30.8	2.1	<0.1	44.2
1.6	0.4	<0.1	1.3	9.4	<0.1	13.2	<0.1	<0.1	28.8	2.4	<0.1	44.4
2.5	0.6	0.1	1.2	18.7	<0.1	27.6	<0.1	0.1	17.8	1.2	0.2	32.4
3.3	0.5	<0.1	1.5	19.1	<0.1	27.5	<0.1	0.1	17.3	2.9	0.1	31.1
4.1	0.4	0.1	1.2	18.6	0.1	26.0	0.1	0.1	19.5	1.9	0.2	31.9
4.9	0.5	0.2	1.7	16.7	<0.1	22.6	<0.1	<0.1	22.5	2.2	0.1	33.4
5.8	0.8	0.1	1.9	18.1	<0.1	24.4	<0.1	0.1	21.2	3.5	<0.1	29.9
6.6	0.8	0.2	1.3	18.5	0.2	20.9	<0.1	0.2	32.5	1.7	0.9	22.8
7.4	0.6	0.2	1.7	12.9	0.2	13.6	<0.1	0.2	43.0	0.9	0.8	26.0
8.2	0.7	0.4	2.4	15.3	0.1	18.5	<0.1	0.2	31.5	0.7	0.3	29.9
9.1	0.7	0.5	2.8	17.7	0.1	24.0	<0.1	0.2	17.7	0.6	0.2	35.5
9.9	1.6	1.2	4.8	11.4	0.2	13.3	<0.1	0.3	34.5	0.4	0.1	32.3
10.7	5.2	4.7	10.6	2.4	1.1	4.9	<0.1	0.6	28.5	0.7	0.1	41.1
11.5	7.0	6.6	16.6	3.7	1.8	6.8	0.1	1.8	15.3	0.4	<0.1	40.0
12.4	7.4	4.2	14.3	11.4	0.8	9.3	0.1	4.3	9.2	0.1	<0.1	38.9

Lith19

(mm)	MgO	Al ₂ O ₃	SiO ₂	P ₂ O ₅	K ₂ O	CaO	MnO	Fe ₂ O ₃	Cu ₂ O	AgO	SnO ₂	PbO
0.0	2.5	0.1	7.7	1.2	0.2	9.4	<0.1	<0.1	20.4	1.1	0.1	57.4
0.8	2.1	0.1	7.3	1.9	0.4	11.2	<0.1	0.1	20.1	1.4	<0.1	55.4
1.6	1.3	<0.1	6.6	2.4	0.4	10.8	<0.1	<0.1	21.5	1.7	<0.1	55.1
2.5	2.7	<0.1	6.5	1.4	0.1	8.8	<0.1	<0.1	22.8	1.8	<0.1	55.9
3.3	2.0	<0.1	4.8	1.0	<0.1	6.6	<0.1	<0.1	22.3	1.6	<0.1	61.7
4.1	2.1	0.1	5.2	1.0	0.1	6.9	<0.1	0.1	21.2	0.9	<0.1	62.4
4.9	1.7	1.0	5.3	1.2	0.1	7.7	<0.1	<0.1	21.2	0.5	<0.1	61.0
5.8	1.5	2.5	6.5	1.0	0.5	10.0	<0.1	0.1	18.8	0.3	<0.1	58.9
6.6	1.7	1.9	6.7	1.0	0.6	8.1	0.2	<0.1	18.2	0.4	<0.1	61.2
7.4	1.3	2.1	5.5	0.8	1.1	5.3	0.1	0.1	21.2	0.4	<0.1	62.0
8.2	1.2	1.9	5.8	0.8	1.4	5.6	<0.1	0.1	23.3	0.4	0.1	59.4
9.1	1.4	1.2	5.6	1.0	1.1	6.1	<0.1	0.1	23.1	0.4	<0.1	60.0
9.9	1.3	1.5	5.7	1.1	1.3	5.9	0.2	0.1	23.6	0.4	<0.1	58.9
10.7	1.4	1.2	5.4	1.1	1.2	5.5	0.2	0.1	23.3	0.4	0.2	59.9
11.5	1.4	1.2	5.4	1.0	1.0	5.4	0.2	<0.1	22.2	0.4	0.1	61.8
12.4	1.6	1.1	5.7	1.3	0.8	5.5	0.2	0.1	24.8	0.1	<0.1	58.8
13.2	1.7	0.9	6.2	1.4	0.7	5.9	0.2	0.1	24.3	0.3	0.1	58.2
14.0	1.2	1.3	6.7	0.9	0.7	5.1	0.2	0.2	19.2	0.2	<0.1	64.3
14.8	1.1	1.4	7.5	1.1	1.0	4.8	0.3	0.3	15.9	0.1	<0.1	66.6
15.7	1.1	1.4	8.2	0.8	1.2	4.5	0.3	0.3	15.6	0.1	<0.1	66.6
16.5	1.0	1.3	8.2	1.0	1.2	4.5	0.3	0.4	15.8	<0.1	0.1	66.2
17.3	0.8	1.8	8.5	0.8	1.5	3.0	0.3	0.5	15.3	<0.1	0.1	67.4
18.1	0.7	0.8	8.6	0.9	0.5	3.6	0.3	0.7	15.1	<0.1	<0.1	68.8
19.0	0.4	1.5	9.2	0.6	1.0	2.4	0.1	0.9	17.3	<0.1	<0.1	66.5
19.8	0.4	2.1	10.9	0.7	1.8	2.5	0.2	1.9	13.3	<0.1	0.1	66.2
20.6	0.4	2.0	9.8	6.7	1.7	6.4	0.1	3.7	4.7	<0.1	<0.1	64.5
21.4	0.4	1.1	5.4	11.1	0.2	11.5	0.1	3.6	1.8	<0.1	<0.1	64.8

Lith22

(mm)	MgO	Al ₂ O ₃	SiO ₂	P ₂ O ₅	K ₂ O	CaO	MnO	Fe ₂ O ₃	Cu ₂ O	AgO	SnO ₂	PbO
0.0	0.3	0.1	1.2	12.2	<0.1	18.6	0.1	<0.1	17.8	<0.1	0.2	49.4
0.8	0.4	<0.1	1.9	14.2	<0.1	22.1	<0.1	<0.1	15.6	0.1	0.1	45.5
1.6	0.4	0.1	1.8	20.2	0.1	29.9	<0.1	0.1	12.1	<0.1	0.2	35.1
2.5	0.5	0.1	2.2	15.6	<0.1	23.2	<0.1	0.1	14.9	0.1	<0.1	43.4
3.3	0.4	<0.1	2.4	14.4	0.1	22.2	<0.1	<0.1	14.0	<0.1	0.2	46.2
4.1	0.5	0.1	2.1	14.3	0.1	22.0	<0.1	0.1	12.8	<0.1	0.1	48.1
4.9	0.4	<0.1	1.5	20.9	0.1	31.1	<0.1	<0.1	9.5	<0.1	0.3	36.3
5.8	0.5	0.1	1.6	16.0	<0.1	24.3	<0.1	<0.1	11.0	<0.1	0.2	46.5
6.6	0.4	0.2	1.0	16.3	<0.1	24.7	<0.1	<0.1	10.6	<0.1	0.3	46.5
7.4	0.4	0.1	1.2	12.8	<0.1	19.1	<0.1	<0.1	13.1	<0.1	<0.1	53.2
8.2	0.2	1.0	2.3	14.7	0.5	17.9	0.1	0.9	6.7	<0.1	<0.1	55.8

Lith23

(mm)	MgO	Al ₂ O ₃	SiO ₂	P ₂ O ₅	K ₂ O	CaO	MnO	Fe ₂ O ₃	Cu ₂ O	AgO	SnO ₂	PbO
0.0	0.2	<0.1	0.6	15.5	<0.1	23.1	<0.1	<0.1	17.3	1.7	<0.1	41.5
0.8	0.2	<0.1	0.5	13.1	<0.1	19.9	0.1	<0.1	18.6	0.3	<0.1	47.3
1.6	0.3	<0.1	0.5	13.4	<0.1	19.5	<0.1	<0.1	23.0	0.4	0.2	42.8
2.5	0.2	<0.1	0.5	12.2	<0.1	17.7	<0.1	<0.1	27.7	0.2	<0.1	41.4
3.3	0.3	<0.1	0.5	17.3	<0.1	25.1	<0.1	<0.1	20.5	0.2	<0.1	36.1
4.1	0.2	<0.1	0.5	14.4	<0.1	20.6	<0.1	<0.1	20.0	3.3	<0.1	41.0
4.9	0.3	<0.1	0.4	15.4	<0.1	17.9	<0.1	<0.1	38.9	10.6	<0.1	16.4
5.8	0.3	<0.1	0.4	23.4	<0.1	26.3	<0.1	<0.1	30.6	3.3	<0.1	15.7
6.6	0.2	<0.1	0.4	18.5	<0.1	18.7	<0.1	<0.1	42.8	7.6	<0.1	11.7
7.4	0.2	<0.1	0.3	18.7	<0.1	18.1	<0.1	<0.1	40.8	5.8	<0.1	15.9
8.2	0.3	<0.1	0.4	21.1	<0.1	23.2	<0.1	<0.1	36.4	2.8	<0.1	15.7
9.1	0.3	<0.1	0.5	21.0	<0.1	26.9	<0.1	<0.1	25.6	1.3	<0.1	24.3
9.9	0.2	<0.1	0.5	15.5	<0.1	21.5	<0.1	<0.1	21.6	0.8	<0.1	39.8
10.7	0.3	<0.1	0.5	17.1	<0.1	21.9	<0.1	<0.1	29.2	0.3	<0.1	30.5
11.5	0.3	0.1	0.5	21.8	<0.1	28.9	<0.1	<0.1	16.0	0.1	0.1	32.3
12.4	0.2	<0.1	0.4	20.3	<0.1	25.4	<0.1	<0.1	24.9	<0.1	0.2	28.6
13.2	0.1	<0.1	0.5	20.3	<0.1	25.1	0.1	<0.1	19.0	0.1	0.1	34.8
14.0	0.2	<0.1	0.6	17.4	<0.1	19.5	<0.1	<0.1	31.8	0.1	0.1	30.3
14.8	0.1	0.1	0.4	22.0	<0.1	30.5	<0.1	0.1	16.6	<0.1	<0.1	30.2
15.7	0.1	0.1	0.5	16.7	<0.1	22.2	0.1	<0.1	23.0	<0.1	<0.1	37.3
16.5	0.1	0.1	0.6	14.1	<0.1	17.7	<0.1	<0.1	29.1	<0.1	0.1	38.3
17.3	0.1	<0.1	0.8	14.4	<0.1	21.9	<0.1	<0.1	11.8	0.2	0.1	50.5
18.1	0.1	<0.1	1.0	14.6	<0.1	21.8	<0.1	<0.1	14.0	<0.1	0.1	48.3
19.0	<0.1	<0.1	1.3	15.9	0.1	23.6	<0.1	0.1	10.5	<0.1	0.2	48.2

Lith27

(mm)	MgO	Al ₂ O ₃	SiO ₂	P ₂ O ₅	K ₂ O	CaO	MnO	Fe ₂ O ₃	Cu ₂ O	AgO	SnO ₂	PbO
0.0	0.2	<0.1	0.7	13.5	0.2	18.0	<0.1	0.1	23.0	2.4	0.3	41.6
0.8	0.2	<0.1	0.7	14.6	<0.1	22.6	0.1	<0.1	14.1	0.9	<0.1	46.8
1.6	0.2	<0.1	0.6	17.3	0.1	25.8	<0.1	0.1	14.6	0.4	0.2	40.6
2.5	0.3	0.1	0.6	15.7	0.1	23.6	<0.1	<0.1	16.4	0.7	0.1	42.5
3.3	0.4	<0.1	0.6	19.4	0.1	29.6	0.1	<0.1	13.6	0.4	0.2	35.7
4.1	0.3	0.1	1.0	19.8	0.2	29.6	0.1	<0.1	13.6	0.4	0.1	34.7
4.9	0.4	<0.1	1.5	16.4	0.2	25.9	<0.1	<0.1	13.5	0.5	0.1	41.6
5.8	0.3	<0.1	1.4	14.7	0.2	22.4	<0.1	<0.1	14.8	0.5	0.1	45.7
6.6	0.4	<0.1	1.5	14.0	0.2	21.5	<0.1	<0.1	16.0	0.4	0.1	46.1
7.4	0.3	<0.1	1.1	14.8	<0.1	22.8	<0.1	<0.1	15.0	0.4	<0.1	45.6
8.2	0.2	<0.1	1.4	16.9	<0.1	25.7	<0.1	<0.1	14.1	0.3	0.2	41.1
9.1	0.3	0.1	2.5	15.4	0.1	23.3	<0.1	<0.1	13.6	0.2	0.1	44.6
9.9	0.2	<0.1	1.6	15.3	0.1	23.1	<0.1	0.1	14.2	0.3	0.1	45.0
10.7	0.3	0.1	1.5	16.8	<0.1	25.6	<0.1	<0.1	12.9	0.3	<0.1	42.5
11.5	0.3	<0.1	1.4	13.9	<0.1	21.9	<0.1	<0.1	12.2	0.2	0.1	50.0
12.4	0.4	<0.1	1.6	13.8	<0.1	21.6	0.1	0.1	12.2	0.2	0.1	49.9
13.2	0.2	0.1	1.4	15.0	<0.1	22.8	<0.1	<0.1	11.0	<0.1	<0.1	49.5
14.0	0.3	<0.1	1.6	15.0	<0.1	23.7	0.1	<0.1	10.8	<0.1	0.1	48.5
14.8	0.2	0.1	1.4	18.1	<0.1	27.5	<0.1	<0.1	9.8	<0.1	0.1	42.8
15.7	0.1	0.1	1.3	13.2	<0.1	21.3	<0.1	0.1	11.0	0.1	0.1	52.9
16.5	0.2	0.1	1.1	15.1	0.1	23.1	<0.1	0.1	10.1	<0.1	0.2	50.0
17.3	0.2	0.1	1.3	15.1	<0.1	23.1	<0.1	<0.1	9.5	<0.1	<0.1	50.7
18.1	0.1	0.1	1.3	12.8	<0.1	18.4	<0.1	<0.1	10.4	<0.1	0.1	56.8
19.0	0.3	<0.1	1.2	18.9	0.1	26.9	0.1	0.3	7.2	0.1	0.3	44.8
19.8	0.3	0.2	1.1	20.0	<0.1	28.9	<0.1	0.3	5.7	<0.1	0.1	43.5
20.6	0.3	0.2	2.7	16.2	<0.1	23.0	<0.1	0.2	7.1	<0.1	<0.1	50.3

Lith35

(mm)	MgO	Al ₂ O ₃	SiO ₂	P ₂ O ₅	K ₂ O	CaO	MnO	Fe ₂ O ₃	Cu ₂ O	AgO	SnO ₂	PbO
0.0	0.2	0.2	1.7	17.1	0.1	23.3	<0.1	<0.1	20.4	2.4	0.2	34.4
0.8	0.2	<0.1	1.8	14.4	0.1	23.1	<0.1	0.1	15.5	4.7	0.2	40.0
1.6	0.4	0.1	1.7	12.8	<0.1	19.0	0.1	<0.1	22.6	2.5	<0.1	40.8
2.5	0.4	0.1	1.7	11.4	<0.1	15.5	<0.1	<0.1	26.8	0.8	0.3	43.0
3.3	0.4	0.1	2.2	12.8	0.1	19.2	<0.1	<0.1	21.3	0.5	0.3	43.1
4.1	0.2	<0.1	1.8	18.2	<0.1	28.1	<0.1	0.1	15.8	0.2	0.1	35.5
4.9	0.3	0.1	2.4	13.4	0.1	20.3	<0.1	<0.1	21.2	<0.1	<0.1	42.2
5.8	0.2	0.1	3.2	12.3	<0.1	18.3	<0.1	<0.1	16.6	0.2	<0.1	49.1
6.6	0.2	0.1	1.9	14.1	<0.1	20.6	<0.1	0.1	8.7	0.1	0.1	54.1
7.4	0.2	0.1	2.0	13.9	0.1	20.8	<0.1	0.1	3.6	<0.1	0.2	59.0
8.2	0.2	0.2	1.8	18.0	0.1	26.3	0.1	0.1	1.9	-0.3	0.3	51.4

Lith36

(mm)	MgO	Al ₂ O ₃	SiO ₂	P ₂ O ₅	K ₂ O	CaO	MnO	Fe ₂ O ₃	Cu ₂ O	AgO	SnO ₂	PbO
0.0	0.9	1.9	9.6	3.5	1.0	7.2	0.1	0.1	28.2	9.5	<0.1	38.0
0.8	1.1	1.5	8.7	1.8	1.1	8.6	0.1	0.1	30.9	6.5	<0.1	39.8
1.6	1.2	1.7	8.0	1.3	1.2	11.4	0.1	0.1	28.7	4.5	0.1	41.5
2.5	1.5	1.4	7.4	1.3	1.2	11.9	0.1	0.1	32.0	5.2	0.2	37.7
3.3	1.6	1.5	7.2	1.2	1.1	8.0	0.2	0.1	32.7	5.6	<0.1	40.8
4.1	1.1	1.6	6.3	1.1	1.1	5.7	<0.1	<0.1	27.9	3.3	<0.1	51.8
4.9	1.0	1.4	6.2	0.9	1.2	6.1	0.2	<0.1	25.1	2.2	0.2	55.5
5.8	1.2	1.0	7.3	1.0	0.8	3.9	0.3	0.1	22.4	1.2	<0.1	60.7
6.6	1.1	0.7	7.3	1.1	0.5	6.5	0.2	0.2	26.4	0.4	<0.1	55.6
7.4	0.8	0.7	7.8	0.7	0.9	4.9	0.2	0.2	25.7	0.3	<0.1	57.8
8.2	1.0	0.7	9.7	1.2	1.1	7.1	0.3	0.4	19.8	0.2	<0.1	58.4
9.1	1.2	0.9	10.0	1.7	1.2	5.2	0.4	0.5	17.0	<0.1	<0.1	61.9
9.9	1.0	0.8	11.2	1.7	0.8	7.2	0.5	0.6	12.9	0.1	0.2	63.2
10.7	0.7	1.1	11.7	2.5	0.9	6.7	0.3	1.6	10.4	<0.1	<0.1	64.0

Lith37

(mm)	MgO	Al ₂ O ₃	SiO ₂	P ₂ O ₅	K ₂ O	CaO	MnO	Fe ₂ O ₃	Cu ₂ O	AgO	SnO ₂	PbO
0.0	0.6	0.5	9.0	5.5	3.3	17.1	0.2	0.1	13.8	0.1	0.1	49.8
0.8	0.5	0.2	7.3	13.3	2.9	26.8	0.1	0.1	9.1	<0.1	0.4	39.4
1.6	0.4	0.1	5.3	22.0	1.3	37.9	0.1	0.1	5.2	0.1	0.3	27.2
2.5	0.2	0.1	6.4	16.8	0.9	31.5	0.1	0.1	8.9	<0.1	0.1	34.9
3.3	0.1	0.1	5.0	13.4	0.3	25.6	<0.1	<0.1	13.6	0.2	0.1	41.6
4.1	<0.1	0.1	5.5	15.3	0.3	26.1	0.1	<0.1	15.9	0.1	0.2	36.4
4.9	0.2	0.1	4.9	14.1	0.3	23.8	<0.1	0.1	20.7	<0.1	<0.1	35.8
5.8	0.1	0.1	4.6	15.9	0.4	27.3	<0.1	<0.1	13.7	<0.1	0.1	37.6
6.6	0.2	0.1	3.4	15.0	0.5	24.8	<0.1	0.1	15.1	0.1	<0.1	40.7
7.4	0.2	0.1	2.2	12.9	0.3	19.9	0.1	0.1	17.1	<0.1	0.3	46.9
8.2	0.1	0.1	1.5	11.9	0.3	18.3	<0.1	0.1	16.7	<0.1	0.1	50.9
9.1	0.1	0.2	1.6	12.0	0.2	18.3	<0.1	0.1	19.0	<0.1	0.1	48.4
9.9	0.2	0.1	1.7	11.4	0.2	17.4	<0.1	0.1	17.5	0.1	0.1	51.2
10.7	0.3	0.1	1.5	17.0	0.2	26.6	0.1	0.1	14.8	0.2	0.1	39.0
11.5	0.3	0.1	1.2	15.3	0.2	24.3	0.1	0.1	13.6	<0.1	0.1	44.7
12.4	0.2	0.2	1.5	12.6	0.2	18.6	0.1	0.1	18.3	<0.1	0.1	48.3
13.2	0.2	0.1	1.5	10.2	0.1	14.9	<0.1	0.1	23.5	0.2	0.1	49.1
14.0	<0.1	0.1	1.5	11.7	<0.1	17.8	0.1	0.1	12.6	0.1	0.1	55.7
14.8	0.2	<0.1	0.9	12.8	0.1	21.6	0.1	0.1	15.9	0.2	0.2	47.8
15.7	0.3	0.1	0.9	16.0	0.1	27.3	<0.1	0.1	11.2	<0.1	0.1	43.8
16.5	0.2	<0.1	0.8	14.1	0.1	23.6	<0.1	<0.1	14.2	<0.1	0.3	46.6
17.3	0.1	0.1	1.0	11.9	0.1	20.6	0.1	<0.1	12.7	0.1	<0.1	53.4
18.1	0.2	<0.1	1.2	11.6	0.2	17.5	0.1	0.1	16.9	0.1	0.4	51.7

Lith38

(mm)	MgO	Al ₂ O ₃	SiO ₂	P ₂ O ₅	K ₂ O	CaO	MnO	Fe ₂ O ₃	Cu ₂ O	AgO	SnO ₂	PbO
0.0	0.5	0.1	2.8	4.8	<0.1	6.3	<0.1	0.1	37.9	0.7	0.1	46.6
0.8	0.2	0.1	2.6	8.3	<0.1	12.6	0.1	0.1	27.8	0.7	<0.1	47.5
1.6	0.3	0.2	2.3	11.0	0.1	17.4	<0.1	0.1	14.6	0.3	<0.1	53.7
2.5	0.3	0.2	2.4	10.8	0.1	17.2	<0.1	0.2	15.5	0.2	<0.1	53.0
3.3	0.2	0.2	2.2	11.8	0.1	18.2	<0.1	0.1	17.6	0.6	<0.1	49.1
4.1	0.5	0.1	2.4	9.3	0.1	13.3	<0.1	<0.1	25.0	0.9	0.1	48.5
4.9	0.4	0.2	2.1	11.5	0.1	16.8	<0.1	0.1	13.6	0.2	0.3	54.7
5.8	0.4	0.1	1.5	14.5	0.1	22.5	<0.1	0.1	13.6	0.1	<0.1	47.2
6.6	0.5	0.2	1.6	14.9	<0.1	22.8	<0.1	0.1	13.4	0.2	0.2	46.1
7.4	0.3	0.1	1.8	13.0	0.1	19.5	<0.1	0.1	14.8	<0.1	0.1	50.3
8.2	0.4	0.1	2.5	15.3	0.2	22.3	<0.1	0.1	13.2	0.1	0.5	45.3
9.1	0.2	0.2	4.3	16.2	0.4	23.5	<0.1	0.2	13.9	<0.1	0.3	40.8
9.9	0.4	0.4	4.8	15.8	0.8	24.6	0.1	0.2	6.8	<0.1	0.9	45.3
10.7	0.4	0.5	6.8	14.2	1.1	24.2	0.1	0.3	4.3	<0.1	1.1	47.1
11.5	0.4	0.4	7.2	19.3	0.5	33.4	0.1	0.2	6.5	<0.1	0.7	31.2
12.4	0.4	0.4	7.8	20.4	0.6	35.1	0.1	0.3	4.4	<0.1	0.9	29.6
13.2	0.3	0.5	7.5	14.9	0.7	25.9	0.2	0.3	5.6	<0.1	1.2	43.0



ENGLISH HERITAGE RESEARCH DEPARTMENT

English Heritage undertakes and commissions research into the historic environment, and the issues that affect its condition and survival, in order to provide the understanding necessary for informed policy and decision making, for sustainable management, and to promote the widest access, appreciation and enjoyment of our heritage.

The Research Department provides English Heritage with this capacity in the fields of buildings history, archaeology, and landscape history. It brings together seven teams with complementary investigative and analytical skills to provide integrated research expertise across the range of the historic environment. These are:

- * Aerial Survey and Investigation*
- * Archaeological Projects (excavation)*
- * Archaeological Science*
- * Archaeological Survey and Investigation (landscape analysis)*
- * Architectural Investigation*
- * Imaging, Graphics and Survey (including measured and metric survey, and photography)*
- * Survey of London*

The Research Department undertakes a wide range of investigative and analytical projects, and provides quality assurance and management support for externally-commissioned research. We aim for innovative work of the highest quality which will set agendas and standards for the historic environment sector. In support of this, and to build capacity and promote best practice in the sector, we also publish guidance and provide advice and training. We support outreach and education activities and build these in to our projects and programmes wherever possible.

We make the results of our work available through the Research Department Report Series, and through journal publications and monographs. Our publication Research News, which appears three times a year, aims to keep our partners within and outside English Heritage up-to-date with our projects and activities. A full list of Research Department Reports, with abstracts and information on how to obtain copies, may be found on www.english-heritage.org.uk/researchreports

For further information visit www.english-heritage.org.uk

